

Aus der Abteilung Experimentelle Neurologie
der Medizinischen Fakultät Charité – Universitätsmedizin Berlin

DISSERTATION

**The Relationship between the Blood-Brain Barrier
and Cerebral Ischemia**

zur Erlangung des akademischen Grades
Doctor of Philosophy in Medical Neurosciences
PhD in Medical Neurosciences

vorgelegt der Medizinischen Fakultät
Charité – Universitätsmedizin Berlin

von

Ryan Cordell

aus San Angelo, Texas, USA

Acknowledgments:

I would like to

-sincerely thank Dr. Ana Luisa Pina for supporting me in my final year.

-thank Prof Dr. Ulrich Dirnagl for giving me the opportunity to do my Phd.

-sincerely thank Dr. Jan Klohs for his help and support in my first few years.

-thank Alon Friedman for letting me work in his lab.

-special thanks to Arina Riabinska for her tireless help and patience.

-thank my friends and colleagues Veronika Lang, Margit Müller, Tian Zhang, Francesco Boato, Gina Eom, Ana Ferreira, Cecilia Nicoletti, Dr. Mesba Alam, Anna, Anna Maslarova, Dr. Jens Dreier, Dr. Ferah Yildirim, Denny Milakara, Lutz Steiner, Daniel Margulies, and Menderes Yusuf Terzi

This list would be much larger, if I were to include every single person who has helped me during my PhD thesis project. I apologize to those whose names are not mentioned.

Thanks to all of you. Special thanks to the International Graduate Program Medical Neuroscience of the Charite-Universitätsmedizin Berlin, Germany.

Gutachter/in:

1. Prof. Dr. med. U. Dirnagl
2. Prof. Dr. rer. nat. U. Schäfer
3. Prof. Dr. G. Gutierrez-Ospina

Datum der Promotion: 07-09-2012

Abstract:

Background: Impairment of the blood–brain barrier (BBB) after cerebral ischemia leads to extravasation of plasma constituents into the brain parenchyma and is associated with a larger final lesion volume and more negative outcome.

Hypothesis: Our hypothesis was that an opening in the BBB leads to a larger final lesion volume and a more severe stroke. Here we explored that hypothesis by selectively altering the permeability of the BBB while simultaneously inducing cerebral ischemia.

Results: We first looked at the time course of BBB impairment after transient middle cerebral artery occlusion (MCAO) in mice. An initial BBB impairment was observed at 4–8 hours and a second impairment at 12–16 hours after reperfusion. No EB extravasation was detected at 8–12 hours. We then manipulated the permeability of the BBB after MCAO using hydrodynamic delivery of claudin-5 small interfering RNA (siRNA), transcranial magnetic stimulation (TMS), intracarotid injection of hypertonic arabinose, and intraventricular infusion of Pigment epithelium-derived factor (PEDF). Opening the BBB with hypertonic arabinose led to a larger final lesion volume in mice, and the lesion volume correlated with the size of the opening in the BBB induced by arabinose. Claudin-5 siRNA, TMS, and PEDF had no effect on final lesion volume.

Conclusion: We found that an early opening in the BBB had a detrimental effect on the progression of stroke and lead to a larger final lesion volume in our animal model.

Table of Contents:

<u>Abbreviations</u>	<u>1</u>
1. <u>Introduction and outline</u>	<u>3</u>
2. <u>Time course of BBB opening after cerebral ischemia</u>	<u>6</u>
2.1 <u>Introduction</u>	<u>6</u>
2.2 <u>Materials and methods</u>	<u>6</u>
2.3 <u>Results</u>	<u>9</u>
3. <u>Si-RNA induced pre-emptive opening of the BBB combined with MCAo</u>	<u>15</u>
3.1 <u>Introduction</u>	<u>15</u>
3.2 <u>Materials and methods</u>	<u>16</u>
3.3 <u>Results</u>	<u>18</u>
4. <u>Transcranial magnetic stimulation induced opening of the BBB combined with MCAo</u>	<u>21</u>
4.1 <u>Introduction</u>	<u>21</u>
4.2 <u>Materials and methods</u>	<u>21</u>
4.3 <u>Results</u>	<u>25</u>
5. <u>Hypertonic arabinose induced opening of the BBB combined with MCAo</u>	<u>29</u>
5.1 <u>Introduction</u>	<u>29</u>
5.2 <u>Materials and methods</u>	<u>31</u>
5.3 <u>Results</u>	<u>33</u>
6. <u>Closing the BBB with Pigment endothelium derived factor combined with MCAo</u>	<u>38</u>
6.1 <u>Introduction</u>	<u>38</u>
6.2 <u>Materials and methods</u>	<u>40</u>
6.3 <u>Results</u>	<u>44</u>
7. <u>Discussion and conclusions</u>	<u>47</u>
7.1 <u>Time course of BBB opening after MCAo</u>	<u>47</u>
7.2 <u>Si-RNA induced pre-emptive opening of the BBB combined with MCAo</u>	<u>48</u>
7.3 <u>TMS induced pre-emptive opening of the BBB combined with MCAo</u>	<u>49</u>
7.4 <u>Hypertonic arabinose induced pre-emptive opening of the BBB combined with MCAo</u>	<u>50</u>
7.5 <u>Closing the BBB with PEDF combined with MCAo</u>	<u>51</u>
<u>Results addendum</u>	<u>52</u>
<u>Appendix A: Laboratory materials and suppliers</u>	<u>53</u>
<u>Appendix B: Opening BBB with focused ultrasound</u>	<u>57</u>
<u>Appendix C: Review of BBB and cerebral ischemia</u>	<u>59</u>
<u>References</u>	<u>87</u>
<u>Eidesstattliche Erklärung</u>	<u>105</u>

Index of Figures & Tables:

<u>Table 1: Animals used in experiment 1 – 1st part of study</u>	<u>7</u>
<u>Table 2: Animals used in experiment 1 – 2nd part of study</u>	<u>7</u>
<u>Table 3: Animals used in experiment 1 – 3rd part of study</u>	<u>8</u>
<u>Figure 1: Biphasic opening in the BBB</u>	<u>10</u>
<u>Figure 2: Opening of the BBB imaged with NIRF</u>	<u>12</u>
<u>Table 4: BBB impairment measured with NIRF-BSA and EB</u>	<u>13</u>
<u>Table 5: BBB impairment measured with NIRF-BSA and EB</u>	<u>14</u>
<u>Table 6: Animals used in experiment 2</u>	<u>17</u>
<u>Figure 3: T1 MRI after high pressure injection of Cldn-5 and NT siRNA</u>	<u>19</u>
<u>Figure 4: Final lesion volume after MCAo in Cldn-5 and NT siRNA groups</u>	<u>20</u>
<u>Figure 5: Transcranial magnetic stimulation</u>	<u>22</u>
<u>Table 7: Animals used in experiment 3 – 1st part of study</u>	<u>23</u>
<u>Table 8: Animals used in experiment 3 – 2nd part of study</u>	<u>24</u>
<u>Table 9: Animals used in experiment 3 – 3rd part of study</u>	<u>24</u>
<u>Figure 6 Opening of the BBB after transcranial magnetic stimulation</u>	<u>27</u>
<u>Figure 7: Opening of BBB after TMS</u>	<u>28</u>
<u>Figure 8: Lesion volume after MCAo in animals receiving TMS</u>	<u>28</u>
<u>Figure 9: Osmotic opening of the BBB</u>	<u>30</u>
<u>Table 10: Animals used in experiment 4 – 1st part of study</u>	<u>31</u>
<u>Table 11: Animals used in experiment 4 – 2nd part of study</u>	<u>32</u>
<u>Table 12: Animals used in experiment 4 – 3rd part of study</u>	<u>32</u>
<u>Figure 10: Opening of the BBB after hyperosmotic arabinose injection</u>	<u>34</u>
<u>Figure 11: Opening of the BBB after hyperosmotic arabinose injection II</u>	<u>35</u>
<u>Figure 12: Gadofluorine-M extravasaton compared with final lesion volume after 45 minute MCAo</u>	<u>36</u>
<u>Figure 13: Lesion volume of arabinose vs. saline</u>	<u>37</u>
<u>Figure 14: Osmotic pump</u>	<u>41</u>
<u>Table 13: Animals used in experiment 5 – 1st part of study</u>	<u>42</u>
<u>Table 14: Animals used in experiment 5 – 2nd part of study</u>	<u>42</u>
<u>Figure 15: VEGF, PEDF, and MMP-9 levels in the brain after 1 hr MCAo</u>	<u>45</u>
<u>Figure 16: Albumin levels in the brain after 1 hr MCAo</u>	<u>45</u>
<u>Figure 17: Final lesion volume after 1 hr MCAo in mice recieving PEDF or CSF</u>	<u>46</u>
<u>Figure 18: Molecular imaging matrix</u>	<u>48</u>

Abbreviations:

ABC	ATP Binding Cassette
AJ	Adherens junctions
AMPA	α -amino-3-hydroxy-5-methyl-4-isoxazole propionic acid
AP	Alkaline phosphatase
ATP	Adenosine triphosphate
BBB	Blood-brain barrier
BCA	Bicinchoninic acid
BSA	Bovine serum albumin
CAMP	Cyclic adenosine monophosphate
CASK	Calcium-dependent serine protein kinase
CCD	Charge coupled device
Cd-31	Cluster of differentiation molecule
CNS	Central Nervous System
Da	Daltons
DABCO	Diazabicyclooctane
EB	Evans blue
ECM	Extracellular matrix
ELISA	Enzyme Linked Immunoabsorbent Assay
ERK	Extracellular signal-regulated kinase
Gd-DTPA	Gadolinium-diethylene triamine penta-acetic acid
Gf	Gadofluorine-M
GFAP	Glial fibrillary acidic protein
GLUT-1	Glucose transporter-1
GSK3- β	Glycogen synthase kinase 3 beta
GTP	Guanosine triphosphate
HIF	Hypoxia inducible factor
Iba-1	Ionized calcium binding adaptor molecule 1
ICAM-1	Inter-Cellular Adhesion Molecule 1
IL-1 β	Interleukin-1 Beta
iNOS	Inducible nitric oxide synthase
JACOP	Junction-associated coiled-coil protein
JAM	Junction adhesion molecule

Relationship between the Blood-Brain Barrier and Cerebral Ischemia

MAGUKs	Membrane-associated guanylate kinase-like family of proteins
MAP	Mitogen activated protein
MAPKAPK-2	MAP kinase-activated protein kinase-2
MCAo	Middle cerebral artery occlusion
MMP	Matrix-metalloproteinase
MRI	Magnetic resonance imaging
NIRF	Near-infrared fluorescence
NMDA	N-methyl-d-aspartic acid
NT	Non targeting
PBS	Phosphate buffered saline
PEDF	Pigment epithelium-derived factor
Pgp	P-glycoprotein
PI3K	Phosphatidylinositol 3-kinase
PIP2	Phosphorylation of phosphatidylinositol (4,5)-bisphosphate
PIP3	Phosphatidylinositol (3,4,5)-trisphosphate
PK	Protein kinase
RIPA	Radio-immunoprecipitation assay
RNA	Ribonucleic Acid
ROI	Region of interest
RT	Room temperature
SDS	Sodium dodecyl sulphate
SEM	Standard error of the mean
siRNA	Small interfering RNA
SLC	Solute carrier transporters
TBR	Target-to-Background ratio
TJ	Tight Junctions
TMS	Transcranial magnetic stimulation
TNF- α	Tumor necrosis factor alpha
uPA	Urokinase
uPAR	Urokinase receptor
VEGF	Vascular endothelial growth factor
VSM	Vascular smooth muscle
ZO	Zonula occludens
γ -GTP	γ -Glutamyltranspeptidase

1. Introduction and Outline:

The BBB can be found in every organism with a central nervous system. It most likely evolved in order to maintain homeostasis within the brain, protect the brain from neurotoxic substances in the blood, and to minimize cross talk between the central and peripheral nervous systems. The BBB is able to successfully perform these functions due to its complex make-up and the inter-communication between various cells and protein structures from which it is derived.

The endothelial cells provide the primary barrier of the BBB. Access to the paracellular pathways between adjacent endothelial cells is restricted by tight junctions and adherens junctions working in concert. Surrounding the endothelial cells are pericytes and the extracellular matrix with astrocytes and neurons next in line. Each of these cell types plays a role in forming the BBB phenotype and in the response to various pathophysiological conditions including cerebral ischemia.

Cerebral ischemia results from a transient or permanent reduction in cerebral blood flow of a major brain artery. The reduction in flow is typically caused by the occlusion of a cerebral artery by an embolus or local thrombosis (Dirnagl et al., 1999). This sudden decrease or loss of blood circulation to an area of the brain, ultimately involves the destruction and/or dysfunction of brain cells resulting in a corresponding loss of neurological function (Donnan et al., 2008). With an incidence of approximately 250–400 in 100,000 and a mortality rate of around 30%, stroke remains the third leading cause of death in industrialized countries (Dirnagl et al., 1999).

The BBB plays an important role in the pathophysiology after cerebral ischemia. When closed it prevents the delivery of therapeutic and diagnostic agents, thus preventing treatment when it is most needed. In subsequent stages, the BBB becomes more permeable to blood born substances. According to various studies after stroke, the incidence of BBB disruption varies from 15% to 66% and is biphasic and possibly triphasic in nature. The BBB's loss of integrity allows for extravasation of immune cells, erythrocytes, and potentially toxic substances into the brain tissue. The leakage of blood cells into the brain parenchyma can result in hemorrhagic transformation. Finally, water passively follows the extravasation of large molecules into the brain tissue. This can

result in vasogenic edema which can increase overall brain volume and possibly lead to additional tissue damage through intracranial hypertension.

In experimental and clinical studies, it has been shown that an opening in the BBB is a good predictor of a more intense stroke and larger final lesion volume. However, it is not known which precedes which. Does a more severe stroke lead to an up regulation of various factors such as bradykinin, VEGF, active MMPs and/or other proteases that directly and indirectly give rise to an opening in the BBB; or does an opening in the BBB (through pathways not fully understood and regardless of the severity of the initial stroke) lead to an influx of substances from the blood and a further disruption of the chemical milieu in the region of interest thus giving rise to a more severe stroke and larger final lesion volume? My working hypothesis was the latter, that an opening in the BBB gives rise to a more severe stroke and larger final lesion volume.

In order to test this hypothesis, I was charged with implementing new techniques that would allow for the manipulation in permeability of the BBB to be combined with our animal model of cerebral ischemia. My objective was to induce an artificial opening (or closing) in the BBB during cerebral ischemia and to use the volume of the lesion as a marker for stroke severity. I subsequently broke this overarching goal down into three discrete parts which would provide the roadmap for my work.

1. The first goal of my PhD was to better understand the timing of the increase in BBB permeability after cerebral ischemia in our animal model. By understanding when the BBB was opening and closing it would be possible to try and manipulate it at these time points.
2. The second goal of my PhD was to apply and adapt a series of techniques that would lead to a change in the permeability of the BBB and which could possibly be applied in conjunction with cerebral ischemia. Many techniques for affecting the permeability of the BBB have been developed over the years. However, many are themselves harmful to brain tissue and would therefore have a confounding effect if applied in conjunction with cerebral ischemia. I have implemented a more benign set of methods for opening the BBB.

3. The third goal of my PhD was to demonstrate that the previously mentioned techniques could be used in conjunction with our MCAo model, and to determine what if any effect an increase in permeability might have on development of the stroke. The resulting lesion volume was chosen as our indicator for stroke severity in our ischemic model.

In the paper that follows, I have broken down my work into the five experiments we undertook to better understand the role of the BBB after cerebral ischemia. The first experiment deals with trying to better understand the increase in permeability in the BBB that occurs after MCAo in our animal model, C57Bl6/N mice. In the next three experiments, I discuss the methods we used to try and open the BBB (hydrodynamic delivery of claudin-5 small interfering RNA, transcranial magnetic stimulation, and intracarotid injection of hypertonic arabinose) along with the results of combining these methods with our model of cerebral ischemia. In the final experiment, I discuss the technique we used to try and close the BBB (intraventricular infusion of PEDF) along with the result of combining this technique with our model of cerebral ischemia. In the final section, I have provided a summary of the work along with a discussion and assessment of the conclusions.

2. Time course of BBB opening after cerebral ischemia:

2.1. Introduction:

Cerebral ischemia causes dysfunction of the tight and adherens junctions of the cerebral endothelium (Petty and Lo, 2002) which leads to an impairment of BBB integrity and thereby to extravasation of plasma constituents and cells into the brain parenchyma. Here we investigated the timing of the increase in BBB permeability after cerebral ischemia in our animal model.

2.2. Materials and methods:

2.2.1 Animal Protocol:

Animal experiments were performed according to institutional and international guidelines. All surgical procedures were approved by the local authorities (G0229/05 LaGeSo, Berlin, Germany). 65 male C57Bl6/N mice (Bundesinstitut fuer Risikoforschung, Berlin, Germany) weighing 18–24 grams were housed under standard conditions.

2.2.2 Focal cerebral ischemia:

MCAo was performed as previously described (Endres et al., 1999; Endres et al., 2000). In brief, anesthesia was induced and maintained with 1.5% isoflurane delivered in a mixture of 70% nitrous oxide and 30% oxygen via a facemask under constant ventilation monitoring. Brain ischemia was induced with an 8.0 nylon monofilament coated with a silicone resin/hardener mixture (Xantopren M Mucosa and Activator NF Optosil Xantopren). The filament was introduced into the common carotid artery and advanced to the middle cerebral artery. After placement of the filament, mice were returned to the heating cage to await reperfusion. After 1 hour, mice were re-anesthetized and the filament was withdrawn to allow reperfusion. During surgery and MCAo, rectal temperature was maintained between 37.0°C and 37.5°C with a heating pad. After reperfusion, the mice were kept in heated cages for the next two hours. The animals were then returned to their home cages and allowed free access to food and water.

2.2.3 Experimental design and administration of probes:

In the first part of the study, BBB impairment was investigated using Evans blue extravasation. Evans blue (EB, 50 mg/kg in saline, Sigma–Aldrich, Hamburg, Germany) was injected intravenously in MCAo mice either immediately after or 4, 8, 12 or 16 hours after reperfusion ($n = 8$ each). Mice were sacrificed under deep anesthesia 4 hour after EB injection. Each brain was inspected for EB extravasation at defined reference sections (i.e., interaural +6.6, +5.34, +3.94, +1.86, and +0.08 mm).

Table 1: Animals used in experiment 1 – 1st part of study

EB inj.	0 hours	4 hours	8 hours	12 hours	16 hours
Time-point					
Number of Animals	n=8	n=8	n=8	n=8	N=8

In the second part of the study, indotricarbocyanine bovine serum albumin conjugate (NIRF–BSA, 50 mg/kg, 3.5 dye molecules per protein on average; Bayer Schering Pharma AG, Berlin, Germany) was injected intravenously in MCAo mice at 4, 8 or 12 hours after reperfusion ($n = 4, 5$ and 5 , respectively). EB was injected 10 minutes after NIRF–BSA injection. NIRF imaging and assessment of EB extravasation was performed 4 hours after injection of the compounds.

Table 2: Animals used in experiment 1 – 2nd part of study:

NIRF-BSA inj.	4 hours	8 hours	12 hours
Time-point			
EB inj.	4 hours	8 hours	12 hours
Time-point	+10 minutes	+ 10 minutes	+10 minutes
Number of Animals	n=4	n=5	n=5

In the third part of the study, NIRF–BSA was injected intravenously in MCAo mice either at 4, 8 or 12 hours after reperfusion ($n = 4, 3$ and 4 , respectively). NIRF imaging was performed 4 hours after injection of NIRF–BSA. Gd–DTPA (Magnevist, 0.5 mmol/kg,

Bayer Schering Pharma AG) was injected at 3.5, 7.5 and 11.5 hours after reperfusion, and T1-weighted MRI was performed before and immediately after Gd-DTPA administration.

Animals used in experiment 1 – 3rd part of study:

NIRF-BSA inj.	4 hours	8 hours	12 hours
Time-point			
Gd-DTPA inj.	3.5 hours	7.5 hours	11.5 hours
Time-point			
Number of Animals	N=4	n=3	n=4

2.2.4 Near Infrared Fluorescence Imaging (NIRF):

NIRF-BSA was injected via the tail vein and allowed to circulate for a predetermined amount of time. For non-invasive NIRF imaging, mice were anesthetized by intraperitoneal injection of chloral hydrate solution (200mg/kg, Merck, Darmstadt, Germany) and the skin overlaying the parietal cortex was depilated. Brains were then removed from the skull under deep anesthesia and used for ex-vivo NIRF imaging. For excitation of the NIRF dye an intensity-controlled laser diode emitting at 682 nm (30 mW) was used. Fluorescence emission was collected by a charge-coupled device (CCD) camera (Vers Array 512, 512×512 pixels. Roper Scientific Inc., Duluth GA, USA) equipped with a focusing lens system (Nikkon macro lens f=50mm, f/1.2, Nikon, Düsseldorf, Germany). Three 780 nm interference filters (FWHM 10 nm, Andover, Salem, NH, USA) and a RG695 filter were used to block the excitation light. Data acquisition times were 60 seconds. Data were normalized and corrected for illumination inhomogeneities as described previously (Klohs et al., 2006). Rectangular regions of interest (ROI) were selected over the left, ischemic and right, non-ischemic hemisphere using non-invasive NIRF images. The average fluorescence intensity of all pixels with the ROI was calculated. Target-to-background ratios (TBR) were calculated by dividing ROI values from the left hemisphere by ROI values from the right hemisphere.

2.2.5 T1-weighted magnetic resonance imaging (MRI):

MRI was performed on a dedicated animal scanner (7T Bruker, Pharmascan 70/16 AS, Bruker Biospin, Ettlingen, Germany) with a 20mm quadrature volume resonator. Mice were placed on a heated circulating water blanket to ensure a constant body temperature of 37°C. Anesthesia was induced and maintained with 1.5% isoflurane delivered in a mixture of 70% N₂O and 30% O₂ via a facemask under constant ventilation monitoring (Small Animal Monitoring & Gating System, SA Instruments, Stony Brook, New York, USA). Tripilot scans were used for accurate positioning of the animal head inside the magnet. T1-weighted images were acquired before and after Gd-DTPA injection (pre- and post-contrast images). For T1-weighted imaging a 2D turbo spin-echo sequence was used (T1 TR/TE = 800/13.2 ms, RARE factor 2, 4 averages). Twenty axial slices with a slice thickness of 0.5mm, a field of view of 2.85cm×2.85cm and a matrix of 256×256 were positioned over the brain excluding the olfactory bulb and cerebellum. On post-contrast images, ROIs were defined in the ipsilateral ischemic hemisphere and its mirror image over the contralateral, non-ischemic hemisphere using Analyze software (AnalyzeDirect, Inc., Lenexa, USA). The mean signal intensity of all pixels within the ROI was calculated. Normalized signal intensities were calculated by dividing ROI values from the ipsilateral hemisphere by ROI values from the contralateral hemisphere.

2.2.6 Statistical Analysis:

Analyses between the amount of extravasated EB and TBR and between lesion volume and TBR were performed using the nonparametric Spearman rank correlation coefficient. Statistical analysis was performed using Sigma Stat software.

2.3. Results:

2.3.1 Evans blue detects biphasic impairment of the BBB ex-vivo

The time course of BBB impairment was explored with EB after 1 hour MCAo in mice. EB was injected at different time points after reperfusion and allowed to circulate for 4 hours. The time points of marker injection and circulation times were selected in order to

maximize the utility of a finite cohort of animals and were chosen based on a thorough examination of the existing literature and previous unpublished work of groups within our laboratory. Extravasation of EB was macroscopically detected as diffuse blue tissue coloration (Fig. 1A). Not every animal that underwent 1 hour MCAo demonstrated an opening in the BBB at the times points under consideration. For those that did have an opening in the BBB the color intensity and spatial distribution of EB extravasation were variable between individual animals. Our results indicated a biphasic pattern of BBB impairment after 1 hour MCAo in mice (Fig. 1B). An initial BBB impairment was observed at 4–8 hours after reperfusion and a second impairment at 12–16 hours after reperfusion. No BBB impairment was observed in MCAo mice at 8–12 hours after reperfusion.

(A)

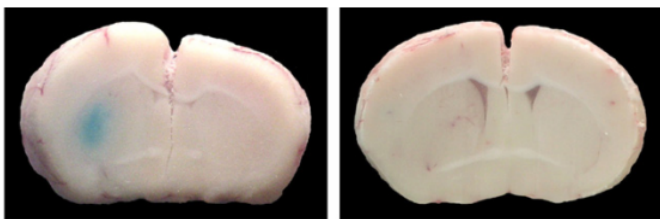
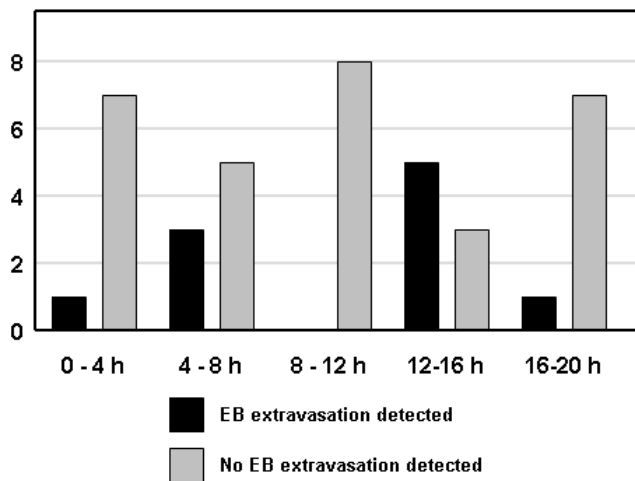


Figure 1: Biphasic opening in the BBB.

Evans blue (EB) was injected at different time points after reperfusion and allowed to circulate for 4 h. Brains were inspected for EB extravasation at defined reference regions. At 4–8 h after reperfusion, EB extravasation was apparent in a coronal brain slice approximately interaural 3.94 mm (A, left) while no EB extravasation was seen at 8–12 h after reperfusion (A, right). Edema was visible in the ischemic hemisphere of both brains.

(B)



. Eight animals were investigated per time point (B). An opening in the BBB was not apparent in all animals at the time points selected. The extravasation of EB seems to follow a biphasic pattern with impairment at 4–8 and 12–16 h after reperfusion. (Klohs et al., 2009)

2.3.2 Biphasic impairment of the BBB detected non-invasively and ex-vivo with NIRF:

In the second part of the study, NIRF-BSA was injected intravenously in MCAo mice at 4, 8 or 12 hours after reperfusion ($n = 4, 5$ and 5 , respectively). EB was injected 10 minutes after NIRF-BSA injection. Non-invasive and ex-vivo NIRF imaging was performed at 8, 12, or 16 hours after reperfusion, i.e., 4 hours after compound injection (Fig. 2). Higher fluorescence intensities over the ischemic hemisphere compared to the contralateral side were detected non-invasively in MCAo mice at 4–8 hours and 8–16 hours after reperfusion (Fig. 2A). NIRF imaging of the brain after removal from the skull revealed intense fluorescence over the ischemic MCA territory, suggesting extravasation of NIRF-BSA (Fig. 2C). No differences between the brain hemispheres were seen on non-invasive and ex-vivo NIRF images of MCAo mice examined at 8–12 hours after reperfusion, suggesting that no NIRF-BSA extravasation had occurred (Fig. 2B and D). ROI analysis of non-invasive NIRF images reveals BBB impairment at 4–8 and 12–16 hours after reperfusion (Fig. 2E). In two mice, no differences were seen between the hemispheres on non-invasive NIRF images, but a difference was noticed when the brains were acquired with ex-vivo NIRF imaging (Table 4). Brains were cut into 1mm thick sections for subsequent inspection of EB extravasation. EB extravasation was detected in brain slices at 4–8 and 12–16 hours after reperfusion, while no EB extravasation was observed at 8–12 hours after reperfusion, confirming biphasic BBB impairment. In those mice in which intense fluorescence over the ischemic hemisphere of the brain was observed with ex-vivo NIRF imaging, extravasation of EB was seen upon inspection of the brain slices. Conversely, in mice where no differences between hemispheres were seen on ex-vivo NIRF images, no EB extravasation was detected in brain slices.

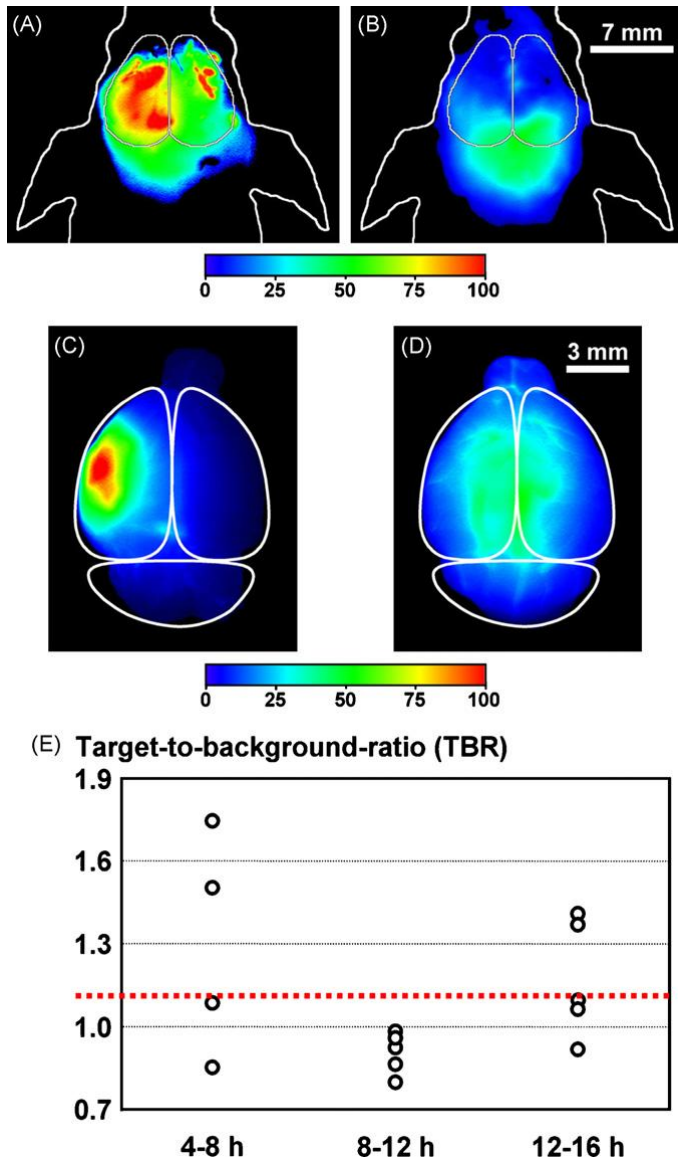


Figure 2: Opening of the BBB imaged with NIRF: Non-invasive NIRF (A and B) and the corresponding ex-vivo NIRF (C and D) images of MCAo mice injected with NIRF-BSA. NIRF-BSA was injected at different time points after reperfusion. NIRF was performed 4 h after compound injection. Higher fluorescence intensities over the ischemic hemisphere compared to the contralateral hemisphere were detected in MCAo mice at 4–8 h after reperfusion (A and C), indicative of an impaired BBB. No differences between the hemispheres were seen in MCAo mice at 8–12 h after reperfusion, showing no extravasation of NIRF-BSA (B and D). TBR calculated from ROI analysis (E). The dotted line indicates the lowest TBR, at which differences between the ischemic and non-ischemic hemisphere can be observed. (Klohs et al., 2009)

Table 4: BBB impairment measured with NIRF-BSA and EB

. Yes = presence, No = absence of marker

4-8 hours				8-12 hours				12-16 hours			
Mouse	NIRF	NIRF	EB	Mouse	NIRF	NIRF	EB	Mouse	NIRF	NIRF	EB
	in	ex-			in	ex-			in	ex-	
	vivo	vivo			vivo	vivo			vivo	vivo	
1	Yes	Yes	Yes	5	No	No	No	10	No	No	No
2	No	No	No	6	No	No	No	11	Yes	Yes	Yes
3	No	Yes	Yes	7	No	No	No	12	Yes	Yes	Yes
4	Yes	Yes	Yes	8	No	No	No	13	No	Yes	Yes
				9	No	No	No	14	No	No	No

2.3.3. NIRF imaging shows biphasic BBB impairment while contrast-enhanced MRI shows invariable BBB impairment

In the third part of the study, MCAo mice were co-injected with NIRF-BSA and Gd-DTPA at different time points after reperfusion. NIRF imaging and MRI were performed at 8, 12 or 16 hours after reperfusion. Due to differences in the plasma half-life of the two probes, different circulation times were chosen. NIRF imaging was performed 4 hours after NIRF-BSA injection. MRI was performed immediately after Gd-DTPA injection. Higher fluorescence intensities over the ischemic hemisphere compared to the contralateral side were seen on non-invasive images of MCAo mice at 4–8 and 12–16 hours after reperfusion. No differences between hemispheres were seen on non-invasive NIRF images of mice examined at 8–12 hours after reperfusion. Subtracting pre-contrast T1-weighted from post-contrast T1-weighted images yielded contrast-enhancement in brains of MCAo mice at 8, 12 and 16 hours after reperfusion. ROI analysis of post-contrast T1-weighted images revealed contrast-enhancement at all time points. While NIRF imaging confirmed the biphasic impairment of the BBB at 8 and 16 hours after reperfusion, T1-weighted images showed contrast-enhancement at all time points (Table 5).

Relationship between the Blood-Brain Barrier and Cerebral Ischemia

Table 5: BBB impairment measured with NIRF-BSA and EB.

Yes = presence, No = absence of marker

4-8 hours			8-12 hours			12-16 hours		
Mouse	NIRF	MRI	Mouse	NIRF	MRI	Mouse	NIRF	MRI
1	Yes	Yes	5	No	Yes	8	Yes	Yes
2	Yes	Yes	6	No	Yes	9	No	Yes
3	Yes	Yes	7	No	Yes	10	Yes	Yes
4	No	Yes				11	No	Yes

3. Si-RNA induced pre-emptive opening of the BBB combined with MCAo.

3.1. Introduction:

Tight junctions (TJs) associated with the BBB are composed of a complex of intracellular and transmembrane proteins that include various claudins, occludin, JAMs, and ZOs along with several other molecules. While many of these proteins can be found in endothelial and epithelial cells throughout the body, claudin-5 is considered to be endothelial-cell-specific and to be of primary importance to TJs of the CNS (Jiao et al., 2011).

The BBB of claudin 5^{-/-} mice has been shown to be compromised. While the BBB was still able to form in these animals and did remain intact and impervious to larger molecules it was unable to prevent the passage of molecules 800 Da or smaller (Nitta et al., 2003). Drugs that increase claudin-5 expression have been reported to increase transendothelial electrical resistance and decrease BBB permeability (Jiao et al., 2011). It has also been shown that VEGF disrupts the expression of Claudin-5 and that a VEGF mediated disruption of the BBB correlates with the down-regulation of Claudin-5 in endothelial cells (Argaw et al., 2009). When mice are exposed to hypoxic conditions they exhibited decreased claudin-5 expression. This decreased expression resulted in a phenotype similar to that seen in claudin-5-deficient mice; there was a disruption of the blood-retinal barrier (BRB) which subsequently allowed for the passage of small molecules into the tissue (Koto et al., 2007). Claudin-5 may take part in the formation of paracellular channels that allow for selective ion permeability (Anderson et al., 2001). Thus a mechanism may be activated that allows for increases in size-selective paracellular diffusion across the BBB of claudin-5 knockout mouse.

Building upon work of several other groups, Campbell et al.; (2008) used systemic hydrodynamic (high-volume) delivery of claudin-5 siRNA, delivered via the tail vein, to endothelial cells within the brain in order to suppress claudin-5 gene expression at the BBB (Herweijer et al., 2007; Furuse et al., 1998; Lewis et al., 2002; McCaffrey et al., 2002; Kiang et al., 2005). According to Campbell et al.,(2008) there was a suppression of claudin-5 protein beginning at 24 hours and peaking at 48 hours post-injection with levels of expression returning to normal at 72 hours to 1 week later. During the time frame of increased BBB permeability they found that molecules up to 742 Da were able

to cross the barrier. In addition, this technique showed no effect on the expression of levels of the TJ-associated proteins claudin-1 and occludin, both of which have been implicated in mediating changes in the paracellular permeability of TJs.

After cerebral ischemia, a breakdown of the TJs or a disruption in their expression profile results in an opening in the BBB. The degree and duration of the opening correlate with the severity of the stroke. It is not fully understood if the severity of the stroke leads to an opening in the BBB or if an opening in the BBB gives rise to a more severe stroke and larger final lesion volume. According to our previous experiment the BBB opens within 4 to 8 hours after a stroke, closes, and then opens again 12 to 16 hours later. It was decided to try and preemptively open the BBB by hydrodynamic delivery of siRNA before initiating the stroke in order to determine what if any effect on final lesion volume this might have.

3.2. Materials and methods:

3.2.1. Animal Protocol:

Animal experiments were performed according to institutional and international guidelines. All surgical procedures were approved by the local authorities (G0229/05 LaGeSo, Berlin, Germany). Twenty-two male C57Bl6/N mice (Bundesinstitut fuer Risikoforschung, Berlin, Germany) weighing 18–24 grams were housed under standard conditions.

3.2.2. Focal cerebral ischemia:

MCAo was performed as previously described in this paper (Endres et al., 1999; Endres et al., 2000).

3.2.3. Experimental design and hydrodynamic delivery of siRNA:

The animals were divided into two groups (n=11 per group) and rapid high-pressure, high-volume tail vein injections were carried out as previously described (Kiang et al., 2006). Briefly, mice were anesthetized in a chamber with isoflurane (2% isoflurane in a

2:1 mixture of nitrous oxide and oxygen), and then restrained inside a 60 mL volume plastic tube. The protruding tail was warmed for 5 minutes prior to injection under a 60 W lamp and the tail vein clearly visualised by illumination from below. Twenty micrograms of Cld5-targeting siRNA (Cld5-siRNA), or nontargeting siRNA (NT) diluted in PBS (to a volume in mL of 10% of the body weight in grams of the animal) was injected into the tail vein at a rate of 1 mL/s using a 26-gauge (26G 3/8) needle.

Table 6: Animals used in experiment 2:

siRNA inj.	Cld5 siRNA	Non-targeting siRNA
Number of mice	n=11	n=11

Forty-eight hours after receiving the injection of NT/Cld5-siRNA, each animal received a tail vein injection of the imaging agent Gd-DTPA (200 µl of 1:3 dilution of magnevist) and then underwent contrast-enhanced T1 weighted MRI in order to determine if the BBB had been successfully opened. If the BBB had not been opened the animal was to be excluded from the rest of the experiment. Immediately after undergoing the contrast enhanced MRI each animal underwent 1 hour MCAo. Twenty-four hours after reperfusion mice were sacrificed under deep anesthesia and the brain was collected. The brains were then sliced and stained with hematoxylin and the lesion volume was quantified using computer-assisted volumetry.

3.2.4. T1-weighted magnetic resonance imaging:

MRI was performed on a dedicated animal scanner (7T Bruker, Pharmascan 70/16 AS, Bruker Biospin, Ettlingen, Germany). Mice were imaged as previously described.

3.2.5. Statistical Analysis:

Analyses between the lesion volume of the NT and Cld5-siRNA groups was performed using the two-tailed t-test. Statistical analysis was performed using Sigma Stat software.

3.3 Results:

The effect of preemptively opening the BBB with siRNA on final lesion development was explored after 1 hour MCAo in mice. Two groups of animals (n=11 per group) received rapid high-pressure, high-volume tail vein injections of either Cld5-siRNA or NT-siRNA. Forty-eight hours later each animal underwent contrast-enhanced T1 weighted MRI in order to determine if the BBB had been successfully opened. In Cld5-siRNA group, if the BBB had not been opened the animal was to be excluded from the rest of the experiment. All animals in the NT-siRNA group showed no signs of BBB opening. Conversely all animals in the Cld5-siRNA group showed an opening in the BBB (Fig 3). Each animal then underwent 1 hour MCAo and was sacrificed 24 hours later in order to ascertain any difference in lesion volume between the two groups. According to the results, there was no statistically significant difference between the Cld5-siRNA and NT-siRNA groups (Fig 4).

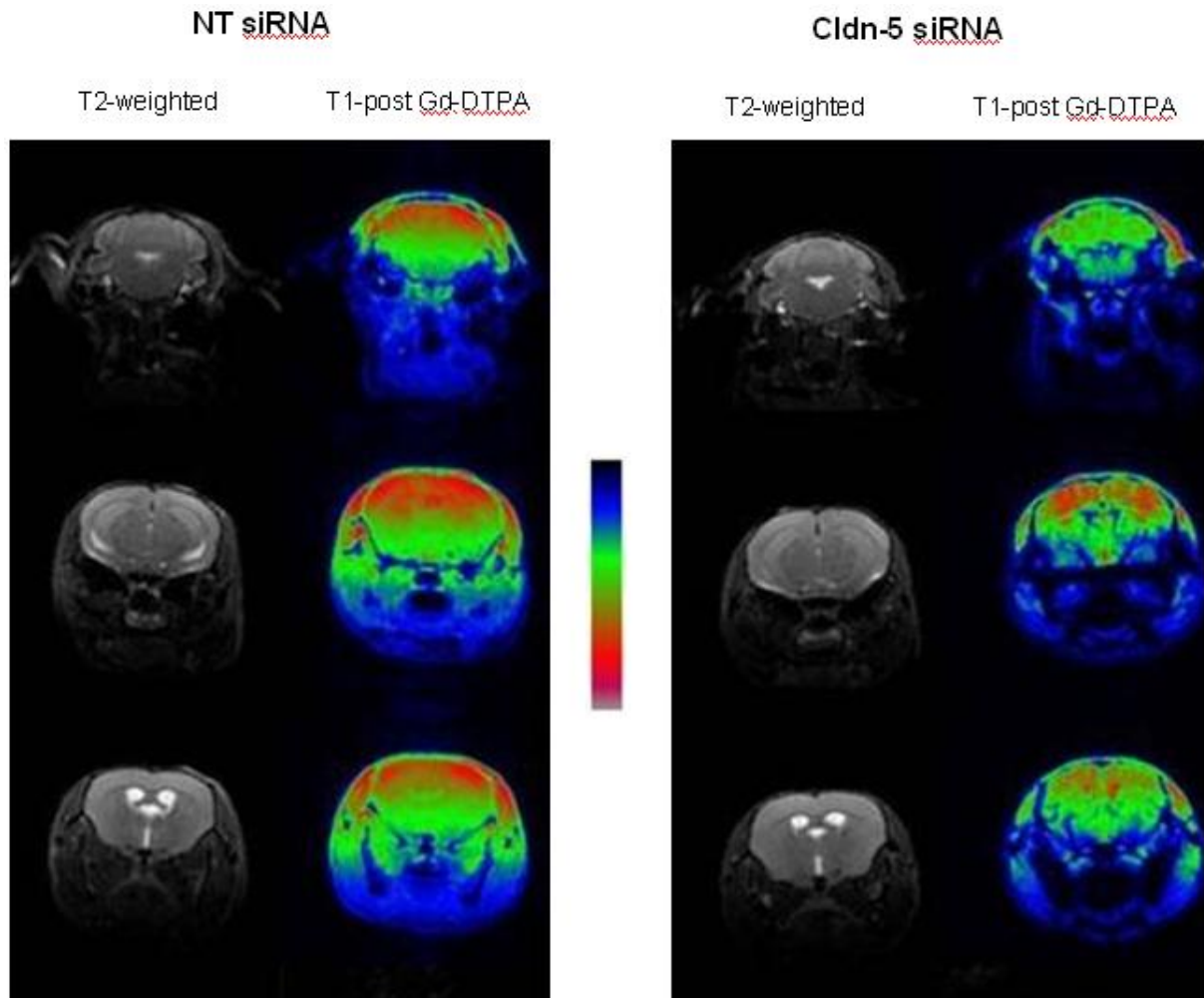


Figure 3: T1 MRI after high pressure injection of Cldn-5 and NT siRNA. NT or Cldn-5 siRNA was injected 48 hours before magnetic resonance imaging. In the image above, the serial brain sections of two animals that received the respective treatments are shown. In the scale above, blue represents a higher concentration of Gd-DTPA and red a lower concentration. In the NT image on the left there is lower concentration of imaging agent in the serial sections of the brain as compared to the Cldn-5 group on the right, thus indicating that the BBB has remained intact in the NT group as opposed to the Cldn-5 group.

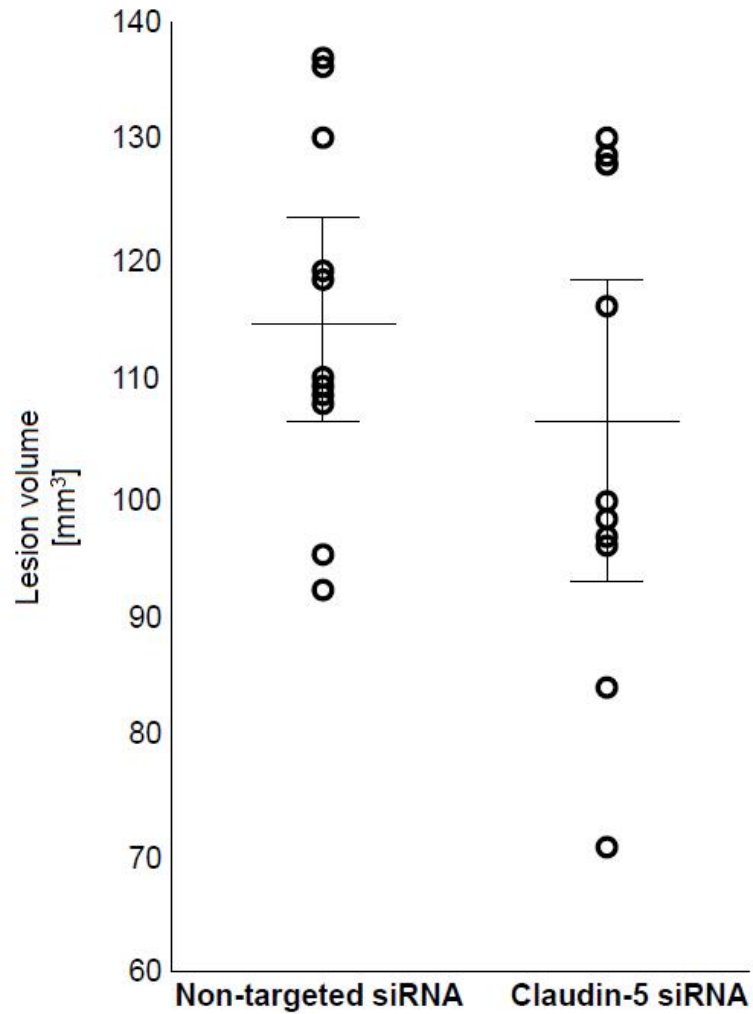


Figure 4: Final lesion volume after MCAo in Cldn-5 and NT siRNA groups. The lesion volume in the Cldn-5 group was not significantly different compared to the NT group. There was a general trend towards a smaller lesion volume in the Cldn-5 group. (two-tailed t-test, $p=0.123$. $n=11$ per group)

4. Transcranial magnetic stimulation induced opening of the BBB combined with MCAo:

4.1 Introduction:

Previous groups have attempted to use transcranial magnetic stimulation (TMS) to open the BBB without success (Ravnborg et al., 1990; Li et al., 2003). Nevertheless the technique has been further modified and new equipment has been developed by Brainsway in Jerusalem, Israel in collaboration with Dr. Alon Friedman in the Department of Physiology and Neurobiology at the Ben-Gurion University of the Negev in Beer Sheva, Israel. While the TMS system developed by Brainsway is able to open the BBB the exact mechanism underlying the mode of action of TMS is currently unknown.

Here we pre-emptively open the BBB with TMS before inducing cerebral ischemia. The objective was to determine what if any effect this opening might have on final lesion volume.

4.2. Materials and methods:

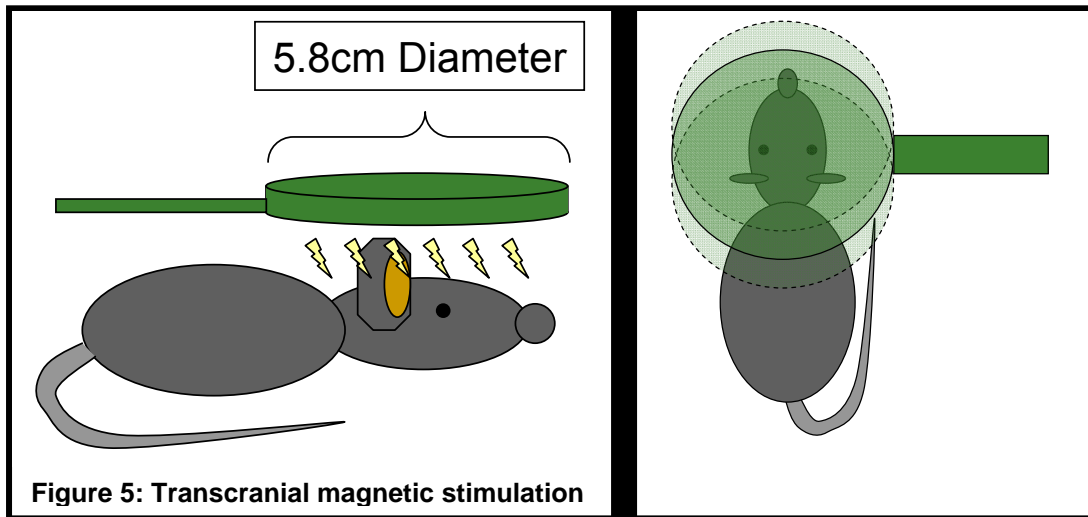
4.2.1. Animal protocol:

Animal experiments were performed according to institutional and international guidelines. All surgical procedures were approved by the local authorities (G 0130/10 LaGeSo, Berlin, Germany). 53 male C57Bl6/N mice (Bundesinstitut fuer Risikoforschung, Berlin, Germany) weighing 18–24 grams were housed under standard conditions.

4.2.2. Focal cerebral ischemia:

MCAo was performed as previously described (Endres et al., 1999; Endres et al., 2000).

4.2.3. Transcranial Magnetic Stimulation:



Mice were anesthetized with an intraperitoneal injection of ketamin (100.0 mg/kg of animal) in combination with xylazin (10 mg/kg of animal). The keratin/xylazin injection was created by mixing 5 mL of Ketavet (100 mg/mL), 5 mL of Rompun (0.02 mg/mL), and 25 mL of saline (0.9%). The scalp was subsequently shaved and the animal fitted in the stereotactic frame. A circular coil (Brainsway, Israel) attached to a magnetic stimulator (Magstim, England) was positioned directly over the center of the skull. The animal's skull was stimulated with 2 sets of 30 pulses at 100% intensity (1,800 volts) or at 1% intensity for controls. After the first two sets of pulses, the coil was moved 1cm towards the anterior end of the animal and stimulated with 2 additional sets of 30 pulses at 100% intensity (1% for controls). The coil was then moved for the third time 1 cm from the middle of the skull towards the posterior end of the animal for the final 2 sets of 30 pulses. Each pulse lasted 1 second and was followed by one second of rest. After each set, the coil was placed in ice and allowed to cool. After a total of 6 sets of 30 pulses, the animal was returned to the heating box and allowed to recover for two hours before being returned to its cage where the animal was given free access to food and water

4.2.4. Experimental design and administration of TMS:

In the first part of the study, the intensity of TMS required to induce and opening in the BBB was investigated using EB extravasation. Mice were divided into four treatment groups (n=3 per group). The first group was stimulated at 60% intensity, the second group at 70% intensity, the third group at 80% intensity and the fourth and final group at 100% intensity. Immediately after TMS the animals were given a 200 μ L tail vein injection of 2% EB. The EB was allowed to circulate for 1 hour before the animal was sacrificed and the brain extracted. The collected brains were sliced in a Zivic brain matrix and then searched for visual signs of Evans blue extravasation with a Zeiss Luma V12 Stereo Microscope.

Table 7: Animals used in experiment 3 – 1st part of study:

TMS Intensity	60%	70%	80%	100%
Mice per group	n=3	n=3	n=3	n=3

In the second part of the study, the duration of the opening of the BBB after TMS was investigated. Eleven animals were divided into four treatment groups (n=2 per group, n=1 for control). Each animal received TMS at 100% intensity. EB was injected intravenously and allowed to circulate for 1 hour. The first group was injected with EB at a time-point immediately after TMS (t=0, n=4), the second group was injected with EB at a time-point 1 hour after stimulation (t=1, n=4), and the third group was injected with EB at a time-point 4 hours after stimulation (t=4, n=4). The 4 hour time point was based on our previous work where it was determined that the first opening in the BBB after MCAo occurred at 4 hours after reperfusion. The control received no TMS but did receive an equivalent amount of EB that was allowed to circulate for 1 hour before sacrifice (n=1). Each animal was sacrificed, perfused, and the brain removed and weighed. The brains were then subdivided into two groups.

In the first group, two brains from each time point plus the one control were separately homogenized in 2 mL of 2% trichloroacetic acid and then centrifuged at 10,000 rpm for 20 minutes. The supernatant was collected and diluted four-fold with ethanol. An aliquot of the resulting solution was again diluted three fold with solvent (50% trichloroacetic acid/ethanol 1:3). Five external standards were created for quantification. 100 to 500 ng

of EB was dissolved in solvent (50% trichloroacetic acid/ethanol 1:3). The standards and the sample were measured at an excitation wavelength of 620 nm and emission wavelength of 680 nm.

In the second group, brains that received injections of EB at a time-point of 1 hour after TMS and 4 hours after TMS (n=2 per group) were snap frozen and sliced on a sliding microtome. The brains were subsequently examined for signs of EB extravasation and stained for signs of apoptosis.

Table 8: Animals used in experiment 3 – 2nd part of study:

Time-point	Control	t=0	t=1	t=4
EB quantification	n=1	N=2	n=2	n=2
Visual detection of EB & Apoptosis		N=2	n=2	n=2

In the third part of the study, the effect of a pre-emptive opening in the BBB by 100% intensity TMS on lesion volume after cerebral ischemia was investigated. Thirty mice were divided into two groups (n=15). The first group received 100% intensity TMS. The second group served as the control and only received stimulation at 1% intensity. One hour after TMS the animal underwent MCAo. The animals were reperfused 45 minutes later. The 45 minute time-point was based on previous work that showed that 1 hour MCAo when combined with 100% TMS lead to an unacceptably high mortality rate. Forty-eight hours after reperfusion each animal was perfused with 4% PFA, and snap frozen. The frozen brains were sliced and stained with hematoxylin and the lesion volume was measured by computer-assisted volumetry.

Table 9: Animals used in experiment 3 – 3rd part of study:

TMS Intensity	100%	1%
Number of Mice	N=15	n=15

4.2.5. Statistical Analysis:

Analysis of lesion volume was performed using the two-tailed t-test. Statistical analysis was performed using Graphpad Prism software.

4.3. Results:

4.3.1. 100% Intensity TMS required to open BBB in mice::

The intensity of TMS required to open the BBB in mice was explored in the first part of the study. The brains that were stimulated at 60%, 70%, and 80% intensity showed no signs of EB extravasation on the cortex or when viewed under the stereo-microscope as serial slices. However the mice that received 100% TMS did demonstrate signs of EB extravasation on the cortex and within the serially sliced brain sections.

4.3.2 Brain opens immediately after TMS and remains open for up to 4 hours and shows no sign of apoptosis:

In the second part of the study, the duration of the opening of the BBB after TMS was investigated. Mice received TMS at 100% intensity and EB was injected immediately after TMS, 1 hour after stimulation, and 4 hours after stimulation. The 4 hour time point was based on our previous work where it was determined that the first opening in the BBB after MCAo occurred around 4 hours after reperfusion. The control received no TMS but did receive an equivalent amount of EB. The brains were then divided into two groups. In the first group, tissue was homogenized and the EB extracted and the concentration analyzed in a fluorometer and plotted. Based on these combined data it was assumed that TMS was able to open the BBB within 1-hour of TMS and that the BBB remained open for at least 4 hours after stimulation (Fig 7). In the second group, brains were snap frozen and serially sliced. Extravasation of EB was macroscopically detected as diffuse blue tissue coloration. Color intensity and spatial distribution of EB extravasation was highly variable between individual animals. The brains were subsequently stained for signs of apoptosis, and no sign of apoptosis were detected (Fig 6)

4.3.3. 100% Intensity TMS has no effect on final lesion volume:

In the third part of the study, the effect of preemptively opening the BBB with TMS on final lesion development in mice after 45 minute MCAO was investigated. The first group (n=15) received 100% intensity TMS, and the second group (n=15) served as the control and only received stimulation at 1% intensity. The animals were reperfused 45 minutes later (the 45 minute time-point was based on previous work that showed that 1 hour MCAo when combined with 100% TMS lead to an unacceptably high mortality rate). Forty-eight hours after reperfusion each animal was sacrificed in order to ascertain any difference in lesion volume between the two groups. According to the results, there was no statistically significant difference between the 100% TMS group and the 1% TMS control (Fig 8)

Evans Blue Inj. Immediately after TMS

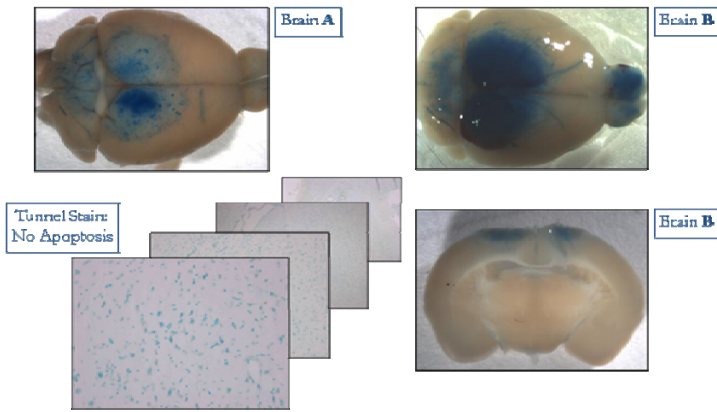
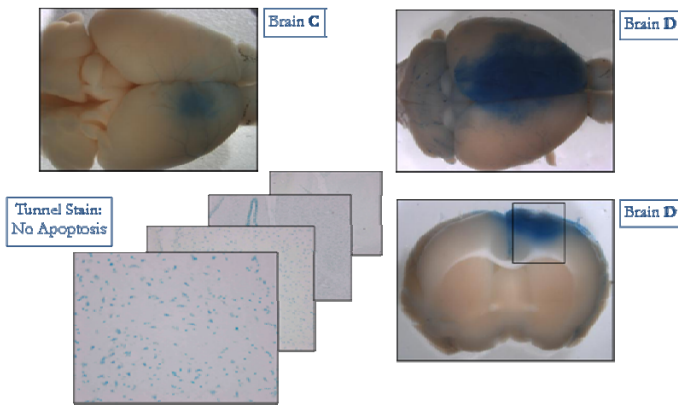


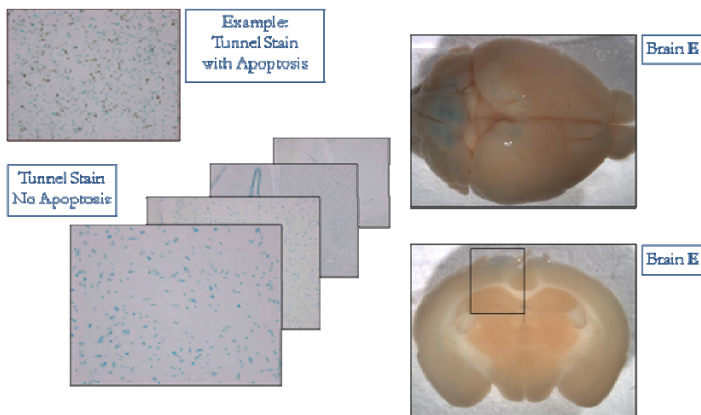
Figure 6: Opening of the BBB after transcranial magnetic stimulation.

Animals received TMS (100% intensity, 1,800V) and were injected with EB immediately after (n=2), 1 hour after stimulation (n=2) or 4 hours after stimulation (n=2). The control did not receive TMS but did receive EB. Brains were removed and homogenized, and EB extravasation was quantified.

Evans Blue Inj. 1hour after TMS



Evans Blue Inj. 4 hours after TMS



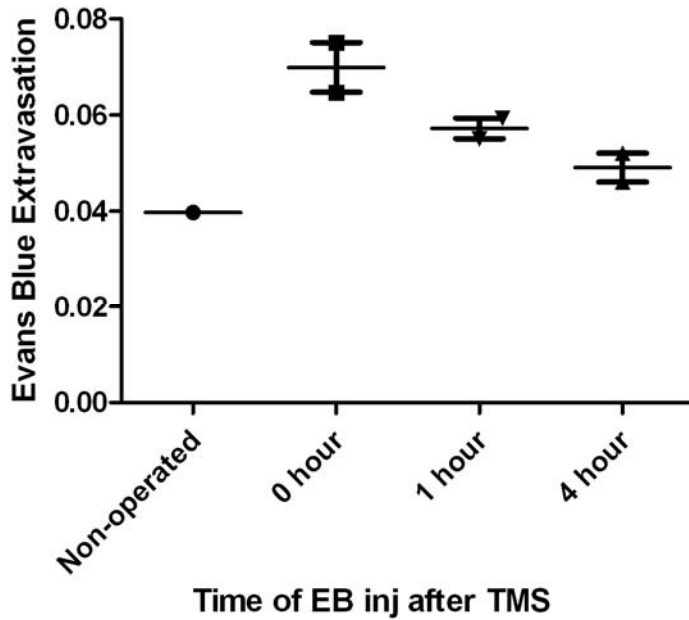


Figure 7: Opening of BBB after TMS:

Animals received TMS (100% intensity, 1,800V) and were injected with EB immediately after, 1 hour after stimulation, or 4 hours after stimulation.

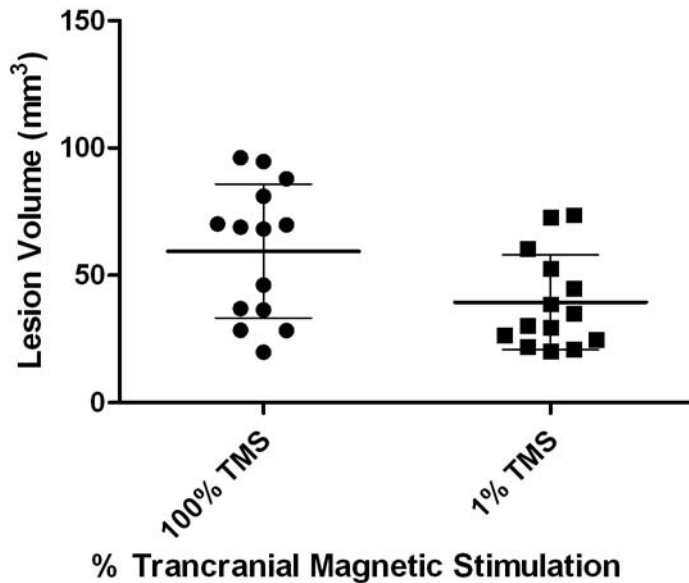


Figure 8: Lesion volume after MCAo in animals receiving TMS.

Animals were divided into two groups: the first received TMS at 100% (n=14) capacity and the second at 1% capacity (n=14). Immediately after TMS, 45 minute MCAo was performed. 48 hours later animals were sacrificed and the lesion volume analyzed. There was no significant difference between the two groups. There was a general trend towards a larger lesion volume in the 100% group.

5. Hypertonic arabinose induced opening of the BBB combined with MCAo:

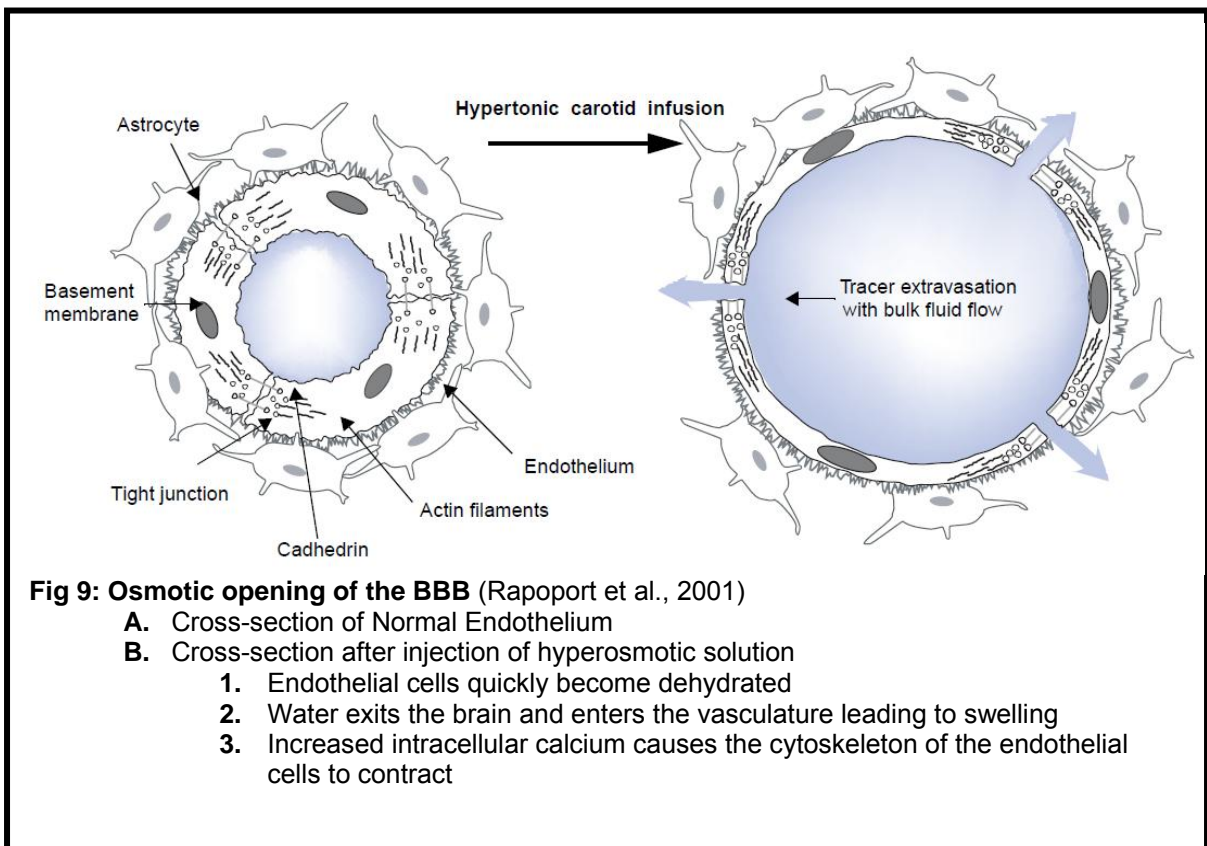
5.1 Introduction:

Hypertonic mannitol or arabinose infusion have both been used in a variety of animals including mice, rats, rhesus monkeys and baboons in order to open the BBB to a plethora of intravascular substances including plasma proteins, neutralising antibodies to measles virus, monoclonal antibodies to melanoma monoclonal immuno-conjugates with anticancer drugs, noradrenaline and albumin, lysosomal enzymes, methotrexate bilirubin-albumin complex, human interferon alpha, iron oxide nanoparticles, recombinant adenovirus vectors and herpes simplex virus, EDTA, gadolinium contrast agents, carboplatin boronphenylalanine, and glial cell line derived neurotrophic factor (Rapoport, 2001). According to the analysis of water composition and volumes of the intracranial compartments in dogs and PET and MRI measurements in animals and humans, the acute exposure of the brain to hypertonic arabinose or mannitol solutions leads to transient brain edema, equivalent to a 1 to 1.5% increase in brain water which eventually resumes normal levels with no tissue damage (Rapoport, 2001; Rapoport, 2000).

Osmotic opening of the BBB by intracarotid infusion of a hypertonic arabinose or mannitol solution works via one of two theoretical mechanisms. In the first mechanism, vessels dilate and the cerebrovascular endothelial cells shrink (Rapoport, 2000) resulting in an increased diffusion of intravascular substances (10-fold for small molecules) and bulk fluid flow across the tight junctions (Rapoport, 2000). These processes may be facilitated by calcium-mediated contraction of the endothelial cytoskeleton which results in a widening of the interendothelial tight junctions to an estimated radius of 200 Å (Rapoport et al., 2000). Other studies have failed to observe separation of tight junctions following osmotic disruption of the BBB (Farrell et al., 1984; Hansson et al., 1980; Houthoff et al., 1982; Nagy et al., 1984; Westergaard et al., 1977). Instead, they have observed an increase in the number of pinocytotic vesicles in the cerebrovascular endothelium and even the fusion of vesicles to form transendothelial channels (Farrell et al., 1984; Hansson et al., 1980; Houthoff et al., 1982; Westergaard et al., 1977).

Regardless of the route of passage, the increase in blood brain barrier permeability is largely reversed within 10 to 20 minutes. This rapid recovery has been demonstrated in

rats as well as in monkeys using positron emission tomography (PET), and the course of recovery has been demonstrated using PET with [68Ga] EDTA (ethylenediaminetetracetic acid) (Rapoport, 2000). Reversibility was confirmed in baboons and in humans, using PET with 82Rb (Rapoport, 2000). In order to follow up on the two previous experiments involving opening the BBB with TMS and siRNA, the administration of hypertonic arabinose was chosen. Despite the uncertainty behind the mechanism underlying an osmotic opening in the BBB, the technique looks promising. It has been used in a plethora of animal models with much success, it is benign to local brain tissue, and the effects of the opening are quickly reversed. Here we investigated the effect of pre-emptively opening the BBB with hypertonic arabinose before inducing cerebral ischemia in order to determine what if any effect this opening might have on final lesion volume.



5.2 Materials and methods:

5.2.1 Animal protocol

Animal experiments were performed according to institutional and international guidelines. All surgical procedures were approved by the local authorities (G 0130/10 LaGeSo, Berlin, Germany). 43 male C57Bl6/N mice (Bundesinstitut fuer Risikoforschung, Berlin, Germany) weighing 18–24 grams were housed under standard conditions.

5.2.2 Focal cerebral ischemia

MCAo was performed as previously described (Endres et al., 1999; Endres et al., 2000).

5.2.3 Experimental design and administration of hyperosmotic arabinose:

In the first part of the study, the ability of a carotid infusion of hypertonic arabinose to open the BBB when compared to saline was investigated with NIRF imaging. Mice were divided into two groups (n=3). Each animal was given an intravenous injection of NIRF-BSA. Surgery was then performed and either 300 μ L of hyperosmotic 2.0 M arabinose or 300 μ L of 0.9% saline was injected into the carotid artery. The conjugate was allowed to circulate for ten minutes before the animal was sacrificed. The brain was removed and imaged in the planar NIRF imaging system. The brain was then sliced in a Zivic brain matrix and again imaged with the NIRF system.

Table 10: Animals used in experiment 4 – 1st part of study:

Carotid Injection	2.0 M arabinose	0.9% saline
Number of Animals	N=3	n=3

In the second part of the study, the duration of the opening of the BBB after a carotid infusion of hypertonic arabinose was investigated. Mice were divided into three groups (n=3 per group). Each animal received an injection of 300 μ L of 2.0 M arabinose into the carotid artery. The NIRF-BSA conjugate was then injected via the tail vein immediately after, 10 minutes, or 20 minutes after the arabinose injection. In each case, the conjugate was allowed to circulate for 10 minutes before the animal was sacrificed. The

brain was removed and imaged in the planar NIRF imaging system. It was then sliced in a Zivic brain matrix and again imaged with the NIRF system.

Table 11: Animals used in experiment 4 – 2nd part of study:

Time-point of conjugate inj.	t=0 min	t=10 min	t=20 min
Number of animals	n=3	n=3	n=3

In the third part of the study, our ability to non-invasively image the opening of the BBB with MRI was investigated. The animals (n=2) received an intravenous injection of Gadofluorine-M (0.1mmol/kg body weight). Immediately afterwards, surgery was performed and 300 µL of hyperosmotic 2.0 M arabinose was injected into the carotid. The animal was then serially scanned in the MRI over the course of two hours (T1 scan approximately every seven to ten minutes) in order to observe the extravasation of the arabinose.

In the fourth part of the study, the effect of opening the BBB with hyperosmotic arabinose on cerebral ischemia was investigated. Mice were divided into two groups (n=13). Before surgery each animal was anesthetized with ketamin/xylazin and received an intravenous injection of 0.1 mM Gadofluorine-M diluted in 300 µL of 0.9 % saline. After the intravenous injection, each animal was operated and 300 µL of hyperosmotic 2.0 M arabinose or 0.9% saline was injected into the carotid. Immediately after the carotid injection 45 minute MCAo was performed. The 45 minute time-point was based on previous work that showed that 1 hour MCAo when combined with a carotid injection of arabinose lead to an unacceptably high mortality rate.

Table 12: Animals used in experiment 4 – 4th part of study:

Carotid Injection	2.0 M arabinose	0.9% saline
Number of animals	n=13	n=13

Approximately 1 hour after occluding the middle cerebral artery (approximately 15 minutes after reperfusion) each animal underwent contrast-enhanced T1 weighted MRI in order to determine if the Gadofluorine-M had extravasated into the brain tissue - a sign that the BBB had successfully been opened or that it had remained closed. Twenty-

four hours after reperfusion the mice underwent contrast-enhanced T1-weighted MRI in order to determine the final lesion volume resulting from the MCAo.

5.2.4 T1-weighted MRI and NIRF:

NIRF imaging and T-1 weighted MRI were performed as previously described in this paper.

5.2.5 Statistical Analysis:

Analysis of lesion volume was performed using the two-tailed t-test. Statistical analysis was performed using Graphpad Prism software.

5.3 Results:

5.3.1 Intracarotid injection of hypertonic arabinose opens the BBB in mice:

In the first part of the study, the ability of a carotid infusion of hypertonic arabinose to open the BBB when compared to saline was investigated with near infrared fluorescence imaging. Animals were divided into two groups with the first group receiving an intracarotid injection of 2.0M arabinose and the second an injection of 0.9% saline. The three animals that received the arabinose injection demonstrated extravasation of the conjugate in the left affected hemisphere. The three animals that received the intracarotid saline injections showed no sign of extravasation of the conjugate. From this we concluded that arabinose was able to open the BBB and that the BBB probably opened immediately or within a few minutes of injection.

5.3.2 Intracarotid injection of arabinose opens the BBB for up to 20 minutes:

In the third part of the study, the duration of the opening in the BBB after an intracarotid injection of arabinose was investigated. Mice were divided into three groups with each group receiving an injection of arabinose. A NIRF albumin conjugate was then injected immediately after, or 10 minutes, or 20 minutes after the arabinose injection. In each case, the conjugate was allowed to circulate for 10 minutes before the animal was

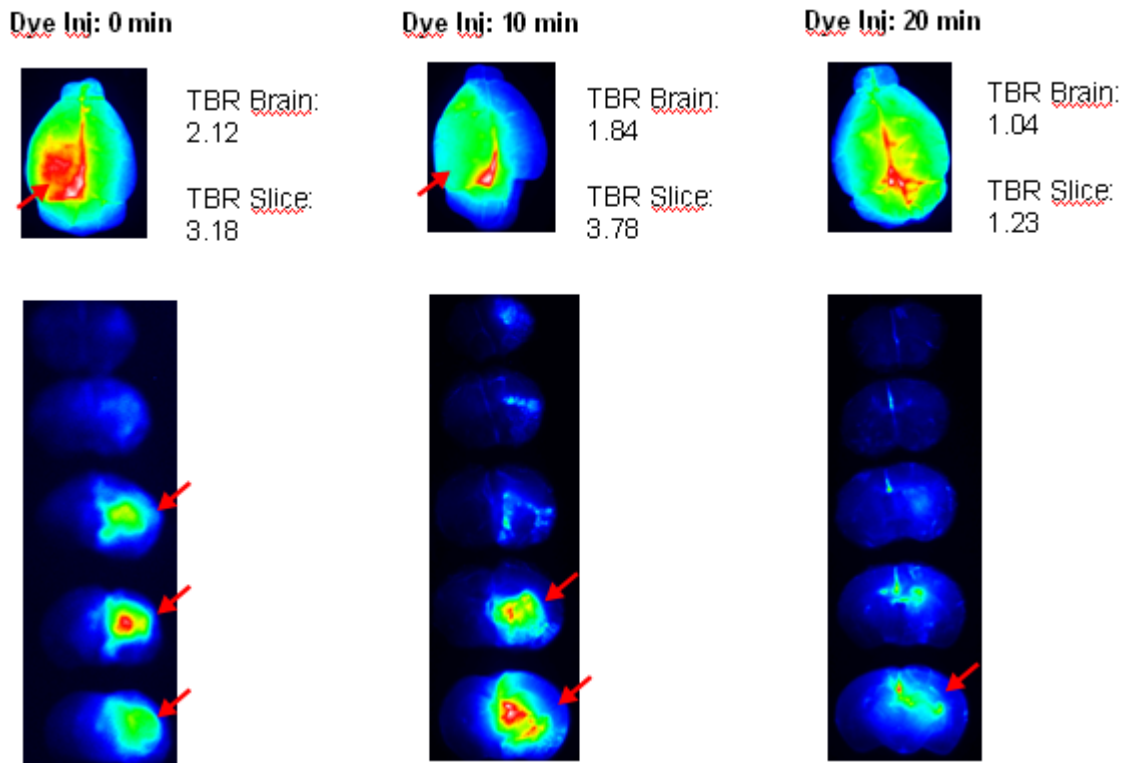


Figure 10: Opening of the BBB after hyperosmotic arabinose injection I. 300 μ L of 2 M arabinose was injected into the carotid artery. A fluorescent imaging agent was injected at immediately after, 10 minutes after or 20 minutes after the arabinose and allowed to circulate for 10 minutes before the animal was sacrificed. The animals were sacrificed and the whole brains imaged with the NIRF imaging system. The brains were then sliced into coronal sections and re-imaged. Extravasation of the agent was apparent at 0min and 10min. There was still some extravasation at the 20min time point.

sacrificed. The brain was removed and imaged in the planar NIRF imaging system. According to the results, intracarotid injection of hyperosmotic arabinose opens the BBB immediately after being injected and the BBB remains open for approximately 20 minutes thereafter (Fig 10).

5.3.3 Opening of the BBB with arabinose can be non-invasively imaged:

In the third part of the experiment, the ability to non-invasively image the opening of the BBB with MRI was investigated. The animal received an injection of Gadofluorine-M, and immediately afterwards arabinose was injected into the carotid. The animal was then serially scanned in the MRI over the course of two hours in order to observe the extravasation of the arabinose (Fig 11). According to our results, the Gadofluorine-M

was seen in the affected hemisphere as soon as the first scan. The signal grew in intensity up to a time point of roughly 1 hour. Since our NIRF experiment demonstrated that the BBB closes after twenty minutes it was likely that the Gadofluorine-M extravasated into the brain during the 20 minute opening, was trapped there after the BBB closed, and continued to passively diffuse during the remaining time period.

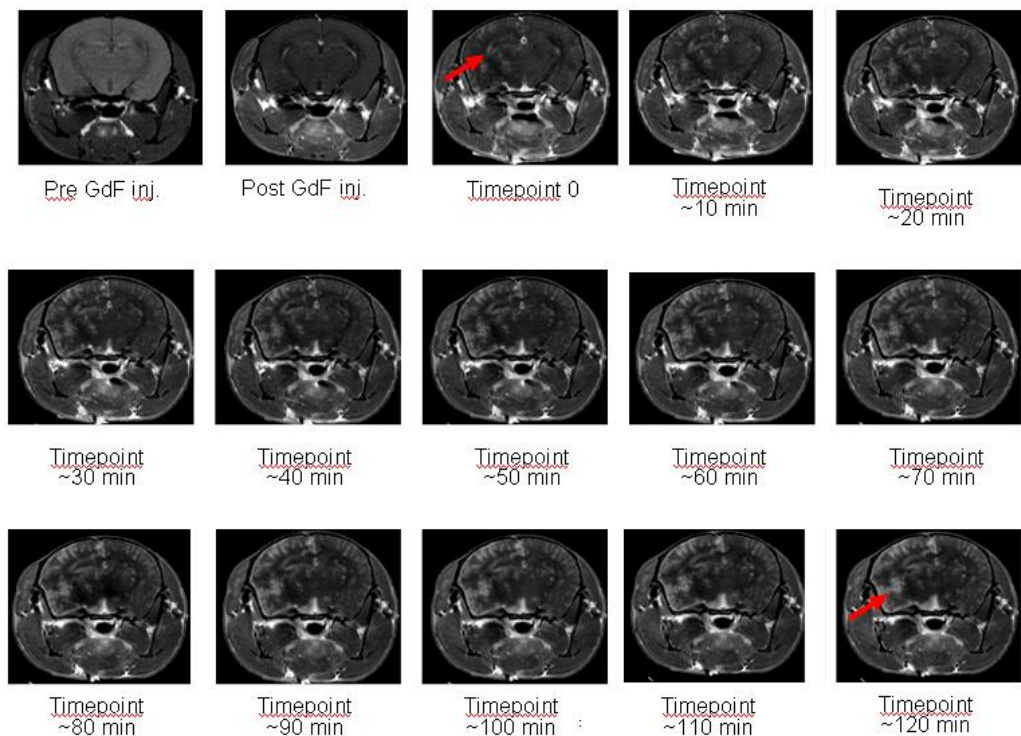


Figure 11: Opening of the BBB after hyperosmotic arabinose injection II. Gadofluorine-M was injected followed by hyperosmotic arabinose into the carotid artery. The animal was placed in MRI scanner and serially scanned over the following two hours. Gadofluorine-M can be seen extravasating into the brain immediately after arbinose injection (time point 0).

5.3.4 Opening the BBB with arabinose leads to a measurable difference in lesion volume after MCAo in mice:

In the fourth part of the study, the effect of opening the BBB with hyperosmotic arabinose on cerebral ischemia was investigated. Mice were divided into two groups; each animal received an intravenous injection of Gadofluorine-M. The first group was injected with hyperosmotic arabinose and the second with saline, and then 45 minute MCAo was performed. The 45 minute time-point was based on previous work that showed that 1 hour MCAo when combined with a carotid injection of arabinose lead to

an unacceptably high mortality rate. 1 hour after MCAo (approximately 15 minutes after reperfusion) each animal underwent MRI to determine if the Gadofluorine-M had extravasated into the brain tissue - a sign that the BBB had successfully been opened or that it had remained closed. All animals included in the final arabinose group showed a successful opening of the BBB. Twenty-four hours after reperfusion each animal was sacrificed in order to ascertain any difference in lesion volume between the two groups. According to the results, pre-emptively opening the BBB with arabinose lead to a significant increase in the size of the final lesion volume as opposed to those animals that were only treated with saline (Fig 13). Furthermore, the final lesion volume correlated with the size of the opening in the BBB that was induced with arabinose (Fig 12).

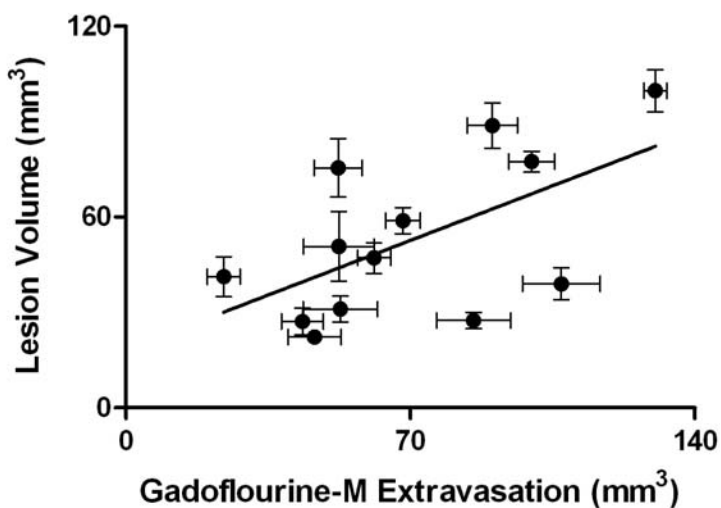


Figure 12: Gadofluorine-M extravasation compared with final lesion volume after 45 min MCAo.

There was a correlation between Gf extravasation and lesion volume in the animals that received arabinose in the carotid artery. Animals that received saline showed no sign of Gf extravasation. (two tailed correlation: $p= 0.036$, $r =0.5842$)

two tailed, correlation: $p=0.036$

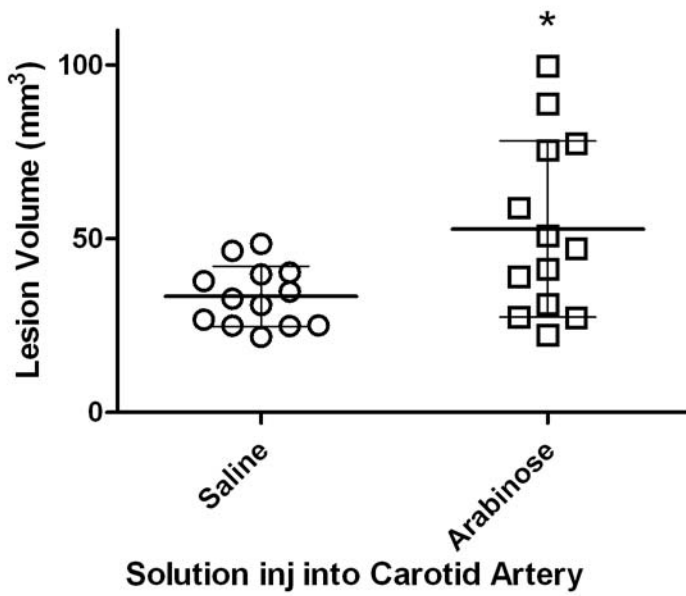


Figure 13: Lesion volume of arabinose vs. saline mice. Mice were divided into two groups and received either 300µL of 2M arabinose or 300 µL of 0.9% NaCl. Immediately after 45min MCAo was performed. When the final lesion volume was measured the mice that received the arabinose had a larger lesion volume than those receiving saline. (two-tailed unpaired t-test: p=0.0158)

two-tailed, unpaired t-test: p = 0.0158

6. Closing the BBB with PEDF after cerebral ischemia:

6.1 Introduction:

During an ischemic event, hypoxic conditions develop in the infarcted tissues which in turn result in the expression of Hypoxia Inducible Factor 1 and 2 (HIF-1 and HIF-2) (Marti et al, 2000, Hermann et al 2009). These two factors drive the expression VEGF which is up regulated in the ischemic periphery within 1 to 3 hours after a stroke and reaches its peak expression 3 to 12 hours later (Marti et al, 2000, Hayashi et al, 1997, Plate et al, 1997). VEGF has many knock-on effects. For example it induces angiogenesis (Marti et al, 2000, Hermann et al 2009; Zhang et al, 2000) and it up regulates glucose transport into the brain tissue (Connolly et al, 1991). Possibly of greater importance however is that VEGF leads to an up regulation of MMP-9 which in turn has been shown to break down the BBB and cleave PEDF (Adibhatla et al, 2008, Notari et al, 2005).

PEDF is a 50 kDa secreted glycoprotein that was first described in the late 1980s after being identified and isolated from conditioned medium of cultured primary human fetal retinal pigment epithelial cells (Tombran-Tink and Johnson, 1989). PEDF is widely expressed throughout fetal and adult tissues, including the adult central nervous system (Tombran Tink et al., 1996). Initially, PEDF was identified as an effective neurotrophic factor, able to convert active Y79 retinoblastoma cells into differentiated non-proliferating neurons (Tombran-Tink et al, 1991). Further studies have shown that PEDF possesses multiple and varied biological properties, not only neurotrophic, but also neuroprotective, antitumorigenic, and potent antiangiogenic activity (Tombran-Tink and Barnstable, 2003). It protects neurons in some regions of the central nervous system against insults such as glutamate excitotoxicity and oxidative damage (Barnstable and Tombran-Tink, 2004). It seems to control the transit of cells through the cell cycle, promoting their entry into a quiescent state (Pignolo et al, 2003).

Both VEGF and PEDF are involved in angiogenesis and neuronal survival, and in the vascular endothelial cell system VEGF and PEDF have counterbalancing proangiogenic and antiangiogenic activities, respectively, with PEDF antagonizing the vascular permeability effects of VEGF (Greenberg and Jin, 2005). Furthermore, PEDF has been

proven to have influence in microglia in vitro (as has been previously mentioned microglia migrating to the ischemic lesion release MMP-9 which disrupts the BBB), inducing their resting state and blocking their proliferation (Takanohashi et al., 2005). PEDF has been shown to block VEGF-induced phosphorylation of extracellular signal-regulated kinase (ERK), p38 mitogen activated protein (MAP) kinase, the p38 substrate MAP kinase-activated protein kinase-2 (MAPKAPK-2), and glycogen synthase kinase 3 beta GSK3- β . The blocking of these proteins then prevents VEGF-induced activation of the uPA/uPAR system (urokinase and its receptor). A serine protease, uPA can be activated by binding to uPAR and it catalyzes the conversion of plasminogen to plasmin, which can degrade the extracellular matrix, activate latent growth factors such as TGF- β , and convert inactive-MMPs (pro-MMPs), including MMP-2 and -9, into their active forms (Yang et al., 2010). PEDF was shown to inhibit AGE-BSA-induced permeability by the increase expression of the junction protein ZO-1 by suppressing NADPH oxidase activity which leads to decreased generation of ROS (Sheikpranbabu et al., 2010b). In addition, PEDF appears to inhibit phosphatidylinositol 3-kinase (PI3K). PI3K is a signal transduction enzyme that catalyses the phosphorylation of phosphatidylinositol (4,5)-bisphosphate (PIP2) to form phosphatidylinositol (3,4,5)-trisphosphate (PIP3) in response to activation of either receptor tyrosine kinase, G-protein coupled receptors or cytokine receptors. This in turn ultimately plays a role in the regulation of cell growth, differentiation, survival, proliferation, migration and cytokine production (Sheikpranbabu et al., 2010b). PEDF is able to protect the retina from ischemic injury and to effectively abate VEGF and Interleukin-1 Beta (IL-1 β) induced vascular permeability and endothelial cell proliferation and migration (Yamagishi et al., 2007; Sheikpranbabu et al., 2010a; Jinnouchi et al., 2007). In addition, simultaneous injection PEDF was found to counter the permeability induced by intradermal injection of VEGF in nude mice in a dose-dependent manner. (Yamagishi et al., 2007).

According to our previous experiment the BBB opens within 4 to 8 hours after a stroke, closes, and then opens again 12 to 16 hours later. It was decided to try to decrease the permeability of the BBB at these time points by countering the effect of VEGF with PEDF. According to the literature, this is the first time the direct of effect of PEDF on the BBB has been tested.

6.2 Materials and methods:

6.2.1 Animal protocol:

Animal experiments were performed according to institutional and international guidelines. All surgical procedures were approved by the local authorities (G 0130/10 LaGeSo, Berlin, Germany). 50 male C57Bl6/N mice (Bundesinstitut fuer Risikoforschung, Berlin, Germany) weighing 18–24 grams were housed under standard conditions.

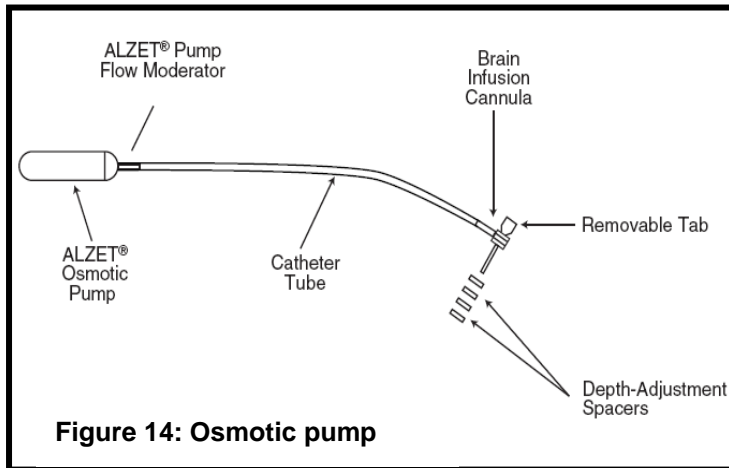
6.2.2 Focal cerebral ischemia:

MCAo was performed as previously described (Endres et al., 1999; Endres et al., 2000). For sham animals the MCAo procedure was performed as normal; however, after the filament was inserted into the carotid it was immediately withdrawn.

6.2.3 Osmotic Pump Implantation:

The pumps were implanted as previously described (Maeda et al., 2011). The pumps (Model 1003D for 3 days, 1.0 μ l/h; Alzet) to be implanted were prepared the day before the surgical procedure. The catheter tube that separated the pump from the cannula measured 3 cm and the depth of the cannula measured 3 mm. The un-primed osmotic pumps were filled with a solution of PEDF dissolved in CSF. The pumps were immersed in sterile saline and incubated overnight at 37 °C to equilibrate pumping. Before surgery the pumps were removed from the incubator and transferred to fresh saline. Mice were anesthetized using ketamine/xylazine (7.5 mg of ketamine and 2.5 mg of xylazine per 100 mg of body weight), the scalp was shaved and then the mice were placed on a warming pad, and secured on a modified stereotactic apparatus. A scalpel was used to make a midline sagittal incision in order to expose the skull. The incision began slightly behind the eyes and continued along the sagittal suture, up to the neck. The skull was gently scraped with the scalpel to remove the periosteal connective tissue. A pocket at the back of the mouse was created to accommodate the pump by

introducing hemostatic scissors through the neck and along the back and



opening and closing them several times in order to spread the connective tissues apart, separating skin from body musculature, and generating enough space to house the mini-osmotic pump. The bregma junction was located and used to identify the target site (stereotactic coordinates: 0.2 antero-posterior, +/-0.7 medio-lateral) which was then labelled with a permanent marker. A 30G needle was used to carefully drill a hole through the skull. The pump was placed under the skin and into the pocket, as a 'backpack' with the flow moderator pointing away from the incision. The infusion cannula was placed into the cannula holder and slowly lowered until the bottom of the cannula reached the skull. The cannula was glued to the skull with dental cement (Heraeus, Hanau, Germany). After the cement had been allowed to dry, the midline sagittal incision was sutured, and the mouse was removed from the stereotactic frame and returned to the heating box cage for two hours before being returned to its cage where the animal was given free access to food and water

6.2.4 Experimental design and administration of PEDF:

According to our first experiment concerning the time course of the opening of the BBB after MCAo, the BBB opens between 4 and 8 hours, closes, and then opens again between 12 and 16 hours after a stroke. In the first part of the study, we investigated the up regulation of the factors thought to play a role in opening/closing of the BBB: VEGF, MMP-9 and PEDF. The three time points that were selected for the upregulation of these factors were based on the BBB opening study previously described in this paper. Albumin was used as a marker for an opening in the BBB. Twenty-six animals were

divided into six groups with two groups (1 hour MCAo and Sham) per time point. The first two groups (6 MCAo animals and 2 sham animals) were sacrificed six hours after reperfusion. The next two groups (7 MCAo animals and 1 sham) were sacrificed 10 hours after reperfusion, and the final two groups (8 MCAo animals and 2 shams) were sacrificed at 14 hours after reperfusion.

Table 13: Animals used in experiment 5 – 1st part of study:

	6 hours	10 hours	14 hours
1 hour MCAo	n=6	n=7	n=8
Sham	n=2	n=1	n=2

The left hemisphere of each brain (ipsilateral to the lesion) was collected and homogenized. The homogenate was then subjected to an ELISA protein detection assay for Albumin and then a second ELISA assay for VEGF, MMP-9, and PEDF.

In the second part of the study, we investigated what effect closing the BBB with PEDF might have on lesion development after cerebral ischemia. Two groups of mice were created (n=12 per group). The first group received a three-day Alzet osmotic pump (pumps 1,0 µl of fluid per hour) with 40mg/mL of PEDF. The second group served as the control and received a three-day Alzet osmotic pump with CSF. Forty-eight hours after pump implantation 1 hour MCAo was performed on each animal. Twenty-four hours after reperfusion the animals were perfused with 4% PFA, snap-frozen, and the lesion volume measured with hematoxylin staining and the number of apoptotic cells with tunnel.

Table 14: Animals used in experiment 5 – 2nd part of study:

Osmotic pump Solution	40mg PEDF /mL of CSF	CSF
Number of mice	n=12	n=12

6.2.5 Enzyme Linked Immunoabsorbent Assay (ELISA) for Mouse Albumin/ VEGF/ PEDF/ MMP-9:

For total cellular protein extraction, mice brains were weighed and then placed in and Eppendorf tube with ristocetin-induced platelet agglutination (RIPA) buffer [50 mM Tris pH 7.4, 150 mM NaCl, 0.1% w/v sodium dodecyl sulphate (SDS), 1% w/v Triton X-100,

1% w/v sodium deoxycholate and protease inhibitor cocktail] (3 mL RIPA buffer was used per gram of brain tissue) and sonicated for 3 x 15 seconds. The lysate was passed through a pipette five times and then through a 25G needle. It was then spun at 10,000g for 10 minutes at 4°C and the supernatant removed. The supernatant was again spun at 10,000g for 20 minutes to pellet remaining tissue debris. Supernatants were collected and stored at -80°C for later use. 100 µL of each standard dilution or diluted sample was pipetted into a microplate well (each standard or sample was done in triplicate). The plate was covered and allowed to incubate at room temperature for 1 hour. Subsequently the plate cover was removed and each well was washed four times with wash solution (50 mM Tris buffered saline, 0.05% Tween in ddH₂O, pH 8.0), 100 µL of detection antibody (Albumin/VEGF/PEDF/MMP-9) was added to each well and the plate was covered and allowed to incubate for 1 hour. The plate cover was removed and each well was again washed four times with wash solution and 100 µL of streptavidin-conjugated horseradish peroxidase (SA-HRP) was then added to each well. The plate was incubated at room temperature for 30 minutes before being washed a final time (4x per well). 100 µL of TMB (3,3',5,5'-tetramethylbenzidine) was then added to each well and the plate incubated at room temperature in the dark for 30 minutes. Finally 100 µL of stop solution was added to each well and the absorbance measured at 450 nm.

6.2.5 ELISA Bicinchoninic Acid (BCA) Protein Assay:

Diluted albumin standards were prepared by diluting a 1 mL ampule of albumin standard (2.0 mg/mL bovine serum albumin in 0,9% saline and 0,05% sodium azide) with RIPA buffer to create eight standards of decreasing concentration and one blank (Ripa buffer with no albumin standard solution). 25 µL of each standard dilution or diluted sample were pipetted into a microplate well (each standard or sample was done in triplicate). 200 µL of working reagent [196,0 µL reagent A (sodium carbonate, sodium bicarbonate, bicinchoninic acid and sodium tartrate in 0.1 M sodium hydroxide) and 4,0 µL reagent B (4% cupric sulphate)] were added to each well. The microplate was covered and allowed to incubate at 37°C for 30minutes. The plate was then cooled to room temperature and the absorbance measured at 562 nm.

6.2.6 Statistical Analysis:

Analysis of lesion volume was performed using the two-tailed t-test. Statistical analysis was performed using Graphpad Prism software.

6.3 Results:

6.3.1 Concentration of VEGF, PEDF, MMP-9, and Albumin increase in brain tissue after MCAo in mice:

In the first part of the study, the up regulation of VEGF, MMP-9 and PEDF along with the extravasation of albumin past the open BBB and into the brain of mice after MCAo was investigated. The three time points that were selected for investigation were based on the previous study that showed that the BBB underwent a biphasic opening during the 24 hour period after MCAo.

We used albumin extravasation as a marker for BBB integrity, because under normal conditions albumin is unable to pass the BBB, thus a larger amount of albumin should correspond to a larger or longer gap in the integrity of the barrier. Since an opening in the BBB would also allow for the extravasation of VEGF, MMP-9, and PEDF into the brain tissue, the albumin concentration was used to normalize the values of these three additional proteins. According to our results, the concentrations of VEGF, MMP-9, and PEDF dramatically increased at 6 hours in mice that underwent MCAo. At 10 and 14 hours the concentration of each protein subsided to some degree but remained well above levels found in sham animals. The concentration of VEGF was approximately four times greater than PEDF (Fig 15). The three sham groups showed minimal albumin in the brain while the three operated groups showed a spike in the amount of albumin at six hours which increased at the 10 hour and 14 hour time points (Fig 16). This increase is a further confirmation of the biphasic opening of the BBB.

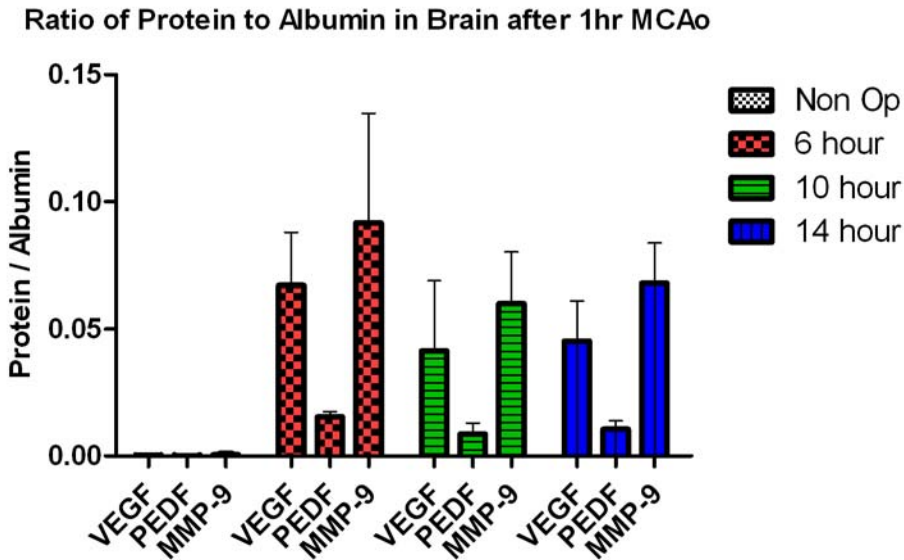


Figure 15: VEGF, PEDF, and MMP-9 levels in the brain after 1 hr MCAo.

Twenty-six animals were divided into six groups. Three of the groups underwent 1hr MCAo and the other three groups served as shams. Protein levels were normalized against the albumin concentration which served as an indicator for a rupture in the BBB. The animals were sacrificed at 6 hr, 10 hr and 14 hrs after reperfusion. At 6 hrs the levels of each protein spiked dramatically when compared to sham animals. At 10hrs and 14hrs the protein concentrations dropped but still remained well above normal levels. (6 hr: n=6, 10 hr: n=7, 14 hr: n=8, Non-operated: n=5)

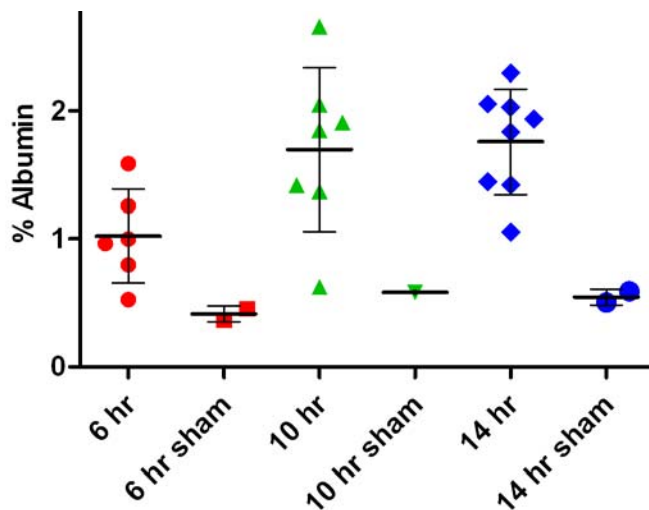


Figure 16: Albumin levels in the brain after 1 hr MCAo.

Twenty-six animals were divided into six groups. Three of the groups underwent 1hr MCAo and the other three groups served as shams. The animals were sacrificed at 6 hr, 10 hr and 14 hrs after reperfusion. Albumin was used as a marker for BBB opening. MCAo animals at all time points showed an increase in albumin in the brain as opposed to the sham animals. The pattern of arabinose extravasation supports the previous results concerning a biphasic opening in the BBB. (6 hr: n=6, 6 hr sham: n=2, 10 hr: n=7, 10 hr sham: n=1, 14 hr: n=8, 14 hr sham: n=2)

6.3.2 PEDF has no effect on lesion volume in mice after MCAo:

PEDF has been shown to counteract VEGF. According to our previous results, the concentration of PEDF in the brain after cerebral ischemia is much lower than that of VEGF. In the second experiment, we investigated what effect an artificial increase of PEDF in the brain might have on final lesion volume. There was no significant difference between the size of lesions in the PEDF group and the control (Fig 17).

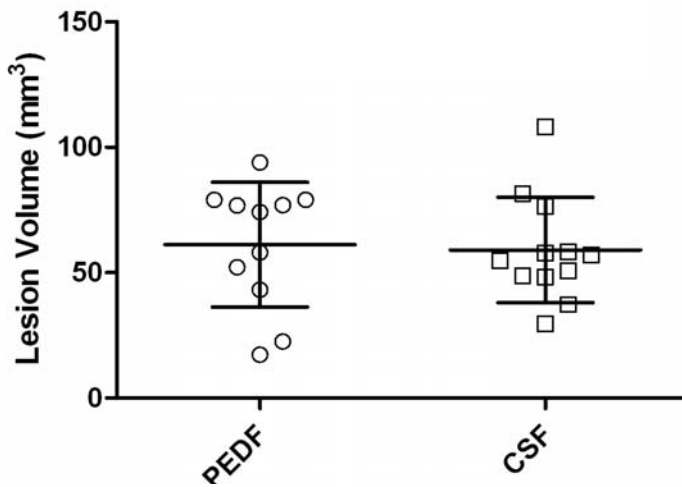


Figure 17: Final lesion volume after 1 hr MCAo in mice receiving PEDF or CSF.

Two days before MCAo mice received an osmotic pump into the ventricle expressing either PEDF or CSF. Mice were sacrificed 24 hrs after reperfusion and the lesion volume analyzed. There was no significant difference between the two groups. (PEDF: n=11, CSF: n=12, difference not significant)

7. Discussion and conclusions:

7.1 Time course of BBB opening after MCAo:

Our primary goal in this experiment was to determine if the BBB did indeed open after an ischemic event in our animal model, and if so at what time point or time points. Our objective was to use this knowledge in subsequent experiments where we attempted to manipulate the permeability of the BBB after cerebral ischemia. Using EB and indotricarbocyanine bovine serum albumin conjugate we saw a biphasic opening in BBB. The initial BBB impairment was observed at 8 hours after reperfusion and a later, second impairment at 16 hours after reperfusion. However, the results were not confirmed with Gd-DTPA. Using Gd-DTPA as a marker the BBB appeared to be open during all the time points that we accounted for which is in accordance with the continuous opening of the BBB reported by Strbian et al. (2008). The discrepancy between Gd-DTPA, EB, and NIRF-BSA might be accounted for by the size of the molecular markers used or even possibly by their chemical profile. Gd-DTPA, which has no binding affinity to plasma albumin, has a molecular weight of approximately 550 Da while NIRF-BSA and EB (which binds to native albumin) both have a molecular weight of approximately 68,000 Da. The smaller molecular size of Gd-DTPA no doubt accounts for its ability to extravasate past the BBB when other larger albumin bound molecules are unable to. Nagaraja et al., (2008) demonstrated molecular markers with approximately similar atomic weights were able to penetrate the BBB with various degrees of success.

The sensitivity of the probe might have also played a role. NIRF is more sensitive than MRI, but still not as sensitive as other imaging techniques available such as SPECT and PET (Fig 18). It is possible that the BBB was in fact permeable to some degree to the albumin bound marker however our imaging technology simply was not sensitive enough to detect the small amounts of marker that were able to extravasate.

However, despite these shortcomings we felt that the biphasic pattern of opening in the BBB after MCAo was most likely to be correct. This pattern was demonstrated by EB extravasation which has traditionally been the gold standard of BBB permeability. The biphasic pattern was further confirmed by NIRF imaging, which is several orders of

magnitude more sensitive than MRI (Fig 18), of Indotricarbocyanine BSA conjugate (which is approximately the same size as EB bound albumin).

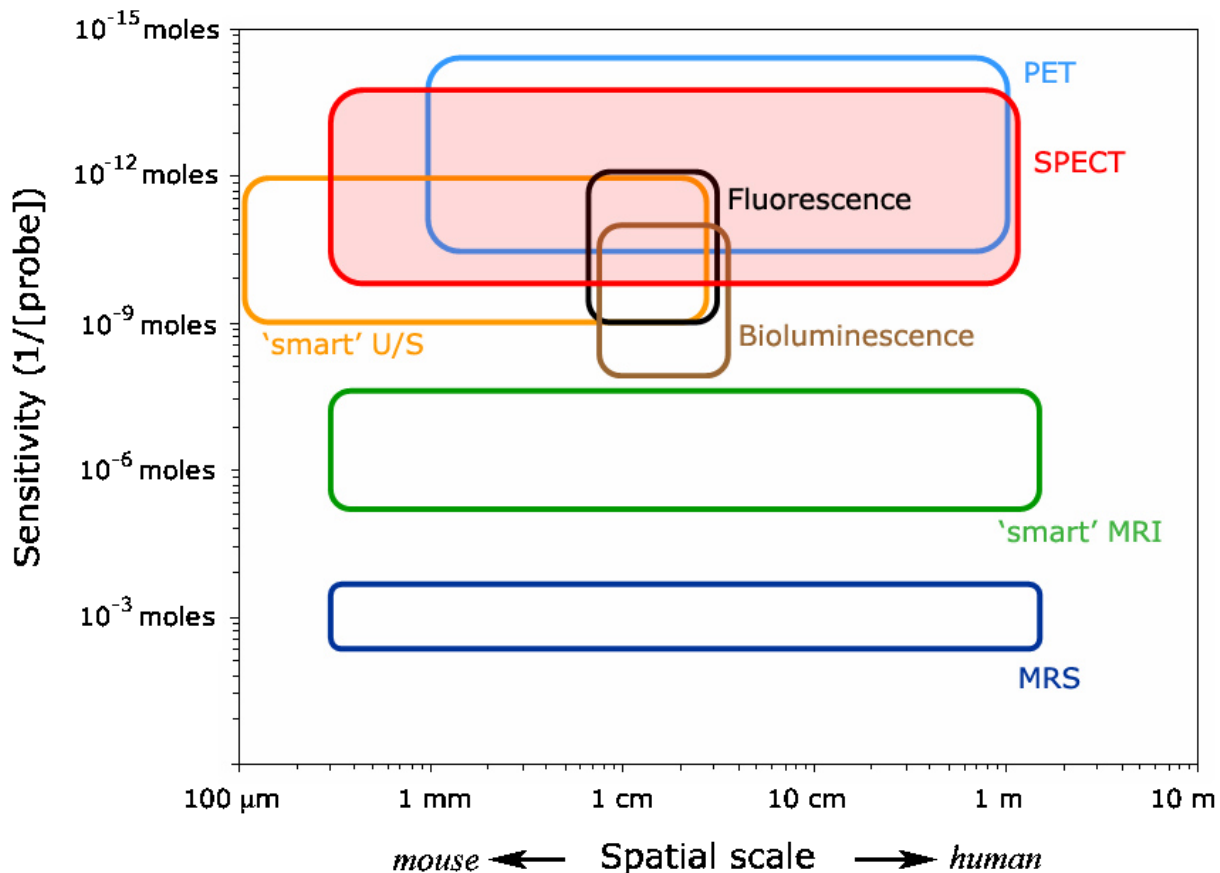


Figure 18: Molecular imaging matrix. “Sensitivity refers to the *in vivo* concentration of the labelled contrast agent (probe) required to elicit a certain signal-to-noise ratio. The spatial scale is the domain bounded by the limiting resolution (left limit) and the depth of penetration of the signal-generating radiation (right limit) for a given technology.” (Meikle et al., 2005)

7.2 Si-RNA induced pre-emptive opening of the BBB combined with MCAo.

The objective of this experiment was to try and pre-emptively open the BBB by hydrodynamic delivery of siRNA before initiating the stroke in order to determine what if any effect on final lesion volume this might have.

When we combined the claudin-5 siRNA induced opening of the BBB with MCAo we found that the results were not significant. Despite finding no clear significance between the two treatment groups we did see a trend towards a smaller lesion volume in the claudin-5 group – the group with the open BBB. It will be necessary to repeat this

experiment with a larger cohort of animals in order to decrease the variance and increase the power.

Up until the experiment is repeated we can possibly speculate about the trend towards a smaller lesion volume in mice with a more permeable BBB. If this trend does prove to be significant when the experiment is repeated it would counter our initial hypothesis that an opening in the BBB leads to a larger lesion volume. According to Campbell et al., the claudin-5 siRNA induced opening in the BBB takes effect within 24 hours after injection. The BBB remains open up to 48 hours after injection. The MCAo was performed 48 hours after the initial injection which means that the BBB was already open for 24 hours preceding the stroke. While speculative it is possible that during this 24 hour period the brains of the treated animals acquired what is known as an induced tolerance to the potentially detrimental effects of an open BBB. This induced tolerance or preconditioning effect might have been the cause behind the tendency towards a smaller lesion volume in the claudin-5 group. According to Dirnagl et al., (2009) preconditioning results when a noxious stimulus that is near to but below the threshold of damage is applied to the tissue. Furthermore, after preconditioning the brain develops an increased tolerance for the same or similar noxious stimuli given beyond the threshold of damage, thus preconditioning protects against subsequent injury.

7.3 TMS induced pre-emptive opening of the BBB combined with MCAo:

Our initial aim in this experiment was to determine if we could use TMS to open the BBB in mice without collateral damage to the surrounding nervous tissue. We successfully demonstrated that we could open the BBB in mice. According to our results, the BBB opened within an hour of the TMS and remained open for at least 4 hours afterwards without causing significant damage in the surrounding tissue. Since we did not study EB extravasation beyond 4 hours after stimulation, we cannot exclude BBB impairment at time points later than 4 hours.

When we combined the TMS induced opening of the BBB with MCAo we found that the results were not significant. The opening induced in the BBB by TMS was highly variable and may have played a role in the lack of statistical significance. Advances to the technology underlying TMS will be required in order to reduce the variability in the BBB

opening between animals. If it proves possible to decrease this variability then TMS could prove to be an invaluable technique for non-invasively targeting discrete areas of the brain to induce greater BBB permeability. Until the point that TMS advances sufficiently, focused ultrasound could be useful in repeating this experiment (see Appendix B for more on focused ultrasound). It causes minimal or no damage, has been used successfully in a plethora of animal models, and the opening induced by the sonification process is tightly focused (within several millimeters), and not as variable as TMS.

Until the technology advances and the experiment is repeated, we can possibly speculate about the trend towards a larger lesion volume in mice that received 100% TMS. This result contrasts with the siRNA experiment where we saw a general trend towards a smaller lesion volume. We demonstrated that the TMS did not lead to apoptosis in the brain. Therefore if the trend towards a larger lesion volume in the treated group is correct we can assume that it is due to the pre-emptive opening of the BBB.

7.4 Hypertonic arabinose induced pre-emptive opening of the BBB combined with MCAo :

Our initial aim was to determine if we could repeat the work of Fredericks et al., (1988) and use arabinose to open the BBB in mice. Our second objective was to determine how long the BBB remained open after arabinose infusion and if it could be visualized using non-invasive imaging techniques such as MRI. Our third objective was to use hyperosmotic arabinose to pre-emptively open the BBB in mice and then induce a stroke via MCAo. Our goal, as before, was to determine what if any effect the pre-emptive opening of the BBB might have on the final lesion volume after the stroke.

According to the results, pre-emptively opening the BBB with arabinose lead to a significant increase in the size of the final lesion volume as opposed to those animals that were only treated with saline. Furthermore, the final lesion volume correlated with the size of the opening in the BBB that was induced with arabinose. This experiment supports the generally held hypothesis that an opening of the BBB is detrimental after cerebral ischemia.

7.5 Closing the BBB with PEDF combined with MCAo:

Our goal was to determine if we could directly administer PEDF to the ischemic brain in order to inhibit the acute angiogenic activity and consequential loss of vascular integrity that results from VEGF expression. The objective was to potentially prevent the death of viable brain tissues and the mortality resulting from edema and hemorrhage by using PEDF to effectively close the BBB after cerebral ischemia.

According to our results PEDF has no effect on the final lesion volume after MCAo. This contrasts with Sanagi et al., (2008) who used gene transfer of PEDF to attenuate ischemic brain damage after 70 minutes of MCAo in rats. He observed that the infarct volume and degree of edema of the PEDF-treated group were both significantly reduced compared to the control group 24 hours after MCAo. These differences might be due to the effective concentration of PEDF or its ability to permeate the tissue. If this experiment is revisited it will be necessary to more firmly confirm that PEDF is counteracting an opening in the BBB and not simply inhibiting the action of VEGF. While PEDF may have counteracted the effects VEGF on the BBB it may not prevent an opening in the BBB. After an ischemic event there are a plethora of growth factors, cytokines, and chemokines released into the brain's local environment – such as MMP-9 which has been shown to degrade PEDF. It is not only feasible but likely that many of these play a role in opening up the BBB either directly or indirectly. By inhibiting the effects of VEGF it is not clear that we were able to effectively prevent the opening of the BBB. Furthermore it will be necessary to determine if PEDF is able to permeate fully into the tissue from the ventricle or if another mode of delivery or higher concentration is necessary.

It will also be necessary to look at other time points after a stroke and possibly prolong treatment with PEDF. In this experiment, animals were sacrificed 24 hours after MCAo. The stroke lesion while well developed at 24 hours continues to mature for another 24 to 48 hours, and given that Strbian et al., (2008) found that the BBB was impaired up to three weeks after MCAo, it is possible that the effect of closing the BBB on lesion volume is not significant until later time points.

Results Addendum:

Experiment 1: Time Course of BBB Opening after cerebral ischemia was carried out in the Clinic for Neurology at Charite Hospital in Berlin. The results were obtained under a collaboration lead by Dr. Jan Klohs and supervised by PD Dr. Andreas Wunder. The full results have been published the Journal of Neuroscience Methods (Klohs et al., 2009).

Experiment 2: Pre-emptive opening of the BBB with Si-RNA combined with cerebral ischemia was carried out in the Clinic for Neurology at Charite Hospital in Berlin, Germany. The results were obtained under a collaboration lead by Dr. Jan Klohs and Dr. Matthew Campbell and supervised by Dr. Andreas Wunder

Experiment 3: Pre-emptive opening of the BBB with TMS combined with cerebral ischemia was carried out in the Laboratory of Experimental Neurosurgery at the Ben-Gurion University of the Negev in Beer-Sheva, Israel. The results were obtained under collaboration with Prof. Dr. Alon Friedman.

Experiment 4: Pre-emptive opening of the BBB with hypertonic arabinose combined with cerebral ischemia was carried out in the Department of Neurosurgery at Charite Hospital in Berlin. The results were obtained under collaboration with Dr Ana Luisa Pina. The full results are currently being written up in a manuscript which will be submitted for publication before the end of the year.

Experiment 5: Closing the BBB with PEDF after cerebral ischemia was carried out in the Department of Neurosurgery at Charite Hospital in Berlin. The results were obtained under collaboration and supervision with Dr Ana Luisa Pina. The full results are currently being written up in a manuscript which will be submitted for publication before the end of the year.

Appendix A: Laboratory Materials:

Anesthetics:

Product	Supplier
Chloral Hydrate	Merck
Isoflurane (Forene)	Abbott
Ketamin (Ketavet 100mg/mL)	Pfizer
Xylazin (Rompun 2%)	Bayer

3.1.2 Chemicals:

Product	Supplier
DABCO	Triton
0,9 % NaCl	B-Braun
Acetic acid (CH ₃ COOH)	Sigma Aldrich
Arabinose	Sigma
Dipotassium phosphate K ₂ HPO ₄	Sigma
Ethanol	J.T. Baker
Evans Blue	Sigma Aldrich
Harris hematoxylin	Merck
Hydrochloric Acid	Merck
Hydrochloric acid (HCl)	Sigma
Isopentane/2-methylbutan	Roth
Monopotassium phosphate (KH ₂ PO ₄)	Sigma
Monosodium phosphate NaH ₂ PO ₄	Sigma
Neutral Red	Sigma Aldrich
Paraformaldehyde	Merck
PBS Tablets	Invitrogen
Polyvinyl alcohol with diazabicyclooctane	Sigma Aldrich
Potassium aluminum sulphate KAl(SO ₄) ₂	Sigma Aldrich
Potassium Ferrocyanide K ₄ Fe(CN) ₆	Sigma Aldrich
Potassium monohydrogenphosphate (K ₂ HPO ₄)	Merck
Protease inhibitor cocktail	Thermo Scientific
RIPA buffer	Millipore
Sodium bicarbonate (NaHCO ₃)	Sigma

Relationship between the Blood-Brain Barrier and Cerebral Ischemia

Sodium dodecyl sulphate (SDS)	Sigma
Sucrose	Sigma
Trichloroacetic acid	Sigma Aldrich
Tween-20	Sigma
Xylene	Sigma Aldrich

Antibodies, Reagents, and Kits:

Product	Supplier
Bovine Serum Albumin	Sigma Aldrich
Milk powder (blocking grade)	Roth
Chicken derived polyclonal	
Anti-laminin primary antibody	Abcam
Rat derived anti-mouse CD31 primary antibody	BD BioSciences Pharmingen
Rabbit derived anti-Iba1 primary antibody	Wako Chemical
Mouse derived anti-GFAP primary antibody	Millipore
DyLight 488-conjugated secondary antibody	Jackson Immuno Research Laboratories
Dylight 549-conjugated secondary antibody	Jackson Immuno Research Laboratories
ApopTag	Millipore
Dental cement	Heraeus
si-RNA	Trinity College in Dublin, Ireland
PEDF	BioProducts
Streptavidin-conjugated horseradish peroxidase	Vector Laboratories
VEGF	PeproTech
BCA Protein Assay Kit	Thermo Scientific
VEGF, Albumin, MMP-9 Elisa Kit	Bethyl Laboratories
PEDF Elisa Kit	BioProducts MD
Milk powder (blocking grade)	Roth

3.1.3 Imaging Agents:

Product	Supplier
Gadofluorine-M	Gift from Prof. Dr. Guido Stoll and Schering

Gd–DTPA (Magnevist)	Bayer Schering Pharma AG
Indotricarbocyanine BSA conjugate	Bayer Schering Pharma AG

3.1.4 Tools and Equipment:

Product	Supplier
0.28 mm, 0.61mm Polyethylene tubing	SIMS Portex
0.45 µm Filter	Sarstedt
30G needle	BD Microlance
7Tesla MRI	Biospin
Alzet Model 1003D Osmotic Pump	Sulzfeld
CCD Camera	Roper Scientific
Fluorescent Microscope Camera	Mbf Bioscience
Fluorescent Microscope Olympus BX61	Olympus
Gastight 1800 Syringe	Hamilton
Heating cage	Pesco Services
Heating pad	Harvard Apparatus
Insumed 31G needle	Picindolor
Magnetic Stimulator	Magstim
Nikkor Focusing lens system	Nikon
NIRF interference Filters	Andover
Nylon monofilament	Suprama
Pipette	Eppendorf
Scalpel blades	Feather
Silicone resin/hardener	Heraeus
Sliding microtome	Leica
Sonicator, Sonorex Super 10P	Bandelin Electronic
Stereotactic frame	Stoelting
SuperFrost slides (25x75x1.0 mm)	Langenbrinck
Tecan infinite M200	Tecan Group Ltd.
Trancranial Magnetic Coil	Brainsway

3.1.6 Software:

Product	Supplier
Fluorescent Microscope Software	Cell^P
Plate Reader Software	Magellen V 6.5
Sigma Scan Pro 5 volumetric software	Sigma Scan

3.1.7 Animals:

Product	Supplier
C57/Bl6 mice	Charles River

Appendix B: Opening the BBB with focused ultrasound:

Focused Ultrasound (FU) uses the sonic excitation of commercially available contrast agents consisting of albumin coated microbubbles to open the BBB (Hynynen et al., 2001). The presence of these microbubbles circulating in the vasculature confines the effects of the ultrasound to the blood vessel walls resulting in BBB disruption with minimal damage to surrounding brain tissue (Hynynen et al., 2005). The microbubbles allow for the selective disruption of the BBB at much lower acoustic power levels than would otherwise be possible due to the skull's tendency to absorb ultrasound thus resulting in heating during sonication (McDannold et al., 2005).

FU allows for acoustic energy to be concentrated into point of only a few millimetres in diameter and has been used in a variety of animal subjects. (Choi et al., 2007; McDannold et al., 2005; Kinoshita et al., 2005; Jalali et al., 2010). The exact mechanisms by which the BBB is disrupted by contrast-enhanced FU is not known; however, it is probably due to a combination of cavitation and acoustic radiation forces (Vykhodtseva et al., 2008).

Electron microscopy of animal brains after FU suggests that sonication results in transendothelial transport by both transcellular and paracellular pathways. These pathways include: transcytosis, endothelial cell cytoplasmic openings, passage through leaking tight junctions and, and (at high powers) passage through injured endothelium (Sheikov et al., 2006; Sheikov et al., 2004; Kinoshita et al., 2006). There is evidence suggesting that FU may lead to a breakdown of tight junctions leading to increased permeability in the brain's vasculature (Sheikov et al., 2008). Immunoelectron microscopy for tight junction-specific proteins after FU has shown a loss of immunosignals for occludins, claudin-5 and ZO-1 as early as 1 hour following sonication (Sheikov et al., 2008). The barrier function of the tight junction appears completely restored 4–5 h following sonication. After FU an increase in BBB permeability has been seen as soon as 10 minutes and for up to 5 hours (Vykhodtseva et al., 2008).

FU induced BBB disruption does not appear to result in brain tissue damage. According to (McDannold et al., 2005) after FU induced BBB disruption there was no ischemic or apoptotic areas which would indicate a compromised vasculature or regions of neuronal

Relationship between the Blood-Brain Barrier and Cerebral Ischemia

damage. The mild damage that has been observed was completely abated within four weeks of the FU process (McDannold et al., 2005).

Appendix C: Review of the BBB and cerebral ischemia:

1.	The Blood Brain Barrier Overview	63
1.1	The Cerebral Vasculature and the BBB	63
1.2	Transport Across the BBB	68
1.3	Neurons	70
1.4	Astrocytes	70
1.5	Pericytes	71
1.6	Basal Lamina / Extracellular Matrix	72
1.7	Microglia	73
1.8	Endothelial Cells	73
1.9	Tight Junctions, Junctional Adhesion Molecules and Adherens Junctions	74
1.9.1	Occludin	76
1.9.2	Claudin	77
1.9.3	JAM	78
1.9.4	MAGUK	78
1.9.5	Adherens Junctions	80
2.	Cerebral Ischemia Overview	81
2.1	Energy failure	83
2.2	Excitotoxicity	84
2.3	Oxidative stress	85
2.4	Inflammation	86
2.5	Cell death	87
2.6	Cerebral reperfusion injury	88
2.7	Current treatment for stroke	89

1. The Blood-Brain Barrier Overview:

1.1 The Cerebral Vasculature and the BBB:

The cerebral vasculature is the largest interface for blood exchange with a surface area between 150 and 200 cm²/g tissue depending on the anatomical region (Abbott et al., 2010). The cerebral vasculature or circulation can be categorized based on vessel size and location. Arterial macrocirculation starts in the neck and goes to the pial arteries, and its primary function is the conductance of blood. The arterial microcirculation is composed of the pial and penetrating arterioles, the capillaries and the venules, and its primary function is the regulation of blood flow, substrate delivery and waste removal. The brain vasculature can also be grouped into extrinsic and intrinsic components. The former is composed of the large conductance vessels or the macrocirculation and the pial circulation. The penetrating arterioles transition to the intracerebral small arterioles, capillaries and venules. Pial vessels can be found either in the subarachnoid space or at the brain surface (Kulik et al., 2008). The arterioles then descend into the brain tissue where their basement membrane eventually makes contact with the astrocyte end-feet (Kulik et al., 2008). The large conductance arteries, the pial arteries and arterioles, and penetrating arterioles all have a BBB (Kulik et al., 2008).

The first evidence for the existence of the BBB was uncovered by Paul Ehrlich around the end of the 19th century. Through a series of experiments he was able to demonstrate that various water-soluble dyes when injected into the circulatory system were unable to stain the brain and spinal cord (Hawkins et al., 2005). Ehrlich initially presumed that this was due to the nervous tissue's low affinity for the dyes; however, Ehrlich's student, Edwin Goldmann, took the next logical step and injected trypan blue directly into the cerebrospinal fluid (CSF). The dye was subsequently able to stain the brain tissue (Hawkins et al., 2005). Max Lewandowsky built upon this work reasoning that there must be some form of barrier between the CNS and the peripheral circulation. Lewandowsky eventually coined the term *Bluthirnschranke* or Blood-Brain Barrier (Hawkins et al., 2005).

All organisms with a well developed CNS have a BBB (Abbott, 2010). The BBB consists of an interdependent network of cells which acts as a diffusion barrier between the CNS

and the peripheral circulation (Sandoval et al., 2008). While the barrier plays a critical role in segregating the sensitive nervous tissue from substances found in the circulation, certain parts of the nervous system are not afforded protection by the BBB. The circumventricular organs (CVOs) which are found bordering the 3rd and 4th ventricle are sites of communication between the brain and peripheral organs and therefore lack a BBB (Kulik et al., 2008). The CVOs include the pineal gland, median eminence, subfornical organ, area postrema, subcommissural organ, and organum vasculosum of the lamina terminalis (Kulik et al., 2008).

The BBB maintains the delicate homeostasis of the brain while simultaneously providing a constant supply of nutrients and oxygen to the CNS (Sandoval et al., 2008). Neurons within the central nervous system communicate using a combination of both chemical and electrical signals and proper neuronal function requires a highly regulated extracellular milieu, where concentrations of ions such as calcium, potassium, and sodium must be maintained within very narrow ranges. For example, the concentration of potassium in mammalian plasma is roughly 4.5 mM and can fluctuate greatly after a meal; however, in the CSF it is kept at a relatively steady 2.5–2.9 mM (Hawkins et al., 2005). It is presumed that this requirement for a fairly static local environment was one of the major evolutionary pressures leading to the development of the BBB (Abbott, 2010).

Under normal circumstances neurons in the CNS are unable to divide and replace themselves, and by and large the CNS does not have the ability to regenerate in any significant capacity if it is damaged. While the CNS is able to compensate for the unavoidable loss of neurons that happens throughout the lifespan of an organism it would be unable to deal with any significant loss without notable and possibly fatal results. It is thus necessary to shield the delicate tissue of the CNS from many of the neurotoxic substances that might otherwise lead to accelerated tissue loss.

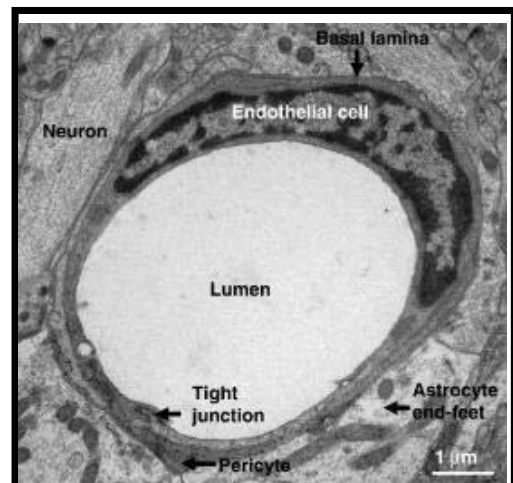
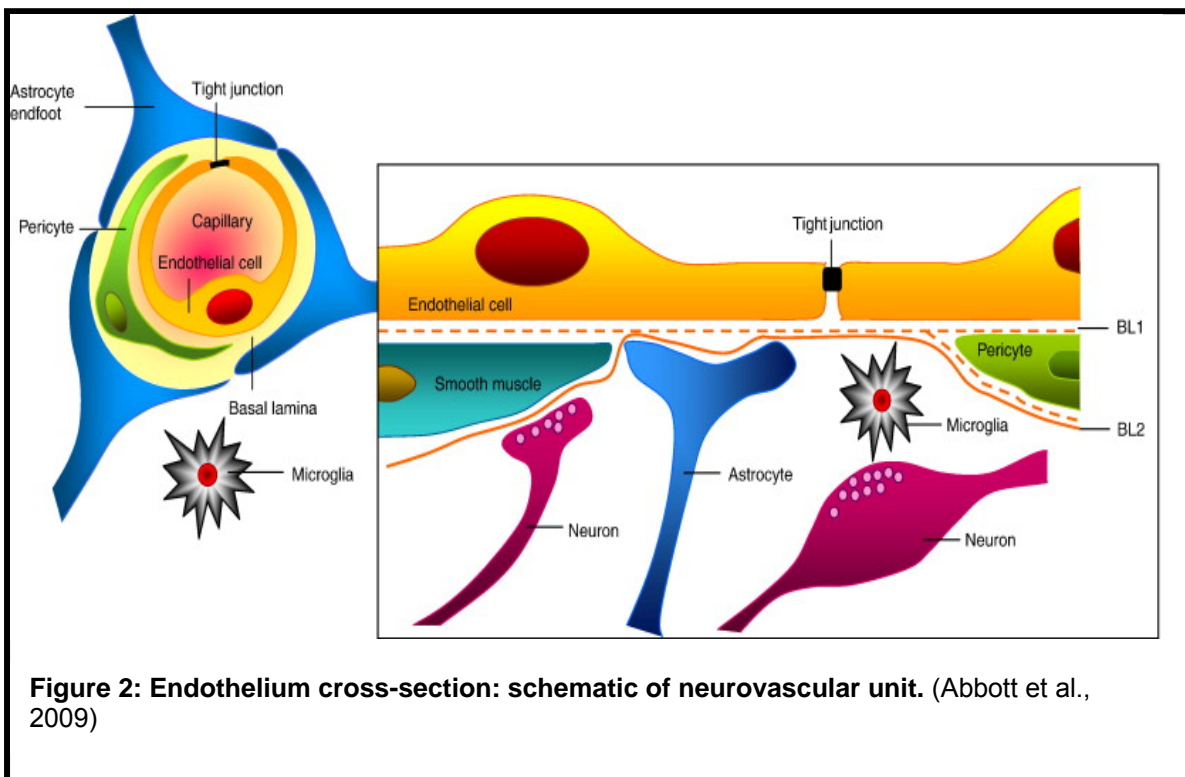


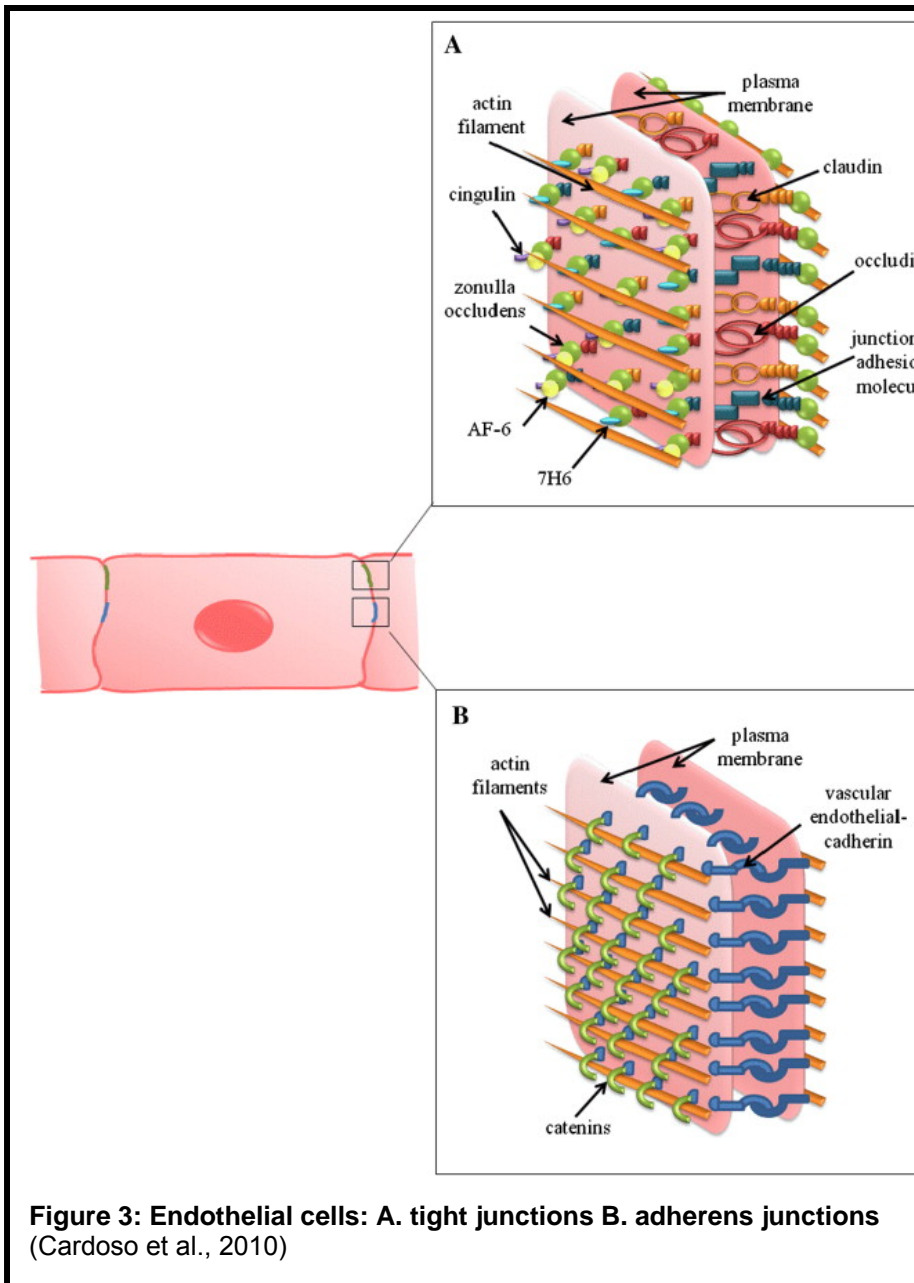
Figure 1: Endothelium cross-section: neurovascular unit.
(Weiss et al., 2009)

The CNS is sensitive to a wide range of substances, many of which are found in a normal diet. These various compounds can be quite neurotoxic; however, they pose no threat to our peripheral organ systems and are readily metabolized and excreted without harm. A classic example is the amino acid glutamate. The blood plasma contains high levels of this neuroexcitatory amino acid and its levels in the peripheral circulation can increase significantly after the eating. However if it is released into the brain in an uncontrolled manner it can cause considerable damage to the brain tissue. In addition, because the central and peripheral nervous systems use many of the same neurotransmitters the BBB is responsible for keeping these transmitter reservoirs separate, thus minimising 'crosstalk' (Abbott et al., 2010).

The plasma contains a much higher level of protein than does the CSF and the composition of various proteins can vary significantly. The BBB is responsible for preventing many of the proteins and macromolecules found in the circulation from finding their way into the neural tissue, because plasma proteins such as albumin, prothrombin and plasminogen can cause cellular activation which can result in apoptosis (Abbott et al., 2010).



Finally, the BBB acts a defence against neurotoxic substances such as xenobiotics ingested in the diet or otherwise acquired from the environment. A number of ABC energy-dependent efflux transporters (ATP-binding cassette transporters) actively pump many of these agents out of the brain.



The BBB is composed of the endothelial cells of the vessel walls and is supported by the neurovascular unit (NVU). The NVU is a concept proposed to highlight the interactions

which control BBB integrity and it provides a basic framework for considering the means of communication between neurons, their surrounding astrocytes and the vessels that supply them with vital gases and nutrients (del Zoppo et al., 2010; Persidsky et al., 2006; Weiss et al., 2008). The NVU is composed of the astrocytes and their astrocytic end-feet which surround the microvessel, the extracellular matrix of the basal lamina, and the pericytes, microglia, and neurons that are in close proximity to the endothelium (Fig1 & Fig2). Oligodendroglial and axonal compartments present in white matter probably also play a role (Persidsky et al., 2006; Lee et al., 2004).

The main features of BBB endothelial cells are an extremely low rate of transcytotic vesicles and a restrictive paracellular diffusion barrier (Lee et al., 2004). In contrast to the endothelium found in the peripheral circulation, the cerebral microvasculature lacks fenestrations, possesses only a small number of pinocytotic vesicles (Abbott, 2002) and has five to six times more mitochondria (Lee et al., 2004; Kulik et al., 2008). The BBB is composed of tight junctions between adjacent endothelial cells that form a continuous network of intramembrane proteins intimately linked to the actin cytoskeleton ((Petty et al., 2001). Tight junctions and Adherens junctions limit the paracellular flux of hydrophilic molecules across the BBB, whereas small lipophilic molecules diffuse freely across plasma membranes along their concentration gradient (Kulik et al., 2008). Tight junctions are composed of trans-membrane molecules (junction-adhesion-molecules, occludin, and claudins) and cytoplasmic proteins (zonula occludens-1 and -2, cingulin, AF-6, and 7H6) linked to an actin cytoskeleton (Fig: 3) (Abbott, 2002). Adherens junctions are composed of the membrane protein cadherin which forms a complex with the submembranal plaque proteins β -catenin and p120-catenin, and α -catenin, and the actin cytoskeleton (Fig:3) (Ballabh et al., 2004; Dejana et al., 2008)

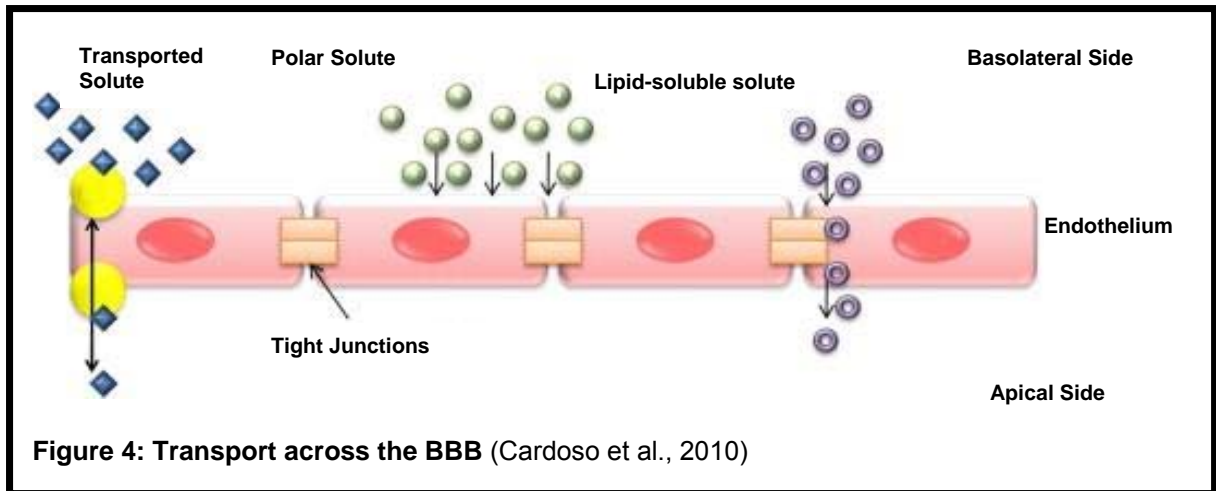
Finally, there is a second permeability barrier, the basal lamina, which is a specialized part of the extracellular matrix (ECM). The basal lamina surrounds the microvascular endothelium and pericytes (Yurchenco et al., 1990). It is 30–40 nm thick and composed of collagen type IV, heparin sulfate proteoglycans, laminin, fibronectin and other extracellular matrix proteins (Ballabh et al., 2004; Hawkins et al., 2005; Persidsky et al., 2006). This lamina is contiguous with the plasma membrane of astrocytic end-feet which ensheathes the cerebral capillaries (Ballabh et al., 2004; Hawkins et al., 2005; Persidsky et al., 2006). Under some circumstances, agents that penetrate the tight junctions of the

BBB may still be impeded by this barrier (Lee et al., 2004). The matrix may also act as a medium for cell-cell signalling thus allowing the cells of the CNS to communicate with each other in order to regulate the BBB (Cserr et al., 1986)

1.2 Transport Across the BBB:

Brain tissue uses oxidative phosphorylation for energy production, and in doing so consumes copious amounts of glucose and oxygen; the CNS accounts for approximately 20% of oxygen consumption in humans (Persidsky et al., 2006; Hawkins et al., 2005). Oxygen and carbon dioxide cross the BBB according to their concentration gradient, thus oxygen supply to the brain and carbon dioxide removal are dependent on blood-flow. Passive diffusion also applies to many lipid-soluble molecules with more lipid-soluble molecules entering the brain at a higher rate (Liu et al., 2004). The same however, can not be said of many essential yet polar nutrients such as glucose and amino acids which are necessary for metabolism. In essence, the presence of inter-endothelial-cell tight junctions give the brain endothelium the functional character of a continuous cell membrane in regards to both the diffusional characteristics of the lipid-bilayer and the properties of the transport proteins located in the cell membrane. Thus the BBB endothelium contains a number of specific solute transporters, most notably the large family of Solute Carrier Transporters (SLC) that supply the CNS with these substances (Abott et al., 2010; Weiss et al., 2009).

Endothelial tight junctions act as a fence in the membrane in order to sequester certain types of transport proteins and lipid rafts to either the luminal or abluminal membrane domain. In effect, TJs prevent these transport proteins and lipid rafts from freely moving from the luminal to the abluminal surface of the endothelium (or vice versa) and thus preserve the polarity of the barrier. Many transport proteins are expressed in either the luminal or abluminal membrane only while others can be found in both membranes of the endothelial cells (Abott et al., 2010). The select location of these transporters most likely results in preferential transport of various molecules in single direction across the BBB.



While the BBB physically prevents most large molecules such as peptides and proteins found in the blood from entering the brain, various endocytotic mechanisms provide routes of entry by which these substances can pass (Abbott et al., 2010). These endocytotic mechanisms involve either adsorptive-mediated transcytosis (AMT) or receptor-mediated transcytosis (RMT).

Cationic, or positively charged, molecules are able to enter the endothelium via AMT. They bind to the cell's surface, are subsequently engulfed by the cell via endocytosis and are then transported across the cell via transcytosis. RMT is used by other macromolecules to transverse the barrier. The ligands of these macromolecules bind to specific receptors on the cell surface, which results in the ligand-receptor complex clustering together to form a caveolus. The caveolus then pinches off into a vesicle which is then transported across the cell. Examples of this are the glucose transporter-1 (GLUT-1) which transports glucose into the brain and the ATP Binding Cassette (ABC) family which transports xenobiotics out of the brain using ATP hydrolysis (Weiss et al., 2009). Monocarboxylic acid, transferrin, insulin, insulin-like growth factor, and leptin also cross the BBB in this manner (Weiss et al, 2009).

Cells from the bone-marrow derived monocyte lineage enter the brain during embryonic development and become resident immunologically-competent microglia (Abbott et al., 2010). However, the BBB acts to prevent most circulating immune cells from entering into the brain thus ensuring that for the most part the brain acts as an immune privileged site. Under pathological conditions however, mononuclear leukocytes, monocytes and

macrophages are recruited to the brain and are able to pass across the BBB (Abott et al., 2010). Mononuclear cells are able to cross the BBB via diapedesis or if the TJs have been disrupted via a paracellular route. During diapedesis the leukocyte adheres to the endothelial cell surface and then enters the cell (Weiss et al., 2009). The luminal membrane is sealed before another opening is created in the abluminal membrane. Thus a fluid-filled channel through the cell that might allow for the extravasation of other blood born particles is never created (Abott et al., 2010). After inflammatory pathological states such as cerebral ischemia the inter-endothelial tight junctions that constitute the first line of defence of the BBB may be temporarily opened allowing for the entry of activated immune cells into the brain tissue (Abott et al., 2010).

1.3 Neurons:

The Neuron can be thought of as the primary unit of the brain, and it is the sensitivity of the neuron to foreign substances that necessitated the creation of the BBB. Despite this there is currently limited knowledge with regard to the neuron's role within the neurovascular unit. However the correlation between brain activity and regional cerebral blood flow and the dynamic nature of neurons' metabolic requirements suggests that neuronal and vascular function must be intrinsically linked (Persidsky et al., 2006)

Communication between the neuron and the other cells that form the NVU is thought to pass either through the astrocytes or directly, via neuronal contact, to the endothelial cell (Koehler et al., 2006 Sandoval et al., 2008). It is also thought that neurons might induce expression of enzymes unique to brain endothelial cells (Persidsky et al., 2006). It has been shown that neurons and glial cells are able to communicate in a bi-directional manner, with glial cells regulating synaptic transmission, neuronal firing thresholds, and plasticity (Sandoval et al., 2008). Astrocytes may also play a role in synaptogenesis in neurons and enhance synaptic performance (Sandoval et al., 2008)

1.4 Astrocytes:

Astrocytes are glial cells that envelop >99% of the BBB endothelium (Hawkins et al., 2005). They are arranged in non-overlapping spatial domains, but coupled to each other in a syncytial network (Kulik et al., 2008). Astrocytes are found between the neurons,

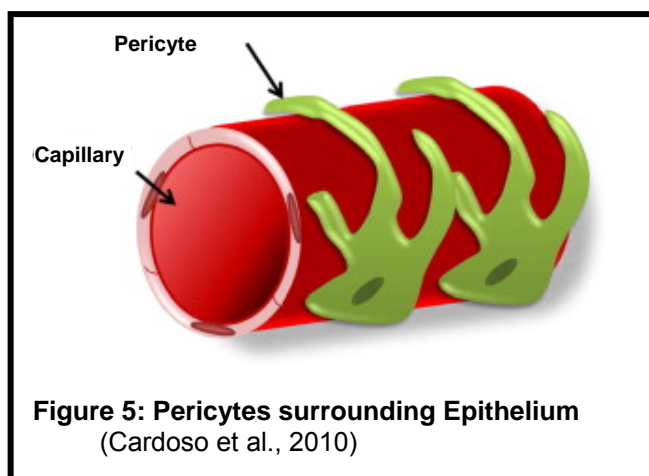
pericytes, and endothelial cells and a single astrocyte can be in contact with upwards of 160,000 synapses (Kulik et al., 2008). Due to this, it is probable that astrocytes are the primary mediators between neuronal activity and the vascular network (Kulik et al., 2008).

Astrocytes play a critical role in cerebral ion homeostasis and transmitter regulation. They contribute to the maintenance and maturation of the BBB and provide structural and metabolic support to neuronal cells (Kulik et al., 2008; Sandoval et al., 2008). Astrocyte end-feet have been shown to mediate regional cerebral blood-flow, and astrocytes have been shown to interact with endothelial cells in order to regulate brain water content and electrolyte balance in both normal and pathological states (Sandoval et al., 2008)

1.5 Pericytes:

Pericytes are the least studied cellular component of the BBB; however, they appear to be actively involved in angiogenesis and vascular branching, endothelial TJ formation, vessel maintenance and integrity, and vasoregulation (Ballabh et al., 2004; Weiss et al., 2009; Persidsky et al., 2006). A lack of pericytes has been associated with endothelial hyperplasia, increased capillary diameter, and changes in TJ proteins. Pericytes have also been shown to migrate away from brain microvessels in response to hypoxia or

brain trauma (Persidsky et al, 2006; Sandoval et al., 2008). Both conditions are associated with increased BBB permeability.



Pericytes are flat, undifferentiated, contractile connective tissue cells that develop around capillary walls. They express non-muscle actins and also contain α -smooth muscle actin which is characteristic of the

vascular smooth muscle (VSM) (Kulik et al., 2008). Pericytes are closely associated with the endothelium and have cellular projections that penetrate the basal lamina and cover

approximately 20 – 30% of the microvascular circumference. The ratio of pericytes to endothelial cells has been correlated with the endothelium's barrier capacity (Persidsky et al., 2006; Weiss et al., 2008)

While it appears certain that pericytes play a role in the endothelium's generation and homeostasis, they have also been attributed with other potential roles within the brain tissue. Pericytes might possess the ability to phagocytise exogenous proteins and present antigens like macrophages (Persidsky et al., 2006). Evidence has also shown that pericytes have contractile properties and might be capable of regulating flow in the capillaries by acting as capillary sphincters (Kulik et al., 2008; Sandoval et al., 2008). In addition, there is evidence that pericytes can communicate directly to endothelial cells through invaginations referred to as "peg-socket" contacts (Armulik et al., 2005). Thus pericytes might facilitate communication between adjacent endothelial cells allowing for an additional layer of communication (Sandoval et al., 2008).

1.6 Basal Lamina/ Extracellular matrix:

The basal lamina is a thin sheet-like network of extracellular matrix components that surrounds the endothelial cells and pericytes, and it is composed of 3 adjacent layers (Weiss et al., 2009). All three layers are composed of different types of collagens, glycoprotein's and proteoglycans (Weiss et al., 2009). All three layers have unique features and are derived from different cell groups. The first is produced by endothelial cells and contains laminin-4 and -5. The second is produced by the astrocytes and contains laminin-1 and -2. The third layer contains collagen IV, is sandwiched between the previous two layers, and both astrocytes and endothelial cells contribute to its construction (Weiss et al., 2009). The extracellular matrix (ECM) of the basal lamina supports the surrounding cells, separates them from each other, and facilitates intercellular communication (Sandoval et al., 2008). The matrix impedes the leakage of red-blood cells during hemorrhage and the transmigration of leucocytes that respond to inflammatory stimuli (del Zoppo et al., 2010). Thus disruption of the extracellular matrix is associated with increased BBB permeability in pathological states (Persidsky et al., 2006). The matrix might also play a role in the expression and maintenance of endothelial TJ proteins.

1.7 Microglia:

Microglia are the resident inflammatory cells of the CNS, they are derived from bone marrow stem cells, and develop from cells of the monocyte/macrophage lineage. Under normal physiological conditions they possess a stellate shape with small bodies and long, thin processes (Cardoso et al., 2010). When they are activated, in response to inflammatory signals, they take on a phagocytic morphology by shifting from long to short processes (Zlokovic, 2008).

Microglia are responsible for surveying the local microenvironment and responding to disturbances of the CNS (Cardoso et al., 2010). They phagocytize debris, release cytotoxic factors, and propagate neuro-inflammation by releasing inflammatory cytokines such as TNF- α and IL-1 β . They are also known to regulate T-cell-mediated immune processes (Aloisi, 2001). Microglia can be found in perivascular space, and it is thought that they might interact with the endothelium and contribute to the properties of the BBB (Cardoso et al., 2010) The exact physiological function of microglia within the NVU is not yet well defined.

1.8 Endothelial Cells:

The brain microvascular endothelial cells are located at the interface between the blood and the brain, and act as the first and most important line of defence between the systemic circulation and the vulnerable brain tissue. Attached at irregular intervals to the abluminal membrane of the endothelium are granular and filamentous pericytes (Hawkins et al., 2005). The brain endothelium not only acts as a barrier to protect the brain, it is also responsible for the transport of micro and macronutrients, receptor-mediated signalling, leukocyte trafficking, and osmoregulation (Persidsky et al., 2006).

There are a number of structural components responsible for these properties. The endothelial cell cytoplasm has uniform thickness with minimal pinocytotic activity, and it has an absence of fenestrations which correlates with the presence of intercellular tight junctions (Hawkins et al., 2005). It has a high number of mitochondria, which are required for the multiple energy dependent processes involved in nutrient support and protection of the brain, and there is a polarized expression of membrane receptors and

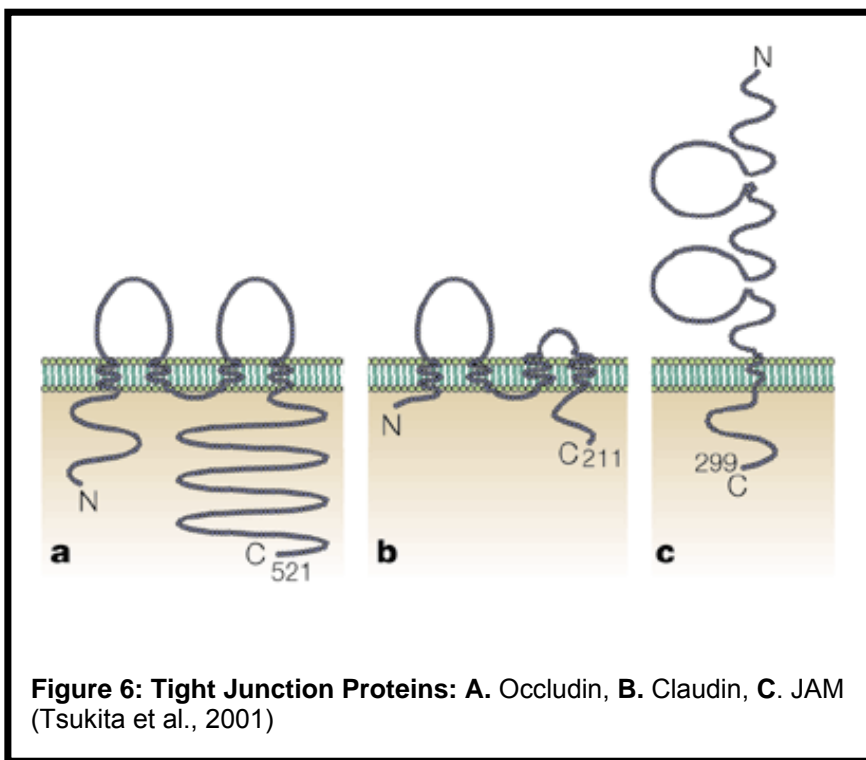
transporters between the luminal and abluminal membrane surfaces of the cell which are responsible for the active transport of blood-borne nutrients to the brain or the efflux of potentially toxic compounds from the brain to the vasculature (Abbott et al., 2005; Hawkins et al., 2005; Sandoval et al., 2008; Persidsky et al., 2006; Weiss et al., 2008). For example, the enzymes alkaline phosphatase (AP) and γ -glutamyltransferase (γ -GTP) are present at the luminal endothelium, whereas Na⁺, K⁺ ATPase and the sodium-dependent neutral amino acid transporter are associated with the abluminal surface of the endothelium. The glucose transporter, GLUT-1, is primarily found on the abluminal surface while drug efflux transporters, such as P-glycoprotein (Pgp) are primarily found on the luminal membrane surface (Abbott et al., 2005; Persidsky et al., 2006). In addition, the endothelium contains several families of molecules that are integral to forming the barrier that sustains the brain's homeostasis. These molecules include:

- Tight junctions (TJ) which are composed of occludin, claudins, zonula occludens (ZO), AF6, and 7H;
- Junctional adhesion molecules (JAM).
- Adherens junctions (AJ) which are composed of cadherins, catenins, vinculin, and actinin

1.9 Tight Junctions, Junctional Adhesion Molecules, and Adherens Junctions:

TJs are responsible for limiting the paracellular flux of hydrophilic molecules across the BBB. TJs, along with adherens junctions, form a seal between adjacent endothelial cells (ECs) (Sandoval et al., 2008). This seal also has a fencing function by separating the luminal side from the abluminal side of the plasma membrane (Sandoval et al., 2008). Under normal physiological conditions, substances with a molecular weight greater than 180 Da do not gain access through the TJs (Mitic and Anderson, 1998). TJs also serve as an impediment to ion movement, resulting in the high in-vivo electrical resistance (approximately 1800 Ω cm²) of the BBB, (Abbott et al., 2010). The barrier function is influenced by the way TJ proteins are organised and interact. The sealing properties of TJs vary between brain endothelial cells at different locations. Tight junctions of the BBB are sensitive to locally produced circulating factors which can on a minute-to-minute basis modulate the properties and the function of the paracellular pathway (Abbott et al., 2010). For example, as endothelial capillaries proceed to post-capillary venules a

reduced sealing capacity is observed (Sandoval et al., 2008). Many of the cell types associated with brain vessels such as microglia and astrocytes can release vasoactive agents and cytokines which can modify tight junction assembly and barrier permeability (Abbott et al., 2010). The regulation of TJs is also mediated by multiple signalling pathways. cAMP is a major regulator of TJs in brain ECs, VEGF has been shown to affect TJ assembly and increase BBB permeability via phosphorylation, and/or degradation (Weiss et al., 2009). TJs have been shown to be regulated by the activity of small G-proteins of the Rho family (Rho GTPases) along with vasoactive compounds such as bradykinin or angiotensin II or adhesion molecules such as ICAM-1. Reactive



oxygen species also play a role. All of these substances have been shown to lead to increases in paracellular permeability as well as trans-endothelial migration of leukocytes (Weiss et al. 2009). In addition, alterations in both intracellular and

extracellular calcium concentration can modulate tight junction assembly, effectively altering the electrical resistance across the endothelium (Abbott et al., 2010; Abbott et al., 2006).

The junctional complexes between endothelial cells are composed of TJs and AJs. The TJs are formed from occludin and claudin proteins that span between cells and junctional adhesion molecules (JAMs) (Wolburg and Lippoldt, 2002). Claudin and occludin are linked to intracellular actin and the cytoskeleton via the intracellular scaffold proteins ZO-1, ZO-2 and ZO-3 and cingulin (Wolburg and Lippoldt, 2002). AJs are

composed of cadherin proteins that span the intercellular cleft and are linked into the cell cytoplasm by the scaffolding proteins alpha, beta and gamma catenin (Abbott et al., 2010). The AJs hold the cells together giving the tissue structural support (Abbott et al., 2010). They are necessary for the formation of TJs, and their degradation inevitably leads to barrier disruption (Wolburg and Lippoldt, 2002).

1.9.1 Occludin:

Occludin is a 60–65 kDa proteins found in high concentrations within the membrane of endothelial cells at BBB TJs (Sandoval et al., 2008). It is composed of four transmembranous domains with the carboxyl and amino terminals found in the cytoplasm and two extracellular loops spanning the intercellular cleft (Furuse et al. 1993). The loops interact homophilically to form intermembranous strands. These strands may contain fluctuating channels allowing the selective diffusion of ions and hydrophilic molecules (Matter and Balda, 2003). The cytoplasmic C-terminal domain connects occludin with the cytoskeleton via accessory proteins, ZO-1 and ZO-2 (Fanning et al. 1998). Occludin is much larger than the claudins and despite their similar two loop transmembrane structure they do not share a similar amino acid sequence (Ballabh et al., 2004).

Occludin's carboxy-terminal binds to ZOs that in turn bind to the actin cytoskeleton (Fanning et al., 1998; Furuse et al., 1994). The carboxy portion of the protein is able to bind to several proteins which can then influence its regulatory actions (e.g. protein kinase-C (PKC), c-Yes, and connexin-26) (Nusrat et al., 2000). The phosphorylation state of occludin may play a role in determining its location and function within the cell membrane. Heavily phosphorylated occludin is concentrated at the cellular membrane (Sakakibara et al., 1997; Wong, 1997). The less phosphorylated form of occludin is located within the cytoplasm and may serve as a pool of reserve protein (Sakakibara et al., 1997; Wong, 1997). Occludin with phosphorylated serine and threonine can be found within the cell membrane while occludin with phosphorylated tyrosine is correlated with a disassociation from intracellular zonula occluden proteins and an increase in TJ permeability (Sandoval et al., 2008).

While occludin may not be necessary for the formation of TJs it seems likely that occludin plays an active role in BBB function: it is found in much lower concentrations in endothelial cells not associated with the CNS, decreased occludin expression has been associated with BBB dysfunction in a number of disease states and, high levels of occludin correlate with greater electrical resistance across the membrane and decreased paracellular permeability (Sandoval et al., 2008).

1.9.2 Claudin:

Claudins are 20–24 kDa proteins and are most likely the major component behind the BBB endothelial cell's impermeability. Claudins share very similar structure and membrane location with occluding - they are composed of four transmembranous domains with the carboxyl and amino terminals found in the cytoplasm and two extracellular loops spanning the intercellular cleft - however, as previously stated, they share no sequence homology with occludin (Morita et al. 1999). The carboxy terminal of claudins binds to cytoplasmic proteins including ZO-1, ZO-2, and ZO-3 (Ballabh et al., 2004). The extracellular loops interact homophilically and heterophilically to form intermembranous strands that form the primary seal of the BBB (Piontek et al., 2008).

There are 24 members in the Claudin family, but only Claudins-3, -5, and -12 have been shown to be present within BBB endothelial cells (Hawkins et al., 2005). Claudin-5 has been shown to have particular importance in regards to the active regulation of small molecule paracellular permeability at the BBB. Increased claudin-5 expression increases transendothelial resistance and decreases BBB permeability (Honda et al., 2006), and decreased claudin-5 expression results in a decrease in BBB integrity to molecules smaller than 800 Da (Nitta et al., 2003). Much like Occludin, Claudins may be regulated via phosphorylation. Phosphorylation of claudin-5 by the protein kinase-A (PKA) or through Rho kinase activation has been shown to increase TJ permeability (Soma et al., 2004; Yamamoto et al., 2008).

1.9.3 JAM:

The third type of TJ-associated membrane protein is the 40 kDa junctional adhesion molecules (JAM) (Ballabh et al., 2004). JAMs are a family of immunoglobulin superfamily proteins that are found on the intercellular cleft of TJs. Intracellularly JAMs bind to ZO-1, afadin (AF-6), partitioning defective protein-3 (PAR-3) and multi-PDZ-protein-1 (MUPP-1) (Ebnet et al., 2003). They have a single membrane-spanning chain with a large extracellular domain (Martin-Padura et al. 1998). The extracellular portion is formed by disulfide bonds and is involved in homophilic and heterophilic interactions (Weber et al., 2007). JAMs participate in the assembly and maintenance of the TJs, signalling of cytoskeletal associated proteins, and cell-to-cell adhesion and monocyte transmigration (diapedesis) through BBB (Aurrand-Lions et al., 2001; Bazzoni et al., 2000; Weber et al., 2007).

Several JAM proteins have been identified: JAM-A, JAM-B, JAM-C JAM-4 and JAML. JAMs-A, -B, and -C are found in endothelial cells (Sandoval et al., 2008). JAM-A is highly expressed in the cerebrovasculature, and homophilic JAM-A interactions are important for the stabilization of cellular junctions and decreasing paracellular permeability (Sandoval et al., 2008). A decrease in JAM-A expression correlates with a decrease in TJ integrity (Yeung et al., 2008).

1.9.4 MAGUK:

The cytoplasmic accessory proteins involved in TJ formation and regulation include cingulin, 7H6, and AF-6, ZO-1 (220 kDa), ZO-2 (160 kDa), and ZO-3 (130 kDa). These are phosphoproteins and members of the membrane-associated guanylate kinase-like family of proteins (MAGUKs) and are capable of forming heterodimeric complexes with one another (Sandoval et al., 2008; Hawkins et al., 2005). They all have homologous sequences and contain three PDZ domains (PDZ1, PDZ2, and PDZ3), one SH3 domain, and one guanyl kinaselike (GUK) domain (Ballabh et al., 2004). These domains function as protein binding molecules and may play a role in the recruitment of the transmembrane TJ proteins to their final destination within the cellular membrane (Bazzoni and Dejana, 2004; Tsukita et al., 2001).

ZO-1 interacts with both ZO-2 and ZO-3, via the PDZ domains, and the PDZ1 domain of all three proteins has been reported to bind directly to the COOH-terminal of claudins (Itoh et al., 1999). Loss or dissociation of ZO-1 from the junctional complexes is associated with increased barrier permeability (Mark and Davis 2002). ZO-1 might also be responsible for communicating the state of the TJs to the interior of the cell or vice versa.

Occludin interacts with the GUK domain on ZO-1 (Ballabh et al., 2004). JAM binds directly to ZO-1 and other PDZ-containing proteins (Ebnet et al., 2000). Actin binds to the proline-rich COOH-terminal of ZO-1 and ZO-2. This protein complex cross-links to the cytoskeleton providing structural support to the endothelial cells (Haskins et al., 1998). ZO-2 binds to transmembranous proteins of the TJs and transcription factors, and it is found in the nucleus during stress and proliferation (Traweger et al. 2003). ZO-2 may be able to act as a replacement for ZO-1, thus facilitating formation of a competent barrier (Sandoval et al., 2008).

Other TJ accessory proteins include Cingulin and AF-6. Cingulin is a 140–160 kDa phosphoprotein found on the cytoplasmic surface of the TJs (Sandoval et al., 2008). It binds to the ZO proteins, myosin, JAM-A, and AF6, and may play a as a structural support within the TJ complex (Bazzoni et al., 2000; Cordenonsi et al., 1999). Cingulin may also act to transfer the mechanical force generated by the contraction of the actin–myosin cytoskeleton, thus participating in TJ permeability (Cordenonsi et al., 1999). 7H6 is a 155 kDa phosphoprotein that is able to reversibly dissociate from the TJ under conditions of adenosine triphosphate (ATP) depletion, and is associated with increased paracellular permeability (Sandoval et al., 2008). AF-6 is a 180 kDa protein that interacts with ZO-1 in order to regulate TJs (Yamamoto et al., 1999).

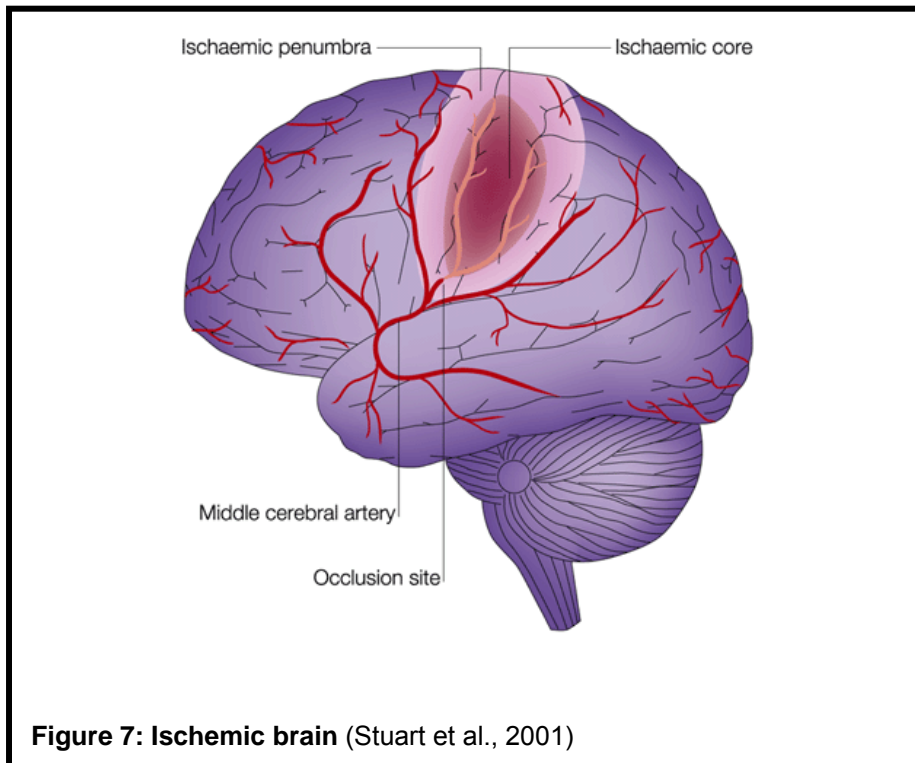
Several other TJ accessory proteins have been identified (e.g. junction-associated coiled-coil protein (JACOP), calcium-dependent serine protein kinase (CASK), regulator of G-protein signaling-5 (RG-5); however, their structural and regulatory roles in regards to the BBB have not yet been determined (Hawkins et al., 2005; Zlokovic, 2008).

1.9.5 Adherens Junctions:

The adherens junctions form a belt around the apical end of the junctional cleft, just below the TJs (Sandoval et al., 2008). It appears that TJs serve as the primary paracellular barrier and AJs act to localize and stabilize the TJs (Dejana et al., 2008). AJs are composed of the membrane protein cadherin which forms a complex with the submembranal plaque proteins β -catenin and p120-catenin, and α -catenin, and the actin cytoskeleton (Ballabh et al., 2004; Dejana et al., 2008). The extracellular calcium-dependent cadherin domains of the AJs interact homophilically to form adhesive contacts between cells – although this extracellular binding domain is thought to be insufficient to promote junction formation (Sandoval et al., 2008).

2. Cerebral Ischemia Overview:

Ischemic stroke results from a transient or permanent reduction in cerebral blood flow of a major brain artery. The reduction in flow is typically caused by the occlusion of a cerebral artery by an embolus or local thrombosis (Dirnagl et al., 1999). This sudden decrease or loss of blood circulation to an area of the brain, ultimately involves the destruction and/or dysfunction of brain cells resulting in a corresponding loss of neurological function (Donnan et al., 2008). With an incidence of approximately 250–400 in 100,000 and a mortality rate of around 30%, stroke remains the third leading cause of death in industrialized countries. (Dirnagl et al., 1999)

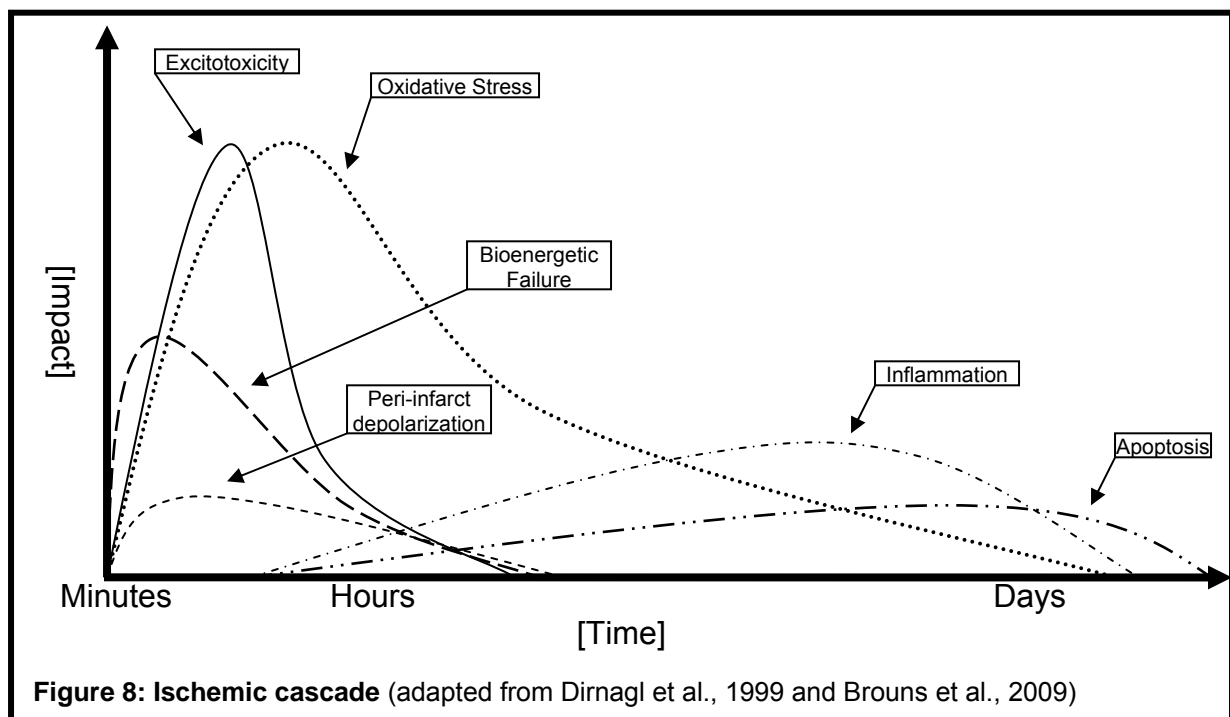


The series of neurochemical processes that are unleashed by transient or permanent focal cerebral ischemia are referred to as the ischemic cascade. This is a complex series of events that evolve in time and space and have over-lapping and redundant features; however, they can be delineated as follows:

Relationship between the Blood-Brain Barrier and Cerebral Ischemia

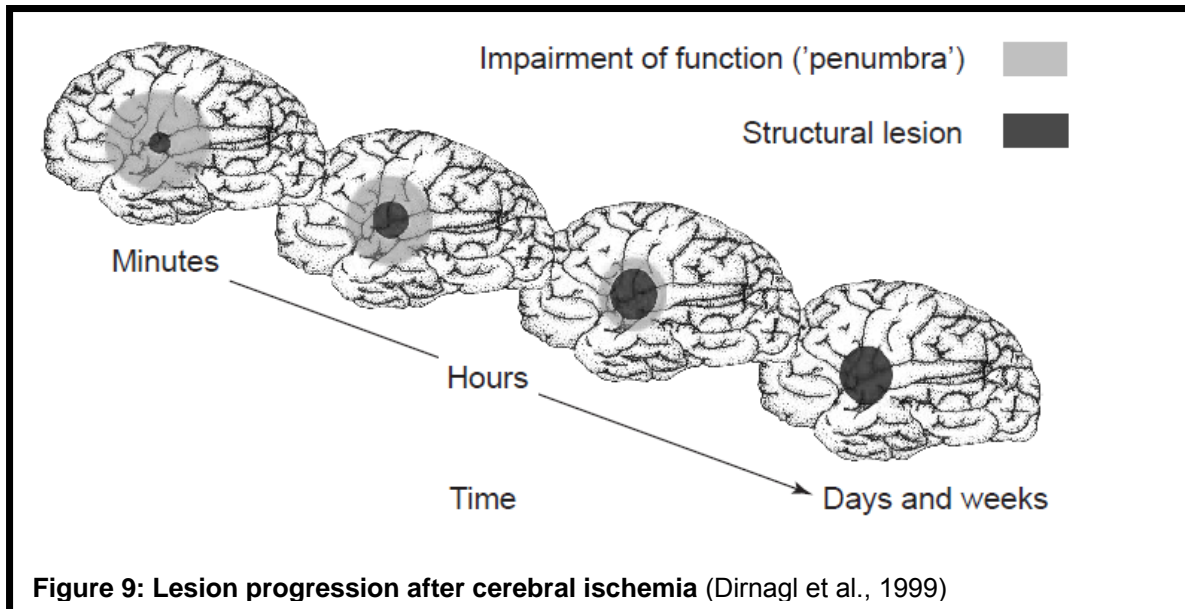
- Depletion of ATP which leads to cellular bioenergetic failure
- Followed by excitotoxicity, excitotoxic glutamate efflux and ionic imbalance component (e.g. increased intracellular calcium)
- Oxidative stress
- Blood–brain barrier dysfunction
- Post-ischemic inflammation
- Finally, cell death of neurons, glia and endothelial cells

Ischemic stroke begins with severe focal hypoperfusion, but cerebral injury continues



over hours or even days and the hemodynamic, metabolic and ionic changes described above do not affect the ischemic territory homogeneously. The amount of permanent damage depends on two factors: the degree and the duration of ischemia. Regions of the brain with severely impaired blood flow (20% below normal) become rapidly and irreversibly injured and are referred to as the ischemic core (Hossmann et al., 1994). Cells in the core are killed rapidly by lipolysis, proteolysis, and disaggregation of microtubules, total bioenergetic failure and breakdown of ion homeostasis (Dirnagl et al., 1999). A region of functionally impaired but structurally intact tissue called the penumbra lies between the lethally damaged core and the normal brain. The penumbra is an area

of inhibited blood flow with partially preserved energy and given time and a lack of treatment it will eventually progress to infarction (Baron et al., 1999; Hossmann et al., 1994; Markus et al., 2004). The penumbra can be salvaged by restoring the blood flow to the affected region or by interfering with the ischemic cascade.



2.1 Energy Failure:

Brain tissue has a relatively high consumption of oxygen and glucose, and depends primarily on oxidative phosphorylation for energy production. Focal hypoperfusion restricts the delivery of essential substrates and causes the brain cells' normal process for adenosine triphosphate (ATP) production for energy to fail. This quickly leads to dysfunction of energy-dependent ion transport pumps which in turn leads to a loss of membrane potential and depolarization of neurones and glia (Martin et al., 1994). Consequently, somatodendritic as well as presynaptic voltage-dependent calcium channels become activated and excitatory amino acids are released into the extracellular space (Dirnagl et al., 1999). At the same time, transport of glutamate from depolarized astrocytes is induced and energy-dependent processes such as the presynaptic reuptake of excitatory amino acids are impeded (Nicholls et al., 1990). This further increases the accumulation of glutamate in the extracellular space (Dirnagl et al., 1999).

2.2 Excitotoxicity:

Excitotoxicity is an important factor when considering tissue damage due to focal cerebral ischemia. Excitotoxic mechanisms can lead to acute cell death via necrosis or pre-programmed and delayed cell death via apoptosis. In addition, the intracellular signalling pathways activated during excitotoxicity trigger the expression of genes that initiate post-ischemic inflammation which is yet another pathogenic process that gives rise to ischemic injury (Dirnagl et al., 1999)

Excitotoxicity refers to the secondary damage caused by pathological activation and calcium uptake by neurons due to abnormal release of excitatory neurotransmitters from dying cells (Meldrum et al., 1985). As described above, excitatory neurotransmitters, especially glutamate, accumulate in the extracellular space. The build-up of glutamate results in over stimulation of α -amino-3-hydroxy-5-methyl-4-isoxazole propionic acid (AMPA), kainate, and N-methyl-d-aspartic acid (NMDA)-type glutamate receptors on other neurons, with consequent influx of Na^+ , Cl^- and Ca^{2+} ions through the channels gated by these receptors (Dirnagl et al., 1999; Chen et al., 2008). These neurons then become depolarized, causing more calcium influx and more glutamate release leading to local amplification of the initial ischemic insult. Additionally, as the influx of sodium and calcium is much larger than the efflux of potassium water passively follows the ion influx, resulting in cytotoxic edema (Brouns et al., 2009). Cytotoxic edema is caused by translocation of interstitial water into the intracellular compartment and results in a net increase in cell ions and water (Betz et al., 1989; Young et al., 1987). Despite the uptake of water by the affected brain cells there is no significant increase in overall brain volume due to the corresponding reduction in extracellular space (Heo et al., 2005).

The intracellular increase of the universal second messenger Ca^{2+} initiates a series of cytoplasmatic and nuclear events among which is the generation of free radicals and the activation of calcium-dependent enzymes. These include proteolytic enzymes that degrade cytoskeletal proteins and extracellular matrix proteins as well as phospholipase A2, calpain, endonucleases, adenosine triphosphatase, cyclooxygenase and nitric oxide synthase type I resulting in extensive cellular damage and generation of free radical species (Choi et al., 1995; Chen et al., 1997; Chan et al., 2001; Cui et al., 2000; El Kossi et al., 2000; Epe et al., 1996; Kelly et al., 2008; Kontos et al., 1985; Kontos et al., 2001;

Nelson et al., 1992). The production of free radicals and activation of degradative enzymes leads to acute cell death through necrosis, but excitotoxic mechanisms can also initiate molecular events that lead to apoptosis. In addition, the intracellular signalling pathways activated during excitotoxicity trigger the expression of genes that initiate post-ischemic inflammation, another process that contributes to ischemic injury.

2.3 Oxidative Stress:

Oxidative stress occurs when the production of free radicals overpowers the endogenous scavenging capacity of cellular antioxidant defences. Data suggest that reactive oxygen and nitrogen molecules are important mediators of tissue injury in acute ischemic stroke (Chan et al., 2001; Cui et al., 2000; El Kossi et al., 2000; Epe et al., 1996; Kelly et al., 2008; Kontos et al., 1985; Kontos et al., 2001; Nelson et al., 1992). The free radicals they give rise to result in release of calcium ions from intracellular stores, protein denaturation, lipid peroxidation, damage to the cytoskeleton and DNA, and inactivation of enzymes (Evans et al., 2004; Liu et al., 1996).

Mitochondrial oxygen radical production is triggered by elevated intracellular calcium, sodium, and adenosine diphosphate levels in ischemic cells. Enzymatic conversions, such as cyclooxygenase-dependent conversion of arachidonic acid to prostanoids, can also produce oxygen radicals (Chan et al., 2001). One such radical is superoxide, which is an intermediary in the electron transport chain. Peroxynitrite is highly toxic to tissue and is formed from superoxide and nitric oxide (Beckman et al., 1996; Ladecola et al., 1997). Nitric oxide is produced from L-arginine by nitric oxide synthase (NOS). NOS type I is calcium-dependent and primarily expressed in neurons. NOS type II is upregulated in response to a variety of cytokines (Masters et al., 1994). Ischemia causes an initial surge in NOS type I activity, and at later stages an increase in NOS type II activity is seen in a cells such as glia and infiltrating neutrophils (Brouns et al., 2009). Once produced, peroxynitrite spontaneously decomposes to form the hydroxyl radical. The hydroxyl radical, while short lived, is the most reactive oxygen species and is the greatest cause of tissue injury.

Free radicals disrupt the inner mitochondrial membrane and oxidate proteins that are responsible for mediating electron transport and production of ATP. Cytochrome-C is

subsequently released from the mitochondria and triggers apoptosis. Moderate oxidation gives rise to apoptosis while severe oxidative stress leads to cell death via necrosis (Evans et al., 2004; Liu et al., 1996).

Oxidative stress also increases BBB permeability through activation of matrix-metalloproteinases (MMP) such as MMP-9, and through endothelial cell damage (Montaner et al., 2003; Rosenberg et al., 1998; Chan et al., 2001; Kontos et al., 1985). Oxidative stress has also been implicated in the disruption of endothelial TJs which results in increased paracellular permeability (Rao et al., 2002; Schreiber et al., 2007). Free radicals also lead to vasoconstriction by altering vascular reactivity to CO₂ by interacting with nitric oxide and superoxide (Kontos 2001). Oxygen radicals have also been shown to increase platelet aggregability (Sandoval et al., 2008).

2.4 Inflammation:

Several different types of cells play a role in post-ischemic inflammation including the native microglia (the resident macrophages of the brain) and astrocytes as well as infiltrating neutrophils, macrophages and monocytes.

The inflammatory response of astrocytes and microglia is triggered by reactive oxygen species (ROS). Four to six hours after an ischemic event astrocytes become hypertrophic and start to secrete inflammatory factors such as cytokines, chemokines and inducible nitric oxide synthase (Che et al., 2001; Dong et al., 2001). During this same time period microglia become activated, retract their processes and become phagocytic in nature (Brouns et al., 2009). They too start to secrete a plethora of cytotoxic substances after their initial activation.

Neutrophils are the first leukocytes to extravasate into the brain and begin to do so within 6 to 48 hours (depending on the severity of the insult) of the initial ischemic event (Buck et al., 2008; Tang et al., 2006). Once they have crossed into the brain they may damage the penumbra by releasing additional pro-inflammatory mediators (Barone et al., 1999; Becker et al., 1998; Danton et al., 2003; Emsley et al., 2002; Wang et al., 2007). Macrophages and monocytes follow neutrophils, migrating into the ischemic territory and becoming the predominant cells five to seven days later (Che et al., 2001; Grau et al., 2001).

Leukocytes are able to pass through the endothelium and over into the brain due to several classes of adhesion molecules including selectins, integrins, and the immunoglobulin superfamily. E and P-selectins become upregulated after ischemia and facilitate leukocyte rolling and recruitment (Haring et al., 1996; Huang et al., 2000). Various chemokines and cytokines activate leukocytes and induce them to express integrins on their cell surface. These integrins are necessary in order for the cell to recognize endothelial adhesion molecules (Matarin et al., 2008).

Cytokines are important inflammatory mediators that are produced by immune cells and resident brain cells after ischemia (Allan et al., 2001). Chemokines are important for cellular communication and inflammatory cell recruitment, and their expression increases leukocyte infiltration (Stamatovic et al., 2003). Chemokines have also been found to play a role in BBB permeability (Dimitrijevic et al., 2006). As previously mentioned, nitric oxide synthases are upregulated in ischemia, especially in circulating leukocytes, microglia, and astrocytes, and they inflict damage through several mechanisms (Forster et al., 1999; Ladecola et al., 1997). Inflammatory cells also generate reactive oxygen species and produce MMPs generating even more damage to the ischemic brain (Gidday et al., 2005).

2.5 Cell Death:

After cerebral ischemia, affected brain cells that have been damaged by glutamate-receptor activation, Ca²⁺ overload, and exposure to reactive oxygen species and have mitochondrial and DNA damage can die by necrosis, apoptosis, or in some cases caspase-independent programmed cell death (Dirnagl et al., 1999; Brouns et al., 2009). After acute, permanent vascular occlusion most cells in the core ischemic territory die via necrosis. In less severe injury, particularly within the ischemic penumbra, apoptosis-like cell death prevails. Caspase-independent programmed cell death is distinct from necrosis and apoptosis and also plays a large role in cell death after an ischemic event (Brouns et al., 2009). Several factors determine which mechanism dominates, including the local degree of ischemia, cell maturity, the concentration of intracellular free Ca²⁺ and the cellular microenvironment (Choi et al., 1995; Brauns et al., 2009).

Necrosis is a form of cell death associated with failure of the plasma membrane and cytotoxic edema of both the cell and internal organelles (Johnson et al., 1993; Martin et al., 1998). If the cell dies through necrosis, it releases more glutamate and toxins into the environment which affects neurons located within the vicinity. In contrast to necrosis is apoptosis, a genetically regulated programme that allows cells to die with very little inflammation and minimal release of genetic material (Choi et al., 1996; Namura et al., 1998). Activation of glutamate receptors may promote apoptosis by activating cellular sensors linked to the apoptosis cascade (Choi et al., 1996; Choi et al., 1995; Namura et al., 1998; Thornberry et al., 1998). Caspase-mediated apoptosis is initiated by release of cytochrome-C from mitochondria (Green et al., 1998).

2.6 Cerebral Reperfusion Injury:

Reperfusion, or the reestablishment of cerebral blood flow to the ischemic brain, is necessary for tissue survival; however, it may also contribute to additional tissue damage or reperfusion injury and may, in some instances lead to hemorrhagic transformation (Albers et al., 2006; Kuroda et al., 1997; del Zoppo et al., 1998). Leukocytes play a part in reperfusion injury via their role in damaging the endothelium, obstructing the microcirculation, and disrupting the BBB. They are also responsible for the release of various cytokines which enhance inflammation (Pan et al., 2007). Platelets also contribute to reperfusion injury by obstructing vessels which leads to the “no-reflow phenomenon”. In addition, they release a variety of biochemical factors that may enhance oxidative stress and the inflammatory cascade (Wong et al., 2008; Brauns et al., 2009).

While many reports are contradictory, there are potentially three phases of increased BBB permeability after reperfusion. The initial phase of reperfusion permeability is associated with acute elevations in regional cerebral blood flow and loss of cerebral autoregulation (Spengos et al., 2006). After the initial hyperemia the no-reflow effect occurs which leads to hypoperfusion of the ischemic area. This latter effect has been attributed to multiple factors: including continued cerebral metabolic depression, microvascular obstruction, occlusion via endothelial and astrocytic end-feet swelling, and the formation of endothelial microvilli. It exasperates the initial ischemic event by depriving the damaged tissue of valuable oxygen and nutrients (Sandoval et al., 2008).

This is then followed by a biphasic permeability response. The first phase of biphasic permeability occurs around three to eight hours after reperfusion and results from inflammatory and oxidative stress of the BBB and degradation of the extracellular matrix (Heo et al., 2005; Wang 2007). The second phase of biphasic permeability occurs within 18-96 hours after reperfusion. This final phase is associated with angiogenesis and vasogenic edema of the damaged tissue and is dependent upon several factors including the degree of insult and the brain region being evaluated (Belayev et al., 1996; Preston et al., 1993; Rosenberg et al., 1998).

2.7 Current treatment for stroke:

At the present time, the only pharmacological treatment for cerebral ischemia with proven efficacy is tissue plasminogen activator (tPA). tPA however, must be administered within 3 to 4.5 hours after stroke onset to be effective and it may increase the chance of developing a hemorrhage in the affected tissue of the brain (Barone et al, 2001). Furthermore only 5 to 8% of patients qualify for treatment within allotted time frame (Barone et al, 2001).

8. References:

- Abbott NJ, Patabendige AA, Dolman DE, Yusof SR, Begley DJ. Structure and function of the blood-brain barrier. *Neurobiol Dis.* 2010 Jan;37(1):13-25. Epub 2009 Aug 5.
- Abbott NJ. Dynamics of CNS barriers: evolution, differentiation, and modulation. *Cell Mol Neurobiol.* 2005 Feb;25(1):5-23.
- Abumiya T, Lucero J, Heo JH, Tagaya M, Koziol JA, Copeland BR, del Zoppo GJ. Activated microvessels express vascular endothelial growth factor and integrin alpha(v)beta3 during focal cerebral ischemia. *J Cereb Blood Flow Metab.* 1999 Sep;19(9):1038-50.
- Adibhatla RM, Hatcher JF. Tissue plasminogen activator (tPA) and matrix metalloproteinases in the pathogenesis of stroke: therapeutic strategies. *CNS Neurol Disord Drug Targets.* 2008 Jun;7(3):243-53.
- Albers GW, Thijs VN, Wechsler L, Kemp S, Schlaug G, Skalabrin E, Bammer R, Kakuda W, Lansberg MG, Shuaib A, Coplin W, Hamilton S, Moseley M, Marks MP; DEFUSE Investigators. Magnetic resonance imaging profiles predict clinical response to early reperfusion: the diffusion and perfusion imaging evaluation for understanding stroke evolution (DEFUSE) study. *Ann Neurol.* 2006 Nov;60(5):508-17.
- Allan SM, Rothwell NJ. Cytokines and acute neurodegeneration. *Nat Rev Neurosci.* 2001 Oct;2(10):734-44. Review.
- Allan SM, Rothwell NJ. Cytokines and acute neurodegeneration. *Nat Rev Neurosci.* 2001 Oct;2(10):734-44.
- Aloisi F. Immune function of microglia. *Glia.* 2001 Nov;36(2):165-79.
- Anderson JM. Molecular structure of tight junctions and their role in epithelial transport. *News Physiol Sci* 2001; 16: 126–130.
- Argaw AT, Gurfein BT, Zhang Y, Zameer A, John GR. VEGF-mediated disruption of endothelial CLN-5 promotes blood-brain barrier breakdown. *Proc Natl Acad Sci U S A.* 2009 Feb 10;106(6):1977-82. Epub 2009 Jan 27.
- Armulik A, Abramsson A, Betsholtz C. Endothelial/pericyte interactions. *Circ Res.* 2005 Sep 16;97(6):512-23.
- Asahi M, Asahi K, Jung JC, del Zoppo GJ, Fini ME, Lo EH. Role for matrix metalloproteinase 9 after focal cerebral ischemia: effects of gene knockout and

- enzyme inhibition with BB-94. *J Cereb Blood Flow Metab.* 2000 Dec;20(12):1681-9.
- Asahi M, Wang X, Mori T, Sumii T, Jung JC, Moskowitz MA, Fini ME, Lo EH. Effects of matrix metalloproteinase-9 gene knock-out on the proteolysis of blood-brain barrier and white matter components after cerebral ischemia. *J Neurosci.* 2001 Oct 1;21(19):7724-32.
- Aschner JL, Lum H, Fletcher PW, Malik AB. Bradykinin- and thrombin-induced increases in endothelial permeability occur independently of phospholipase C but require protein kinase C activation. *J Cell Physiol.* 1997 Dec;173(3):387-96.
- Aurrand-Lions M, Duncan L, Ballestrem C, Imhof BA. JAM-2, a novel immunoglobulin superfamily molecule, expressed by endothelial and lymphatic cells. *J Biol Chem.* 2001 Jan 26;276(4):2733-41.
- Ballabh P, Braun A, Nedergaard M. The blood-brain barrier: an overview: structure, regulation, and clinical implications. *Neurobiol Dis.* 2004 Jun;16(1):1-13.
- Bang OY, Buck BH, Saver JL, Alger JR, Yoon SR, Starkman S, Ovbiagele B, Kim D, Ali LK, Sanossian N, Jahan R, Duckwiler GR, Viñuela F, Salamon N, Villablanca JP, Liebeskind DS. Prediction of hemorrhagic transformation after recanalization therapy using T2*-permeability magnetic resonance imaging. *Ann Neurol.* 2007 Aug;62(2):170-6.
- Barnstable CJ, Tombran-Tink J. Neuroprotective and antiangiogenic actions of PEDF in the eye: molecular targets and therapeutic potential. *Prog Retin Eye Res.* 2004 Sep;23(5):561-77.
- Baron JC. Mapping the ischemic penumbra with PET: implications for acute stroke treatment. *Cerebrovasc Dis.* 1999 Jul-Aug;9(4):193-201.
- Barone FC, Feuerstein GZ. Inflammatory mediators and stroke: new opportunities for novel therapeutics. *J Cereb Blood Flow Metab.* 1999 Aug;19(8):819-34.
- Bazzoni G, Dejana E. Endothelial cell-to-cell junctions: molecular organization and role in vascular homeostasis. *Physiol Rev.* 2004 Jul;84(3):869-901.
- Bazzoni G, Martinez-Estrada OM, Mueller F, Nelboeck P, Schmid G, Bartfai T, Dejana E, Brockhaus M. Homophilic interaction of junctional adhesion molecule. *J Biol Chem.* 2000 Oct 6;275(40):30970-6.
- Becker KJ. Inflammation and acute stroke. *Curr Opin Neurol.* 1998 Feb;11(1):45-9.

- Beckman JS, Ye YZ, Chen J, Conger KA. The interactions of nitric oxide with oxygen radicals and scavengers in cerebral ischemic injury. *Adv Neurol.* 1996;71:339-50; discussion 350-4.
- Beckman JS. Oxidative damage and tyrosine nitration from peroxynitrite. *Chem Res Toxicol.* 1996 Jul-Aug;9(5):836-44.
- Belayev L, Busto R, Zhao W, Ginsberg MD. Quantitative evaluation of blood-brain barrier permeability following middle cerebral artery occlusion in rats. *Brain Res.* 1996 Nov 11;739(1-2):88-96.
- Betz AL, Ennis SR, Schielke GP. Blood-brain barrier sodium transport limits development of brain edema during partial ischemia in gerbils. *Stroke.* 1989 Sep;20(9):1253-9.
- Brightman, M. W., M. Hori, S. I. Rapaport, T. S. Osmotic opening of tight junctions in cerebral endothelium. *J. Comp. Neurol.* 152: 317-325, 1965.
- Brouns R, De Deyn PP. The complexity of neurobiological processes in acute ischemic stroke. *Clin Neurol Neurosurg.* 2009 Jul;111(6):483-95.
- Buck BH, Liebeskind DS, Saver JL, Bang OY, Yun SW, Starkman S, Ali LK, Kim D, Villablanca JP, Salamon N, Razinia T, Ovbiagele B. Early neutrophilia is associated with volume of ischemic tissue in acute stroke. *Stroke.* 2008 Feb;39(2):355-60.
- Campbell M, Nguyen AT, Kiang AS, Tam L, Kenna PF, Dhubhghaill SN, Humphries M, Farrar GJ, Humphries P. Reversible and size-selective opening of the inner Blood-Retina barrier: a novel therapeutic strategy. *Adv Exp Med Biol.* 2010;664:301-8.
- Cardoso FL, Brites D, Brito MA. Looking at the blood-brain barrier: molecular anatomy and possible investigation approaches. *Brain Res Rev.* 2010 Sep 24;64(2):328-63.
- Chamorro A, Hallenbeck J. The harms and benefits of inflammatory and immune responses in vascular disease. *Stroke.* 2006 Feb;37(2):291-3.
- Chan PH. Reactive oxygen radicals in signaling and damage in the ischemic brain. *J Cereb Blood Flow Metab.* 2001 Jan;21(1):2-14.
- Che X, Ye W, Panga L, Wu DC, Yang GY. Monocyte chemoattractant protein-1 expressed in neurons and astrocytes during focal ischemia in mice. *Brain Res.* 2001 Jun 1;902(2):171-7

- Chen M, Lu TJ, Chen XJ, Zhou Y, Chen Q, Feng XY, Xu L, Duan WH, Xiong ZQ. Differential roles of NMDA receptor subtypes in ischemic neuronal cell death and ischemic tolerance. *Stroke*. 2008 Nov;39(11):3042-8.
- Chen ZL, Strickland S. Neuronal death in the hippocampus is promoted by plasmin-catalyzed degradation of laminin. *Cell*. 1997 Dec 26;91(7):917-25.
- Choi DW. Calcium: still center-stage in hypoxic-ischemic neuronal death. *Trends Neurosci*. 1995 Feb;18(2):58-60.
- Choi DW. Ischemia-induced neuronal apoptosis. *Curr Opin Neurobiol*. 1996 Oct;6(5):667-72.
- Choi JJ, Pernot M, Small SA, Konofagou EE. Noninvasive, transcranial and localized opening of the blood-brain barrier using focused ultrasound in mice. *Ultrasound Med Biol*. 2007 Jan;33(1):95-104.
- Clark AW, Krekoski CA, Bou SS, Chapman KR, Edwards DR. Increased gelatinase A (MMP-2) and gelatinase B (MMP-9) activities in human brain after focal ischemia. *Neurosci Lett*. 1997 Nov 28;238(1-2):53-6.
- Cordenonsi M, D'Atri F, Hammar E, Parry DA, Kendrick-Jones J, Shore D, Citi S. Cingulin contains globular and coiled-coil domains and interacts with ZO-1, ZO-2, ZO-3, and myosin. *J Cell Biol*. 1999 Dec 27;147(7):1569-82.
- Cserr HF, Bundgaard M. The neuronal microenvironment: a comparative view. *Ann N Y Acad Sci*. 1986;481:1-6.
- Cui J, Holmes EH, Greene TG, Liu PK. Oxidative DNA damage precedes DNA fragmentation after experimental stroke in rat brain. *FASEB J*. 2000 May;14(7):955-67.
- Danton GH, Dietrich WD. Inflammatory mechanisms after ischemia and stroke. *J Neuropathol Exp Neurol*. 2003 Feb;62(2):127-36.
- Dejana E, Orsenigo F, Lampugnani MG. The role of adherens junctions and VE-cadherin in the control of vascular permeability. *J Cell Sci*. 2008 Jul 1;121(Pt 13):2115-22.
- del Zoppo GJ, Hallenbeck JM. Advances in the vascular pathophysiology of ischemic stroke. *Thromb Res*. 2000 May 1;98(3):73-81.
- del Zoppo GJ, von Kummer R, Hamann GF. Ischaemic damage of brain microvessels: inherent risks for thrombolytic treatment in stroke. *J Neurol Neurosurg Psychiatry*. 1998 Jul;65(1):1-9.

- Dimitrijevic OB, Stamatovic SM, Keep RF, Andjelkovic AV. Effects of the chemokine CCL2 on blood-brain barrier permeability during ischemia-reperfusion injury. *J Cereb Blood Flow Metab.* 2006 Jun;26(6):797-810.
- Dirnagl U, Iadecola C, Moskowitz MA. Pathobiology of ischaemic stroke: an integrated view. *Trends Neurosci.* 1999 Sep;22(9):391-7.
- Dirnagl U, Becker K, Meisel A. Preconditioning and tolerance against cerebral ischaemia: from experimental strategies to clinical use. *Lancet Neurol.* 2009 Apr;8(4):398-412.
- Dong Y, Benveniste EN. Immune function of astrocytes. *Glia.* 2001 Nov;36(2):180-90.
- Donnan GA, Fisher M, Macleod M, Davis SM. Stroke. *Lancet.* 2008 May 10;371(9624):1612-23.
- Ebnet K, Schulz CU, Meyer Zu Brickwedde MK, Pendl GG, Vestweber D. Junctional adhesion molecule interacts with the PDZ domain-containing proteins AF-6 and ZO-1. *J Biol Chem.* 2000 Sep 8;275(36):27979-88.
- El Kossi MM, Zakhary MM. Oxidative stress in the context of acute cerebrovascular stroke. *Stroke.* 2000 Aug;31(8):1889-92.
- Emsley HC, Tyrrell PJ. Inflammation and infection in clinical stroke. *J Cereb Blood Flow Metab.* 2002 Dec;22(12):1399-419.
- Endres M, Meisel A, Biniszkiwicz D, Namura S, Prass K, Ruscher K, Lipski A, Jaenisch R, Moskowitz MA, Dirnagl U. DNA methyltransferase contributes to delayed ischemic brain injury. *J Neurosci.* 2000 May 1;20(9):3175-81.
- Endres M, Fink K, Zhu J, Stagliano NE, Bondada V, Geddes JW, Azuma T, Mattson MP, Kwiatkowski DJ, Moskowitz MA. Neuroprotective effects of gelsolin during murine stroke. *J Clin Invest.* 1999 Feb;103(3):347-54.
- Epe B, Ballmaier D, Roussyn I, Briviba K, Sies H. DNA damage by peroxynitrite characterized with DNA repair enzymes. *Nucleic Acids Res.* 1996 Nov 1;24(21):4105-10.
- Evans MD, Cooke MS. Factors contributing to the outcome of oxidative damage to nucleic acids. *Bioessays.* 2004 May;26(5):533-42.
- Farrell, C. L., and R. R. Shivers. Capillary junctions of the rat are not affected by osmotic opening of the blood-brain barrier. *Acta Neuropathol.* 63: 179-189,1984.
- Feuerstein GZ, Liu T, Barone FC. Cytokines, inflammation, and brain injury: role of tumor necrosis factor-alpha. *Cerebrovasc Brain Metab Rev.* 1994 Winter;6(4):341-60.

- Forster C, Clark HB, Ross ME, Iadecola C. Inducible nitric oxide synthase expression in human cerebral infarcts. *Acta Neuropathol.* 1999 Mar;97(3):215-20.
- Fredericks WR, Rapoport SI. Reversible osmotic opening of the blood-brain barrier in mice. *Stroke.* 1988 Feb;19(2):266-8.
- Furukawa K, Fu W, Li Y, Witke W, Kwiatkowski DJ, Mattson MP. The actin-severing protein gelsolin modulates calcium channel and NMDA receptor activities and vulnerability to excitotoxicity in hippocampal neurons. *J Neurosci.* 1997 Nov 1;17(21):8178-86.
- Furuse M, Sasaki H, Fujimoto K, Tsukita S. A single gene product, claudin-1 or -2, reconstitutes tight junction strands and recruits occludin in fibroblasts. *J Cell Biol* 1998; 143: 391–401.
- Gasche Y, Copin JC, Sugawara T, Fujimura M, Chan PH. Matrix metalloproteinase inhibition prevents oxidative stress-associated blood-brain barrier disruption after transient focal cerebral ischemia. *J Cereb Blood Flow Metab.* 2001 Dec;21(12):1393-400.
- Gasche Y, Fujimura M, Morita-Fujimura Y, Copin JC, Kawase M, Massengale J, Chan PH. Early appearance of activated matrix metalloproteinase-9 after focal cerebral ischemia in mice: a possible role in blood-brain barrier dysfunction. *J Cereb Blood Flow Metab.* 1999 Sep;19(9):1020-8.
- Gidday JM, Gasche YG, Copin JC, Shah AR, Perez RS, Shapiro SD, Chan PH, Park TS. Leukocyte-derived matrix metalloproteinase-9 mediates blood-brain barrier breakdown and is proinflammatory after transient focal cerebral ischemia. *Am J Physiol Heart Circ Physiol.* 2005 Aug;289(2):H558-68.
- Grau AJ, Reis A, Buggle F, Al-Khalaf A, Werle E, Valois N, Bertram M, Becher H, Grond-Ginsbach C. Monocyte function and plasma levels of interleukin-8 in acute ischemic stroke. *J Neurol Sci.* 2001 Nov 15;192(1-2):41-7.
- Green DR, Reed JC. Mitochondria and apoptosis. *Science.* 1998 Aug 28;281(5381):1309-12.
- Greenberg DA, Jin K. From angiogenesis to neuropathology. *Nature.* 2005 Dec 15;438(7070):954-9.
- Hansson, H.A., and B.B. Johansson. Induction of pinocytosis in cerebral vessels by acute hypertension and hyperosmolar solutions. *J. Neurosci. Res.* 5: 183-190, 1980.

- Haring HP, Berg EL, Tsurushita N, Tagaya M, del Zoppo GJ. E-selectin appears in nonischemic tissue during experimental focal cerebral ischemia. *Stroke*. 1996 Aug;27(8):1386-91; discussion 1391-2.
- Haskins J, Gu L, Wittchen ES, Hibbard J, Stevenson BR. ZO-3, a novel member of the MAGUK protein family found at the tight junction, interacts with ZO-1 and occludin. *J Cell Biol*. 1998 Apr 6;141(1):199-208.
- Hawkins BT, Davis TP. The blood-brain barrier/neurovascular unit in health and disease. *Pharmacol Rev*. 2005 Jun;57(2):173-85.
- Heo JH, Han SW, Lee SK. Free radicals as triggers of brain edema formation after stroke. *Free Radic Biol Med*. 2005 Jul 1;39(1):51-70.
- Heo JH, Lucero J, Abumiya T, Koziol JA, Copeland BR, del Zoppo GJ. Matrix metalloproteinases increase very early during experimental focal cerebral ischemia. *J Cereb Blood Flow Metab*. 1999 Jun;19(6):624-33.
- Heo JH, Han SW, Lee SK. Free radicals as triggers of brain edema formation after stroke. *Free Radic Biol Med*. 2005 Jul 1;39(1):51-70.
- Hermann DM, Zechariah A. Implications of vascular endothelial growth factor for postischemic neurovascular remodeling. *J Cereb Blood Flow Metab*. 2009 Oct;29(10):1620-43. Epub 2009 Aug 5.
- Herweijer H, Wolff JA. Gene therapy progress and prospects: hydrodynamic gene delivery. *Gene Ther* 2007; 14: 99–107.
- Hewett SJ, Misko TP, Keeling RM, Behrens MM, Choi DW, Cross AH. Murine encephalitogenic lymphoid cells induce nitric oxide synthase in primary astrocytes. *J Neuroimmunol*. 1996 Feb;64(2):201-8.
- Hjort N, Wu O, Ashkanian M, Sølling C, Mouridsen K, Christensen S, Gyldensted C, Andersen G, Østergaard L. MRI detection of early blood-brain barrier disruption: parenchymal enhancement predicts focal hemorrhagic transformation after thrombolysis. *Stroke*. 2008 Mar;39(3):1025-8.
- Honda M, Nakagawa S, Hayashi K, Kitagawa N, Tsutsumi K, Nagata I, Niwa M. Adrenomedullin improves the blood-brain barrier function through the expression of claudin-5. *Cell Mol Neurobiol*. 2006 Mar;26(2):109-18. Epub 2006 Apr 20.
- Hosomi N, Lucero J, Heo JH, Koziol JA, Copeland BR, del Zoppo GJ. Rapid differential endogenous plasminogen activator expression after acute middle cerebral artery occlusion. *Stroke*. 2001 Jun;32(6):1341-8.

- Hossmann KA. Viability thresholds and the penumbra of focal ischemia. *Ann Neurol*. 1994 Oct;36(4):557-65.
- Houthoff, H. J., K. G. Go. The mechanism of blood-brain barrier impairment by hyperosmolar perfusion. *Acta Neuropathol*. 56: 99-112,1982.
- Huang J, Choudhri TF, Winfree CJ, McTaggart RA, Kiss S, Mocco J, Kim LJ, Protosaltis TS, Zhang Y, Pinsky DJ, Connolly ES Jr. Postischemic cerebrovascular E-selectin expression mediates tissue injury in murine stroke. *Stroke*. 2000 Dec;31(12):3047-53.
- Huang ZG, Xue D, Preston E, Karbalai H, Buchan AM. Biphasic opening of the blood-brain barrier following transient focal ischemia: effects of hypothermia. *Can J Neurol Sci*. 1999 Nov;26(4):298-304.
- Hynynen K, McDannold N, Vykhodtseva N, Jolesz FA. Noninvasive MR imaging-guided focal opening of the blood-brain barrier in rabbits. *Radiology*. 2001 Sep;220(3):640-6.
- Hynynen K, McDannold N, Sheikov NA, Jolesz FA, Vykhodtseva N. Local and reversible blood-brain barrier disruption by noninvasive focused ultrasound at frequencies suitable for trans-skull sonications. *Neuroimage*. 2005 Jan 1;24(1):12-20.
- Itoh M, Morita K, Tsukita S. Characterization of ZO-2 as a MAGUK family member associated with tight as well as adherens junctions with a binding affinity to occludin and alpha catenin. *J Biol Chem*. 1999 Feb 26;274(9):5981-6.
- Jalali S, Huang Y, Dumont DJ, Hynynen K. Focused ultrasound-mediated bbb disruption is associated with an increase in activation of AKT: experimental study in rats. *BMC Neurol*. 2010 Nov 15;10:114.
- Jiao H, Wang Z, Liu Y, Wang P, Xue Y. Specific Role of Tight Junction Proteins Claudin-5, Occludin, and ZO-1 of the Blood-Brain Barrier in a Focal Cerebral Ischemic Insult. *J Mol Neurosci*. 2011 Feb 12. [Epub ahead of print]
- Jinnouchi Y, Yamagishi S, Matsui T, Takenaka K, Yoshida Y, Nakamura K, Ueda , Imaizumi T. Administration of pigment epithelium-derived factor (PEDF) inhibits cold injury-induced brain edema in mice. *Brain Res*. 2007 Sep 5;1167:92-100.
- Johnson EM Jr, Deckwerth TL. Molecular mechanisms of developmental neuronal death. *Annu Rev Neurosci*. 1993;16:31-46.
- Kiang AS, Palfi A, Ader M, et al. Toward a gene therapy for dominant disease: validation of an RNA interference-based mutation-independent approach. *Mol Ther* 2005; 12: 555–561

- Kinoshita M, McDannold N, Jolesz FA, Hynynen K. Targeted delivery of antibodies through the blood-brain barrier by MRI-guided focused ultrasound. *Biochem Biophys Res Commun*. 2006 Feb 24;340(4):1085-90.
- Kinoshita M, McDannold N, Jolesz FA, Hynynen K. Noninvasive localized delivery of Herceptin to the mouse brain by MRI-guided focused ultrasound-induced blood-brain barrier disruption. *Proc Natl Acad Sci U S A*. 2006 Aug 1;103(31):11719-23.
- Kamiya T, Katayama Y, Kashiwagi F, Terashi A. The role of bradykinin in mediating ischemic brain edema in rats. *Stroke*. 1993 Apr;24(4):571-5; discussion 575-6.
- Kastrup A, Engelhorn T, Beaulieu C, de Crespigny A, Moseley ME. Dynamics of cerebral injury, perfusion, and blood-brain barrier changes after temporary and permanent middle cerebral artery occlusion in the rat. *J Neurol Sci*. 1999 Jul 1;166(2):91-9.
- Kelly PJ, Morrow JD, Ning M, Koroshetz W, Lo EH, Terry E, Milne GL, Hubbard J, Lee H, Stevenson E, Lederer M, Furie KL. Oxidative stress and matrix metalloproteinase-9 in acute ischemic stroke: the Biomarker Evaluation for Antioxidant Therapies in Stroke (BEAT-Stroke) study. *Stroke*. 2008 Jan;39(1):100-4.
- Kidwell CS, Latour L, Saver JL, Alger JR, Starkman S, Duckwiler G, Jahan R, Vinuela F; UCLA Thrombolysis Investigators, Kang DW, Warach S. Thrombolytic toxicity: blood brain barrier disruption in human ischemic stroke. *Cerebrovasc Dis*. 2008;25(4):338-43.
- Kidwell CS, Saver JL, Mattiello J, Starkman S, Vinuela F, Duckwiler G, Gobin YP, Jahan R, Vespa P, Villablanca JP, Liebeskind DS, Woods RP, Alger JR. Diffusion-perfusion MRI characterization of post-recanalization hyperperfusion in humans. *Neurology*. 2001 Dec 11;57(11):2015-21.
- Klohs J, Steinbrink J, Bourayou R, Mueller S, Cordell R, Licha K, Schirner M, Dirnagl U, Lindauer U, Wunder A. Near-infrared fluorescence imaging with fluorescently labeled albumin: a novel method for non-invasive optical imaging of blood-brain barrier impairment after focal cerebral ischemia in mice. *J Neurosci Methods*. 2009 May 30;180(1):126-32.
- Knight RA, Nagaraja TN, Ewing JR, Naghesh V, Whitton PA, Bershad E, et al. Quantitation and localization of blood-to-brain influx by magnetic resonance imaging and quantitative autoradiography in a model of transient focal ischemia. *Magn Reson Med* 2005;54:813–21

- Kontos HA. George E. Brown memorial lecture. Oxygen radicals in cerebral vascular injury. *Circ Res*. 1985 Oct;57(4):508-16.
- Kontos HA. Oxygen radicals in cerebral ischemia: the 2001 Willis lecture. *Stroke*. 2001 Nov;32(11):2712-6.
- Koto T, Takubo K, Ishida S, et al. Hypoxia disrupts the barrier function of neural blood vessels through changes in the expression of claudin-5 in endothelial cells. *Am J Pathol* 2007; 170: 1389–1397.
- Kulik T, Kusano Y, Aronhime S, Sandler AL, Winn HR. Regulation of cerebral vasculature in normal and ischemic brain. *Neuropharmacology*. 2008 Sep;55(3):281-8.
- Kuroda S, Siesjö BK. Reperfusion damage following focal ischemia: pathophysiology and therapeutic windows. *Clin Neurosci*. 1997;4(4):199-212.
- Kuroiwa T, Ting P, Martinez H, Klatzo I. The biphasic opening of the blood–brain barrier to proteins following temporary middle cerebral artery occlusion. *Acta Neuropathol* 1985;68:122–9.
- Latour LL, Kang DW, Ezzeddine MA, Chalela JA, Warach S. Early blood-brain barrier disruption in human focal brain ischemia. *Ann Neurol*. 2004 Oct;56(4):468-77.
- Ladecola C. Bright and dark sides of nitric oxide in ischemic brain injury. *Trends Neurosci*. 1997 Mar;20(3):132-9.
- Lee NY, Kang YS. The brain-to-blood efflux transport of taurine and changes in the blood-brain barrier transport system by tumor necrosis factor- α . *Brain Res*. 2004 Oct 8;1023(1):141-7.
- Liu PK, Hsu CY, Dizdaroglu M, Floyd RA, Kow YW, Karakaya A, Rabow LE, Cui JK. Damage, repair, and mutagenesis in nuclear genes after mouse forebrain ischemia-reperfusion. *J Neurosci*. 1996 Nov 1;16(21):6795-806.
- Li X, Nahas Z, Lomarev M, Denslow S, Shastri A, Bohning DE, George MS. Prefrontal cortex transcranial magnetic stimulation does not change local diffusion: a magnetic resonance imaging study in patients with depression. *Cogn Behav Neurol*. 2003 Jun;16(2):128-35.
- Lo EH, Pan Y, Matsumoto K, Kowall NW. Blood–brain barrier disruption in experimental focal ischemia: comparison between in vivo MRI and immunocytochemistry. *Magn Reson Imaging* 1994;24:403-11.

- Lorberboym M, Lampl Y, Sadeh M. Correlation of 99mTc-DTPA SPECT of the blood-brain barrier with neurologic outcome after acute stroke. *J Nucl Med.* 2003 Dec;44(12):1898-904.
- Lewis DL, Hagstrom JE, Loomis AG, Wolff JA, Herweijer H. Efficient delivery of siRNA for inhibition of gene expression in postnatal mice. *Nat Genet* 2002; 32: 107–108.
- Maeda S, Arai Y, Higuchi H, Tomoyasu Y, Mizuno R, Takahashi T, Miyawaki T. Induction of apoptotic change in the rat hippocampus caused by ferric nitrilotriacetate. *Redox Rep.* 2011;16(3):114-20.
- Mark KS, Davis TP. Cerebral microvascular changes in permeability and tight junctions induced by hypoxia-reoxygenation. *Am J Physiol Heart Circ Physiol.* 2002 Apr;282(4):H1485-94.
- Markus R, Reutens DC, Kazui S, Read S, Wright P, Pearce DC, Tochon-Danguy HJ, Sachinidis JI, Donnan GA. Hypoxic tissue in ischaemic stroke: persistence and clinical consequences of spontaneous survival. *Brain.* 2004 Jun;127(Pt 6):1427-36.
- Marti HJ, Bernaudin M, Bellail A, Schoch H, Euler M, Petit E, Risau W. Hypoxia-induced vascular endothelial growth factor expression precedes neovascularization after cerebral ischemia. *Am J Pathol.* 2000 Mar;156(3):965-76.
- Martin LJ, Al-Abdulla NA, Brambrink AM, Kirsch JR, Sieber FE, Portera-Cailliau C. Neurodegeneration in excitotoxicity, global cerebral ischemia, and target deprivation: A perspective on the contributions of apoptosis and necrosis. *Brain Res Bull.* 1998 Jul 1;46(4):281-309.
- Martin RL, Lloyd HG, Cowan AI. The early events of oxygen and glucose deprivation: setting the scene for neuronal death? *Trends Neurosci.* 1994 Jun;17(6):251-7.
- Matter K, Balda MS. Holey barrier: claudins and the regulation of brain endothelial permeability. *J Cell Biol.* 2003 May 12;161(3):459-60.
- Masters BS. Nitric oxide synthases: why so complex? *Annu Rev Nutr.* 1994;14:131-45.
- Matarin M, Brown WM, Hardy JA, Rich SS, Singleton AB, Brown RD Jr, Brott TG, Worrall BB, Meschia JF; SWISS Study Group;ISGS Study Group; MSGD Study Group. Association of integrin alpha2 gene variants with ischemic stroke. *J Cereb Blood Flow Metab.* 2008 Jan;28(1):81-9.
- McCaffrey AP, Meuse L, Pham TT, Conklin DS, Hannon GJ, Kay MA. RNA interference in adult mice. *Nature* 2002; 418: 38–39.

- McDannold N, Vykhodtseva N, Raymond S, Jolesz FA, Hynynen K. MRI-guided targeted blood-brain barrier disruption with focused ultrasound: histological findings in rabbits. *Ultrasound Med Biol.* 2005 Nov;31(11):1527-37.
- McDannold N, Vykhodtseva N, Hynynen K. Targeted disruption of the blood-brain barrier with focused ultrasound: association with cavitation activity. *Phys Med Biol.* 2006 Feb 21;51(4):793-807.
- Meikle SR, Kench P, Kassiou M, Banati RB. Small animal SPECT and its place in the matrix of molecular imaging technologies. *Phys Med Biol.* 2005 Nov 21;50(22):R45-61
- Meldrum B, Evans M, Griffiths T, Simon R. Ischaemic brain damage: the role of excitatory activity and of calcium entry. *Br J Anaesth.* 1985 Jan;57(1):44-6
- Mitic LL, Anderson JM. Molecular architecture of tight junctions. *Annu Rev Physiol.* 1998;60:121-42.
- Montaner J, Alvarez-Sabín J, Molina C, Anglés A, Abilleira S, Arenillas J, González MA, Monasterio J. Matrix metalloproteinase expression after human cardioembolic stroke: temporal profile and relation to neurological impairment. *Stroke.* 2001 Aug;32(8):1759-66.
- Montaner J, Molina CA, Monasterio J, Abilleira S, Arenillas JF, Ribó M, Quintana M, Alvarez-Sabín J. Matrix metalloproteinase-9 pretreatment level predicts intracranial hemorrhagic complications after thrombolysis in human stroke. *Circulation.* 2003 Feb 4;107(4):598-603.
- Nagaraja TN, Keenan KA, Fenstermacher JD, Knight RA. Acute leakage patterns of fluorescent plasma flow markers after transient focal cerebral ischemia suggest large openings in blood-brain barrier. *Microcirculation* 2008a;15:1– 14.
- Nagy, Z. H. Peters. Fracture faces of cell junctions in cerebral endothelium during normal and hyperosmolar conditions. *Lab. Invest.* 50: 313-322, 1984.
- Namura S, Zhu J, Fink K, Endres M, Srinivasan A, Tomaselli KJ, Yuan J, Moskowitz MA. Activation and cleavage of caspase-3 in apoptosis induced by experimental cerebral ischemia. *J Neurosci.* 1998 May 15;18(10):3659-68.
- Nelson CW, Wei EP, Povlishock JT, Kontos HA, Moskowitz MA. Oxygen radicals in cerebral ischemia. *Am J Physiol.* 1992 Nov;263(5 Pt 2):H1356-62.
- Nicholls D, Attwell D. The release and uptake of excitatory amino acids. *Trends Pharmacol Sci.* 1990 Nov;11(11):462-8.

- Nitta T, Hata M, Gotoh S, et al. Size-selective loosening of the blood-brain barrier in claudin-5-deficient mice. *J Cell Biol* 2003; 161: 653–660.
- Notari L, Miller A, Martínez A, Amaral J, Ju M, Robinson G, Smith LE, Becerra SP. Pigment epithelium-derived factor is a substrate for matrix metalloproteinase type 2 and type 9: implications for downregulation in hypoxia. *Invest Ophthalmol Vis Sci*. 2005 Aug;46(8):2736-47.
- Nusrat A, Turner JR, Madara JL. Molecular physiology and pathophysiology of tight junctions. IV. Regulation of tight junctions by extracellular stimuli: nutrients, cytokines, and immune cells. *Am J Physiol Gastrointest Liver Physiol*. 2000 Nov;279(5):G851-7.
- Olsen, F. Increased permeability for plasma components of the cerebral vessels during acute angiotensin hypertension in rats. *Acta Pathol. Microbiol. Scand. Sect. A* 85: 572-576, 1977.
- Opdenakker G, Van den Steen PE, Dubois B, Nelissen I, Van Coillie E, Masure S, Proost P, Van Damme J. Gelatinase B functions as regulator and effector in leukocyte biology. *J Leukoc Biol*. 2001 Jun;69(6):851-9.
- Pan J, Konstas AA, Bateman B, Ortolano GA, Pile-Spellman J. Reperfusion injury following cerebral ischemia: pathophysiology, MR imaging, and potential therapies. *Neuroradiology*. 2007 Feb;49(2):93-102.
- Persidsky Y, Heilman D, Haorah J, Zelivyanskaya M, Persidsky R, Weber GA, Shimokawa H, Kaibuchi K, Ikezu T. Rho-mediated regulation of tight junctions during monocyte migration across the blood-brain barrier in HIV-1 encephalitis (HIVE). *Blood*. 2006 Jun 15;107(12):4770-80.
- Petty MA, Wettstein JG. Elements of cerebral microvascular ischaemia. *Brain Res Brain Res Rev*. 2001 Aug;36(1):23-34.
- Petty MA, Lo EH. Junctional complexes of the blood-brain barrier: permeability changes in neuroinflammation. *Prog Neurobiol*. 2002 Dec;68(5):311-23.
- Pignolo RJ, Francis MK, Rotenberg MO, Cristofalo VJ. Putative role for EPC-1/PEDF in the G0 growth arrest of human diploid fibroblasts. *J Cell Physiol*. 2003 Apr;195(1):12-20.
- Piontek J, Winkler L, Wolburg H, Müller SL, Zuleger N, Piehl C, Wiesner B, Krause G, Blasig IE. Formation of tight junction: determinants of homophilic interaction between classic claudins. *FASEB J*. 2008 Jan;22(1):146-58.

- Povlishock, J.T, H.A. Kontos, W.I. Rosenblum. A scanning electronmicroscopic analysis of the intraparenchymal brain vasculature following experimental hypertension. *Actu Neuropathol.* 51: 203-213,1980.
- Preston E, Sutherland G, Finsten A. Three openings of the blood-brain barrier produced by forebrain ischemia in the rat. *Neurosci Lett.* 1993 Jan 4;149(1):75-8.
- Rao RK, Basuroy S, Rao VU, Karnaky Jr KJ, Gupta A. Tyrosine phosphorylation and dissociation of occludin-ZO-1 and E-cadherin-beta-catenin complexes from the cytoskeleton by oxidative stress. *Biochem J.* 2002 Dec 1;368(Pt 2):471-81.
- Rapoport, S.I., Hori, M., Klatzo., I. Testing of a hypothesis for osmotic opening of the blood-brain barrier. *Am. J. Physiol.* 223: 323-331,1972.
- Rapoport SI. Advances in osmotic opening of the blood-brain barrier to enhance CNS chemotherapy. *Expert Opin Investig Drugs.* 2001 Oct;10(10):1809-18.
- Rapoport SI. Osmotic opening of the blood-brain barrier: principles, mechanism, and therapeutic applications. *Cell Mol Neurobiol.* 2000 Apr;20(2):217-30.
- Rapoport SI Reversible opening of the blood-brain barrier by osmotic shrinkage of the cerebrovascular endothelium: opening of the tight junctions as related to carotid arteriography. In: *Small Vessel Angiography*, edited by S. K. Hilal. St. Louis, MO: Mosby, 1973.
- Ravnborg M, Knudsen GM, Blinkenberg M. No effect of pulsed magnetic stimulation on the blood-brain barrier in rats. *Neuroscience.* 1990;38(1):277-80.
- Rosell A, Cuadrado E, Ortega-Aznar A, Hernández-Guillamon M, Lo EH, Montaner J. MMP-9-positive neutrophil infiltration is associated to blood-brain barrier breakdown and basal lamina type IV collagen degradation during hemorrhagic transformation after human ischemic stroke. *Stroke.* 2008 Apr;39(4):1121-6.
- Romanic AM, White RF, Arleth AJ, Ohlstein EH, Barone FC. Matrix metalloproteinase expression increases after cerebral focal ischemia in rats: inhibition of matrix metalloproteinase-9 reduces infarct size. *Stroke.* 1998 May;29(5):1020-30.
- Rosenberg GA, Navratil M, Barone F, Feuerstein G. Proteolytic cascade enzymes increase in focal cerebral ischemia in rat. *J Cereb Blood Flow Metab.* 1996 May;16(3):360-6.
- Rosenberg GA, Estrada EY, Dencoff JE. Matrix metalloproteinases and TIMPs are associated with blood-brain barrier opening after reperfusion in rat brain. *Stroke.* 1998 Oct;29(10):2189-95.

- Rosenberg GA, Cunningham LA, Wallace J, Alexander S, Estrada EY, Grossetete M, Razhagi A, Miller K, Gearing A. Immunohistochemistry of matrix metalloproteinases in reperfusion injury to rat brain: activation of MMP-9 linked to stromelysin-1 and microglia in cell cultures. *Brain Res.* 2001 Mar 2;893(1-2):104-12.
- Rosenberg GA. Matrix metalloproteinases in neuroinflammation. *Glia.* 2002 Sep;39(3):279-91.
- Sakakibara A, Furuse M, Saitou M, Ando-Akatsuka Y, Tsukita S. Possible involvement of phosphorylation of occludin in tight junction formation. *J Cell Biol.* 1997 Jun 16;137(6):1393-401.
- Sanagi T, Yabe T, Yamada H. Gene transfer of PEDF attenuates ischemic brain damage in the rat middle cerebral artery occlusion model. *J Neurochem.* 2008 Aug;106(4):1841-54.
- Sandoval KE, Witt KA. Blood-brain barrier tight junction permeability and ischemic stroke. *Neurobiol Dis.* 2008 Nov;32(2):200-19.
- Schaller B, Graf R. Cerebral ischemia and reperfusion: the pathophysiologic concept as a basis for clinical therapy. *J Cereb Blood Flow Metab.* 2004 Apr;24(4):351-71.
- Schreibelt G, Kooij G, Reijkerkerk A, van Doorn R, Gringhuis SI, van der Pol S, Weksler BB, Romero IA, Couraud PO, Piontek J, Blasig IE, Dijkstra CD, Ronken E, de Vries HE. Reactive oxygen species alter brain endothelial tight junction dynamics via RhoA, PI3 kinase, and PKB signaling. *FASEB J.* 2007 Nov;21(13):3666-76.
- Sheikov N, McDannold N, Vykhodtseva N, Jolesz F, Hynynen K. Cellular mechanisms of the blood-brain barrier opening induced by ultrasound in presence of microbubbles. *Ultrasound Med Biol.* 2004 Jul;30(7):979-89.
- Sheikov N, McDannold N, Jolesz F, Zhang YZ, Tam K, Hynynen K. Brain arterioles show more active vesicular transport of blood-borne tracer molecules than capillaries and venules after focused ultrasound-evoked opening of the blood-brain barrier. *Ultrasound Med Biol.* 2006 Sep;32(9):1399-409.
- Sheikov N, McDannold N, Sharma S, Hynynen K. Effect of focused ultrasound applied with an ultrasound contrast agent on the tight junctional integrity of the brain microvascular endothelium. *Ultrasound Med Biol.* 2008 Jul;34(7):1093-104.
- Sheikpranbabu S, Ravinarayanan H, Elayappan B, Jongsun P, Gurunathan S. Pigment epithelium-derived factor inhibits vascular endothelial growth factor-and interleukin-

- 1beta-induced vascular permeability and angiogenesis in retinal endothelial cells. *Vascul Pharmacol.* 2010 Jan-Feb;52(1-2):84-94.. (a)
- Sheikpranbabu S, Haribalaganesh R, Lee KJ, Gurunathan S. Pigment epithelium-derived factor inhibits advanced glycation end products-induced retinal vascular permeability. *Biochimie.* 2010 Aug;92(8):1040-51. (b)
- Soma T, Chiba H, Kato-Mori Y, Wada T, Yamashita T, Kojima T, Sawada N. Thr(207) of claudin-5 is involved in size-selective loosening of the endothelial barrier by cyclic AMP. *Exp Cell Res.* 2004 Oct 15;300(1):202-12.
- Sood RR, Taheri S, Candelario-Jalil E, Estrada EY, Rosenberg GA. Early beneficial effect of matrix metalloproteinase inhibition on blood-brain barrier permeability as measured by magnetic resonance imaging countered by impaired long-term recovery after stroke in rat brain. *J Cereb Blood Flow Metab.* 2008 Feb;28(2):431-8.
- Sorokin L. The impact of the extracellular matrix on inflammation. *Nat Rev Immunol.* 2010 Oct;10(10):712-23.
- Spengos K, Tsivgoulis G, Zakopoulos N. Blood pressure management in acute stroke: a long-standing debate. *Eur Neurol.* 2006;55(3):123-35.
- Stamatovic SM, Keep RF, Kunkel SL, Andjelkovic AV. Potential role of MCP-1 in endothelial cell tight junction 'opening': signaling via Rho and Rho kinase. *J Cell Sci.* 2003 Nov 15;116(Pt 22):4615-28.
- Strbian D, Durukan A, Pitkonen M, Marinkovic I, Tatlisumak E, Pedrono E, et al. The blood-brain barrier is continuously open for several weeks following transient focal cerebral ischemia. *Neuroscience* 2008;153:175-81.
- Takanohashi A, Yabe T, Schwartz JP. Pigment epithelium-derived factor induces the production of chemokines by rat microglia. *Glia.* 2005 Sep;51(4):266-78.
- Tang Y, Xu H, Du X, Lit L, Walker W, Lu A, Ran R, Gregg JP, Reilly M, Pancioli A, Khoury JC, Sauerbeck LR, Carrozzella JA, Spilker J, Clark J, Wagner KR, Jauch EC, Chang DJ, Verro P, Broderick JP, Sharp FR. Gene expression in blood changes rapidly in neutrophils and monocytes after ischemic stroke in humans: a microarray study. *J Cereb Blood Flow Metab.* 2006 Aug;26(8):1089-102.
- Thornberry NA, Lazebnik Y. Caspases: enemies within. *Science.* 1998 Aug 28;281(5381):1312-6.

- Tombran-Tink J, Johnson LV. Neuronal differentiation of retinoblastoma cells induced by medium conditioned by human RPE cells. *Invest Ophthalmol Vis Sci*. 1989 Aug;30(8):1700-7.
- Tombran-Tink J, Barnstable CJ. PEDF: a multifaceted neurotrophic factor. *Nat Rev Neurosci*. 2003 Aug;4(8):628-36.
- Traweger A, Fuchs R, Krizbai IA, Weiger TM, Bauer HC, Bauer H. The tight junction protein ZO-2 localizes to the nucleus and interacts with the heterogeneous nuclear ribonucleoprotein scaffold attachment factor-B. *J Biol Chem*. 2003 Jan 24;278(4):2692-700.
- Tsukita S, Furuse M, Itoh M. Multifunctional strands in tight junctions. *Nat Rev Mol Cell Biol* 2001; 2: 285–293.
- Tsukita S, Furuse M. The structure and function of claudins, cell adhesion molecules at tight junctions. *Ann N Y Acad Sci*. 2000;915:129-35.
- Vykhodtseva N, McDannold N, Hynynen K. Progress and problems in the application of focused ultrasound for blood-brain barrier disruption. *Ultrasonics*. 2008 Aug;48(4):279-96.
- Wang Q, Tang XN, Yenari MA. The inflammatory response in stroke. *J Neuroimmunol*. 2007 Mar;184(1-2):53-68.
- Weber C, Fraemohs L, Dejana E. The role of junctional adhesion molecules in vascular inflammation. *Nat Rev Immunol*. 2007 Jun;7(6):467-77
- Wei EP, Kontos HA, Beckman JS. Mechanisms of cerebral vasodilation by superoxide, hydrogen peroxide, and peroxynitrite. *Am J Physiol*. 1996 Sep;271(3 Pt 2):H1262-6
- Weiss N, Miller F, Cazaubon S, Couraud PO. The blood-brain barrier in brain homeostasis and neurological diseases. *Biochim Biophys Acta*. 2009 Apr;1788(4):842-57. Epub 2008 Nov 11.
- Westergaard, E. The blood-brain barrier to horseradish peroxidase under normal and experimental conditions. *Acta Neuropathol*. 39: 181-187, 1977.
- Witt KA, Mark KS, Sandoval KE, Davis TP. Reoxygenation stress on blood-brain barrier paracellular permeability and edema in the rat. *Microvasc Res*. 2008 Jan;75(1):91-6.
- Wolburg H, Lippoldt A. Tight junctions of the blood-brain barrier: development, composition and regulation. *Vascul Pharmacol*. 2002 Jun;38(6):323-37.

- Wong CH, Crack PJ. Modulation of neuro-inflammation and vascular response by oxidative stress following cerebral ischemia-reperfusion injury. *Curr Med Chem.* 2008;15(1):1-14.
- Wong V, Gumbiner BM. A synthetic peptide corresponding to the extracellular domain of occludin perturbs the tight junction permeability barrier. *J Cell Biol.* 1997 Jan 27;136(2):399-409.
- Yamagishi S, Abe R, Jinnouchi Y, Matsui T, Imaizumi T, Inoue H. Pigment epithelium-derived factor inhibits vascular endothelial growth factor-induced vascular hyperpermeability both in vitro and in vivo. *J Int Med Res.* 2007 Nov-Dec;35(6):896-9.
- Yamamoto M, Ramirez SH, Sato S, Kiyota T, Cerny RL, Kaibuchi K, Persidsky Y, Ikezu T. Phosphorylation of claudin-5 and occludin by rho kinase in brain endothelial cells. *Am J Pathol.* 2008 Feb;172(2):521-33.
- Yang J, Duh EJ, Caldwell RB, Behzadian MA. Antipermeability function of PEDF involves blockade of the MAP kinase/GSK/beta-catenin signaling pathway and uPAR expression. *Invest Ophthalmol Vis Sci.* 2010 Jun;51(6):3273-80.
- Yeung D, Manias JL, Stewart DJ, Nag S. Decreased junctional adhesion molecule-A expression during blood-brain barrier breakdown. *Acta Neuropathol.* 2008 Jun;115(6):635-42.
- Young W, Rappaport ZH, Chalif DJ, Flamm ES. Regional brain sodium, potassium, and water changes in the rat middle cerebral artery occlusion model of ischemia. *Stroke.* 1987 Jul-Aug;18(4):751-9.
- Yurchenco PD, Schittny JC. Molecular architecture of basement membranes. *FASEB J.* 1990 Apr 1;4(6):1577-90.
- Zhang R, Chopp M, Zhang Z, Jiang N, Powers C. The expression of P- and E-selectins in three models of middle cerebral artery occlusion. *Brain Res.* 1998 Mar 2;785(2):207-14.
- Zlokovic BV. The blood-brain barrier in health and chronic neurodegenerative disorders. *Neuron.* 2008 Jan 24;57(2):178-201.

Erklärung

„Ich, Ryan, Cordell, erkläre, dass ich die vorgelegte Dissertationsschrift mit dem Thema: *The Relationship between the Blood-Brain Barrier and Cerebral Ischemia*, selbst verfasst und keine anderen als die angegebenen Quellen und Hilfsmittel benutzt, ohne die (unzulässige) Hilfe Dritter verfasst und auch in Teilen keine Kopien anderer Arbeiten dargestellt habe.“

Datum

02-09-2012

Unterschrift